ISSN 2518-1491 (Online),
ISSN 2224-5286 (Print)

ҚАЗАҚСТАН РЕСПУБЛИКАСЫ
ҰЛТТЫҚ ҒЫЛЫМ АКАДЕМИЯСЫНЫҢ

Д.В.Сокольский атындағы «Жанармай,
катализ және электрохимия институты» АҚ

Х А Б А Р Л А Р Ы

ИЗВЕСТИЯ

НАЦИОНАЛЬНОЙ АКАДЕМИИ НАУК
РЕСПУБЛИКИ КАЗАХСТАН
АО «Институт топлива, катализа и
электрохимии им. Д.В. Сокольского»

N E W S

OF THE ACADEMY OF SCIENCES
OF THE REPUBLIC OF KAZAKHSTAN
JSC «D.V. Sokolsky institute of fuel, catalysis
and electrochemistry»

SERIES
CHEMISTRY AND TECHNOLOGY

6 (438)

NOVEMBER – DECEMBER 2019

PUBLISHED SINCE JANUARY 1947

PUBLISHED 6 TIMES A YEAR

ALMATY, NAS RK

NAS RK is pleased to announce that News of NAS RK. Series of chemistry and technologies scientific journal has been accepted for indexing in the Emerging Sources Citation Index, a new edition of Web of Science. Content in this index is under consideration by Clarivate Analytics to be accepted in the Science Citation Index Expanded, the Social Sciences Citation Index, and the Arts & Humanities Citation Index. The quality and depth of content Web of Science offers to researchers, authors, publishers, and institutions sets it apart from other research databases. The inclusion of News of NAS RK. Series of chemistry and technologies in the Emerging Sources Citation Index demonstrates our dedication to providing the most relevant and influential content of chemical sciences to our community.

Қазақстан Республикасы Ұлттық ғылым академиясы "ҚР ҰҒА Хабарлары. Химия және технология сериясы" ғылыми журналының Web of Science-тің жаңаланған нұсқасы Emerging Sources Citation Index-те индекстелуге қабылданғанын хабарлайды. Бұл индекстелу барысында Clarivate Analytics компаниясы журналды одан әрі the Science Citation Index Expanded, the Social Sciences Citation Index және the Arts & Humanities Citation Index-ке қабылдау мәселесін қарастыруда. Webof Science зерттеушілер, авторлар, баспашылар мен мекемелерге контент тереңдігі мен сапасын ұсынады. ҚР ҰҒА Хабарлары. Химия және технология сериясы Emerging Sources Citation Index-ке енуі біздің қоғамдастық үшін ең өзекті және беделді химиялық ғылымдар бойынша контентке адалдығымызды білдіреді.

НАН РК сообщает, что научный журнал «Известия НАН РК. Серия химии и технологий» был принят для индексирования в Emerging Sources Citation Index, обновленной версии Web of Science. Содержание в этом индексировании находится в стадии рассмотрения компанией Clarivate Analytics для дальнейшего принятия журнала в the Science Citation Index Expanded, the Social Sciences Citation Index и the Arts & Humanities Citation Index. Web of Science предлагает качество и глубину контента для исследователей, авторов, издателей и учреждений. Включение Известия НАН РК в Emerging Sources Citation Index демонстрирует нашу приверженность к наиболее актуальному и влиятельному контенту по химическим наукам для нашего сообщества.

«ҚР ҰҒА Хабарлары. Химия және технология сериясы».
ISSN 2518-1491 (Online),
ISSN 2224-5286 (Print)
Меншіктенуші: «Қазақстан Республикасының Ұлттық ғылым академиясы» Республикалық қоғамдық бірлестігі (Алматы қ.)
Қазақстан республикасының Мәдениет пен ақпарат министрлігінің Ақпарат және мұрағат комитетінде 30.04.2010 ж. берілген **№1089-Ж** мерзімдік басылым тіркеуіне қойылу туралы куәлік

Мерзімділігі: жылына 6 рет.
Тиражы: 300 дана.

Редакцияның мекенжайы: 050010, Алматы қ., Шевченко көш., 28, 219 бөл., 220, тел.: 272-13-19, 272-13-18,
http://chemistry-technology.kz/index.php/en/arhiv

Типографияның мекенжайы: «Аруна» ЖК, Алматы қ., Муратбаева көш., 75.

«Известия НАН РК. Серия химии и технологии».
ISSN 2518-1491 (Online),
ISSN 2224-5286 (Print)
Собственник: Республиканское общественное объединение «Национальная академия наук Республики Казахстан» (г. Алматы)
Свидетельство о постановке на учет периодического печатного издания в Комитете информации и архивов Министерства культуры и информации Республики Казахстан **№10893-Ж,** выданное 30.04.2010 г.

Периодичность: 6 раз в год
Тираж: 300 экземпляров

Адрес редакции: 050010, г. Алматы, ул. Шевченко, 28, ком. 219, 220, тел. 272-13-19, 272-13-18,
http://chemistry-technology.kz/index.php/en/arhiv

Адрес редакции: 050100, г. Алматы, ул. Кунаева, 142,
Институт органического катализа и электрохимии им. Д. В. Сокольского,
каб. 310, тел. 291-62-80, факс 291-57-22, e-mail:orgcat@nursat.kz
Адрес типографии: ИП «Аруна», г. Алматы, ул. Муратбаева, 75

News of the National Academy of Sciences of the Republic of Kazakhstan. Series of chemistry and technology.
ISSN 2518-1491 (Online),
ISSN 2224-5286 (Print)
Owner: RPA "National Academy of Sciences of the Republic of Kazakhstan" (Almaty)
The certificate of registration of a periodic printed publication in the Committee of Information and Archives of the Ministry of Culture and Information of the Republic of Kazakhstan N 10893-Ж, issued 30.04.2010

Periodicity: 6 times a year
Circulation: 300 copies

Editorial address: 28, Shevchenko str., of. 219, 220, Almaty, 050010, tel. 272-13-19, 272-13-18,
http://chemistry-technology.kz/index.php/en/arhiv

Editorial address: Institute of Organic Catalysis and Electrochemistry named after D. V. Sokolsky
142, Kunayev str., of. 310, Almaty, 050100, tel. 291-62-80, fax 291-57-22,
e-mail: orgcat@nursat.kz

Address of printing house: ST "Aruna", 75, Muratbayev str, Almaty

N E W S
OF THE NATIONAL ACADEMY OF SCIENCES OF THE REPUBLIC OF KAZAKHSTAN
SERIES CHEMISTRY AND TECHNOLOGY
ISSN 2224-5286 **https://doi.org/10.32014/2019.2518-1491.67**
Volume 6, Number 438 (2019), 6 – 11

UDC: 661.669
IRSTI:31.23.15; 61.51.21; 87.53.13

G.T. Smagulova[1,2], P.J.F. Harris[3], Z.A. Mansurov[1,2]

[1]Institute of Combustion Problems, Almaty, Kazakhstan;
[2]Al-FarabiKazakhNationalUniversity, Almaty, Kazakhstan;
[3]University of Reading, Reading, Berkshire, United Kingdom
smagulova.gaukhar@gmail.com

PROCESSING HOUSE HOLD POLYETHYLENE WASTE TO PRODUCE CARBON NANOTUBES

Abstract. The paper presents the results of processing household polyethylene waste by thermal degradation for the synthesis of carbon nanotubes by chemical vapor deposition. A feature of the work is that the decomposition of polyethylene samples and the synthesis of carbon nanotubes were carried out in one stage. The effect of temperature on the decomposition products of polyethylene wastes in the temperature range 200-550 ° C was investigated. It has been determined that even at a temperature of 450 ° C, the decomposition of polyethylene proceeds sufficiently to form carbon nanotubes. The catalyst for the growth of CNTs was cenospheres obtained from the ash and slag waste of thermal power plants during coal combustion. The main components of cenospheres are silicon and aluminum oxides. The active phase of the catalyst was iron nitrate, which is a precursor to the formation of iron clusters on the surface of cenospheres. The decomposition of polyethylene waste and the synthesis of carbon nanotubes was carried out one-stage in a tubular CVD reactor in a nitrogen atmosphere. The temperature of the synthesis of CNTs is 800 ° C. As a result of synthesis, carbon nanotubes with a diameter of 15-28 nm are formed on the surface of cenospheres, which is confirmed by results of SEM analysis and Raman spectroscopy. Based on the studies, the authors proposed a method for processing polyethylene waste for the synthesis of high quality CNTs.

Key words: carbon nanotubes, polyethylene waste, IR spectroscopy, electron microscopy.

INTRODUCTION

Currently, the problem of recycling polymer waste is a critical point in ensuring environmental safety. According to the report of the Eurasian Economic Commission, the world production of polymers in 2013 amounted to 245 megatons [1]. Polymeric waste, which makes up about 40% of all household and industrial waste, is recycled only in small quantities, and is either incinerated or disposed of in landfills. According to [2], in 2015, only 9% of the total volume of plastic waste was recycled, 12% was burnt, and 79% was collected in landfills. There are several ways to recycle plastic waste: mechanical recycling; processing of raw materials (monomerization, blast furnace recovery, chemical processing of raw materials of coke ovens, gasification, liquefaction, etc.); thermal processing (cement kilns and power generation) [3].

The review [4] presents data on the processing of polymer wastes to produce carbon nanomaterials (fullerenes, carbon nanotubes, graphenes, etc.). It is shown that the processing process is energy and resource intensive, however, with the right approach and organization of the process, it is possible to achieve economic profitability. In [5], the authors proposed a method for recycling PET plastic bottles for the production of carbon nanostructures, including fullerenes and graphene sheets. The work [6] presents the results of the synthesis of CNTs with a diameter of 30–50 nm by catalytic pyrolysis of polyethylene waste. Interest in the production of carbon nanotubes is due to the wide range of applications of these nanomaterials in various industries: energy [7], textile industry [8], as sorbent materials for wastewater treatment [9] due to the high values of the specific surface [10].

EXPERIMENTAL PART

As the initial material, household garbage (bags and containers) with the marking PET was used. Household plastic waste was pre-shredded and cleaned. Cleaning was carried out by washing the powdered sample with hot water with the addition of a surfactant. After washing, the samples were dried under normal conditions. At the end of the drying process, the crushed samples were fused without chemical degradation in a porcelain boat by heating at temperatures no higher than 130 °C, in order to obtain compact samples of polyethylene for more convenient loading into the reactor

To study the decomposition process, a three-zone furnace with a quartz reactor was used. The inner diameter of the pipe is 6 cm, length 120.7 cm. A study was made of the effect of temperature on the decomposition of polyethylene. The process of decomposition of polyethylene waste in the temperature range from 200 to 550 °C was investigated. Gaseous and vaporous products of thermal degradation of polyethylene were condensed on a cellulose filter with a pore size of 2-3 $\mu m$and subjected to IR analysis on a Fourier IR spectrometer Spectrum 65.

The synthesis of carbon nanotubes was carried out by thermal destruction of polyethylene waste. The synthesis of carbon nanotubes was carried out in a three-zone CVD reactor. A quartz cuvette with polyethylene samples weighing 4 g was installed in the first zone of the reactor. $P'_{100/500}$cenospherereswere used as the basis for the catalyst for the synthesis of CNTs. To prepare the catalysts, 10 g of cenospherereswere impregnated with an aqueous solution of iron nitrate nonahydrate with a concentration of 100 g/l. Further, the catalyst samples were dried at a temperature of 70 °C for 2-3 hours until the moisture was completely removed. Quartz cuvettes with a 1 g sample of catalyst were installed in the 3rd zone of the furnace. The temperatures in the second and third zones of the furnace were set at 700 and 800 °C, respectively. Nitrogen (99.9%) with a flow rate of 530-540 cm^3/min was used as a transport gas. Synthesis time 30 min. Samples of carbon nanotubes were studied by scanning microscopy (Quanta 200i 3D B JEOL, JSM-6490LA) and Raman spectroscopy (NT-MDT NTegra Spectra), which allowed to evaluate the morphology and structure of the obtained CNT.

RESULTS AND DISCUSSIONS

It was experimentally determined that at a temperature of 200 °C thermal degradation of polyethylene waste does not occur, only a slight sintering of the samples is observed. At a temperature of 300-400 °C, a slight destruction of the sample is observed, however, this temperature is not enough for the complete destruction of polyethylene waste. Thus, it was experimentally determined that the destruction of polyethylene samples proceeds from a temperature of 450 °C. Thermal decomposition of polyethylene waste occurs with the release of white smoke with a specific odor

Figure 1 shows the IR spectrum of the thermal decomposition products of polyethylene at a temperature of 450, 500, 550 °C.

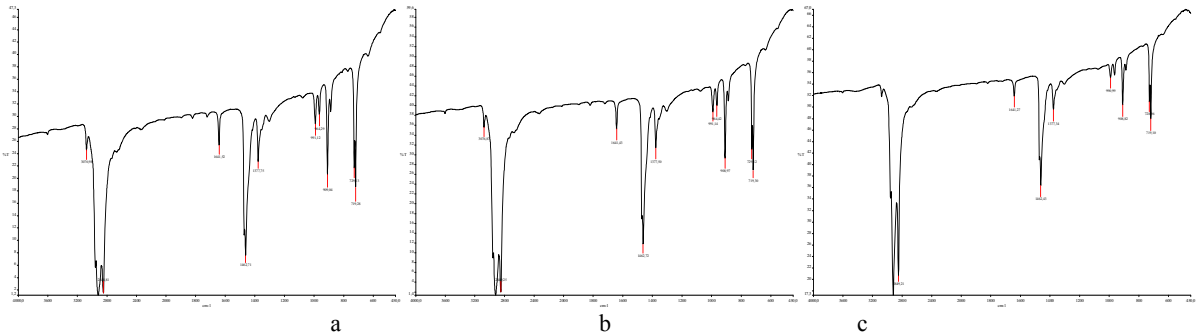

Figure 1 - IR spectra of decomposition of products of polyethylene wastes at various temperatures: a) 450 °C;b) 500 °C; c) 550 °C

Infrared spectroscopy is one of the main methods for identifying organic materials. This is possible due to the different nature of the interaction of infrared radiation with chemical bonds and functional groups of the analyte.

Comparing the spectra presented,it should immediately be noted that all of the peaks described below are most pronounced for the pyrolysis products at 450 °C, and their presence gradually decreases with increasing temperature. So, a weak peak at a frequency of 3077 cm^{-1} corresponds to the stretching vibrations of the C-H bond present in aromatic compounds.

Peaks corresponding to a frequency of 1641 cm^{-1} characterize a double carbon – carbon bond and most likely signal the presence of alkenes in the pyrolysis products. There is other evidence of alkenes in this spectrum. So, at frequencies of 964 and 991 cm^{-1} distinct peaks were observed, corresponding to the vinyl group in trans-disubstituted alkenes and monosubstituted alkenes, respectively.

The well-structured adsorption peak at 1462 cm^{-1} seems to characterize the presence of $-CH_2$ groups.

Vibrations of C-O bonds observed at 909 cm^{-1} indicate the presence of spirits, esters and carboxylic acids. The presence of carboxylic acids is also evidenced by the band clearly pronounced in all spectra at 1377 cm^{-1}.

The bending vibrations of the C-H bonds correspond to the peaks at 729 cm^{-1} and 719 cm^{-1}, which correspond to aromatic compounds, in particular, a monosubstituted benzene ring and a phenyl group.

A group of peaks is also observing, the severity of which increases with increasing pyrolysis temperature, and with decreasing temperature the peak intensity decreases. Thus, in the range of 2915–2940 cm^{-1}, peaks corresponding to aliphatic C-H bonds are observed in all three spectra, and vibrations at a frequency of 2849 cm^{-1} correspond to symmetric methyl groups. Thus,these peaks correspond to the presence of alkanes in the samples.

Thus, the treatment of polyethylene waste at low temperatures contributes to a more noticeable presence of unsaturated compounds, alkenes, aromatics, and oxygen-containing compounds in the pyrolysis products. An increase in temperature during the pyrolysis of polyethylene in turn contributes to an increase in the formation of alkanes.

The results of IR analysis showed that there was no significant difference in the mechanism and products of the decomposition of polyethylene wastes in the temperature range 450-550 °C, thus, for the synthesis of CNTs, the decomposition temperature of polyethylene was 450 °C.

As indicated earlier, the catalyst matrix was $P'_{100/500}$cenospheres (P'-factory marking of cenospheres, 100/500 - cenosphere sizes from 100 to 500 μm) obtained by the flotation method from ash and slag waste of thermal power plants during coal combustion. Images of optical and electron microscopy of cenospheres are presented in Figure 2.

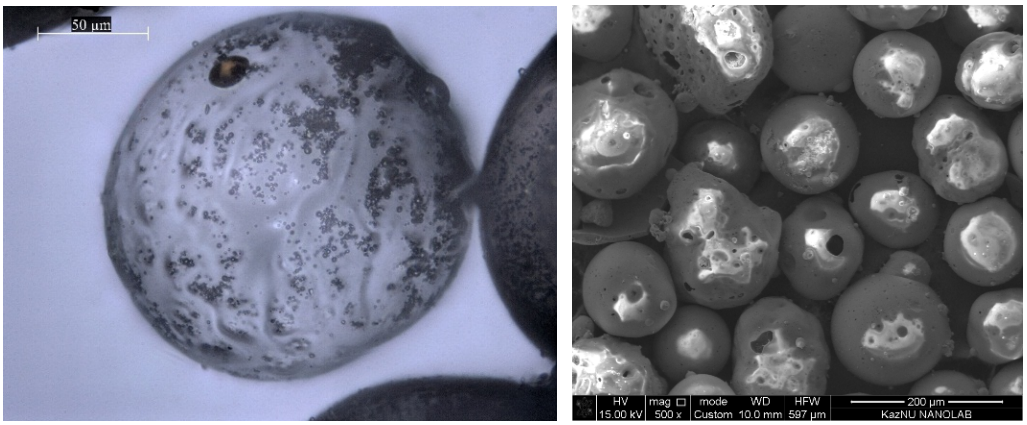

Figure 2 - Micrographs of cenospheres

The cenospheres used as the catalyst matrix are hollow spherical structures. The sizes of the spheres vary from 100 to 500 μm. The composition of the cenospheres: SiO_2 - 58-68%, Al_2O_3 - 32-38%, Fe_2O_3 - 1.4-2%, CaO - 1.9%, MgO - 1%, K_2O + Na_2O - not more than 1.5%. The melting temperature of the cenospheres is 1350-1500 °C. The wall thickness from the diameter of the microspheres is 5-10%.

Figure 3 a,b shows SEM images of the surface of cenospheres coated with CNT.

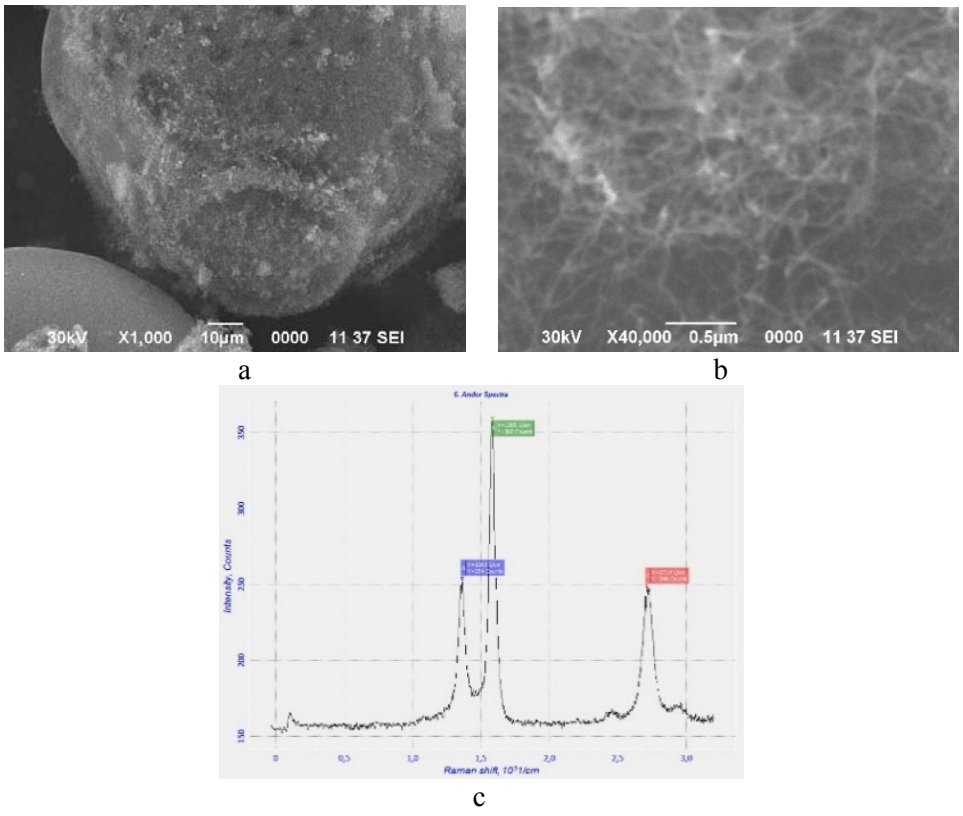

Figure 3 – a, b) SEM images of the surface of cenospheres coated with CNT; c) Raman-spectra of synthesized CNTs

Analysis of SEM images of samples, obtained from polyethylene wastes at a decomposition temperature of 450 °C on a Fe@P'$_{100/500}$ catalyst, shows that in result of synthesis high-quality carbon nanotubes are forming, and completely turbostratic carbon is completely absent. Nanotubes have a diameter of 15 to 28 nm. The Raman spectrum (Fig. 3c) shows a high degree of graphitization and low defectiveness of the obtained CNTs.

CONCLUSION

Based on obtained results, a methodology for processing polyethylene wastes (PET marking) to produce carbon nanotubes is proposed. It was experimentally determined that the optimal temperature of polyethylene decomposition for the synthesis of CNTs is 450 °C. Thus, on the Fe@P'$_{100/500}$ catalyst (cenospheres with Fe $(NO_3)_2 \cdot 9H_2O$) at a synthesis temperature of 800 °C and a synthesis time of 30 min, carbon nanotubes with a diameter of 15-28 nm are formed on the surface of the cenospheres, and turbostratic carbon is completely absent. The results of Raman spectroscopy also confirm the high degree of graphitization of obtained one-dimensional carbon structures, which makes them perceptive for further practical applications.

ACKNOWLEDGMENT

The work was carried out as part of the project «Production of carbon nanotubes in a fluidized catalyst bed reactor and their application in electric-energy systems» (AP05135539) grant financing of the Ministry of Education and Science of the Republic of Kazakhstan.

ӘОЖ: 661.669
ХҒТАК:31.23.15; 61.51.21; 87.53.13

Г.Т. Смагулова[1,2], П. Харрис[3], З.А. Мансуров[1,2]

[1]Жану проблемалары институты, Алматы, Қазақстан;
[2]әл-Фараби атындағы Қазақ ұлттық университеті, Алматы, Қазақстан;
[3]Рединг университеті, Рединг, Беркшир, Ұлыбритания

КӨМІРТЕК НАНОТҮТІКШЕЛЕДІ ӨНДІРУ ҮШІН ПОЛИТЕТИЛЕН ҚАЛДЫҚТАРЫН ӨҢДЕУ

Аннотация. Мақалада тұрмыстық полиэтилен қалдықтарын химиялық будың тұндыруымен көміртекті нанотүтікшелерді синтездеу үшін термиялық тозу арқылы өңдеу нәтижелері келтірілген. Жұмыстың ерекшелігі – полиэтилен үлгілерінің ыдырауы және көміртекті нанотүтікшелердің синтезі бір сатыда жүргізілуі болып саналады. 200-550 °С температура диапазонында полиэтилен қалдықтарының ыдырау өнімдеріне температураның әсері зерттелді. Тіпті 450 °С температурада да полиэтиленнің ыдырауы көміртекті нанотүтікшелерді қалыптастыру үшін жеткілікті болатындығы анықталды. КНТ өсуінің катализаторы ретінде көмірді жағу кезінде жылу электр станцияларының күл мен шлак қалдықтарынан алынған ценосфера болды. Ценосфераның негізгі компоненттері – кремний және алюминий оксидтері. Катализатордың белсенді фазасы темір нитраты болды, ол ценосфера бетінде темір кластерлерінің пайда болуының алғышарты болып табылады. Полиэтилен қалдықтарының ыдырауы және көміртекті нанотүтікшелер синтезі азот атмосферасындағы құбырлы CVD реакторында бір сатылы жүргізілді. КНТ синтезінің температурасы 800 °С құрайды. Синтез нәтижесінде диаметрі 15-28 нм болатын көміртекті нанотүтікшелер пайда болады, бұл СЭМ анализі және Раман спектроскопиясының нәтижелерімен расталады. Зерттеулер негізінде авторлар жоғары сапалы УНТ синтезі үшін полиэтилен қалдықтарын өңдеу әдісін ұсынды.

Түйін сөздер: көміртекті нанотүтікшелер, полиэтилен қалдықтары, ИК-спектроскопия, электронды микроскопия.

УДК: 661.669
МРНТИ:31.23.15; 61.51.21; 87.53.13

Г.Т. Смагулова[1,2], П. Харрис[3], З.А. Мансуров[1,2]

[1]Институт проблем горения, Алматы, Казахстан;
[2]Казахский национальный университет им. аль-ФарабиАлматы, Казахстан;
[3]Университет Рединга, Рединг, Беркшир, Великобритания

ПЕРЕРАБОТКА БЫТОВЫХ ПОЛИЭТИЛЕНОВЫХ ОТХОДОВ ДЛЯ ПОЛУЧЕНИЯ УГЛЕРОДНЫХ НАНОТРУБОК

Аннотация. В статье представлены результаты переработки бытовых полиэтиленовых отходов путем термической деструкциидля синтеза углеродных нанотрубок методом химического парофазного осаждения. Особенностью работы является то, что процесс разложения полиэтиленовых образцов и синтез углеродных нанотрубок проводили в одну стадию. Было исследовано влияние температуры на продукты разложения полиэтиленовых отходов в интервале температур 200-550 °С. Установлено, что уже при температуре 450 °С разложение полиэтилена идет в достаточной степени для формирования углеродных нанотрубок. Катализаторомроста УНТ служили ценосферы, полученные из золо-шлаковых отходов ТЭЦ при сжигании угля. Основными компонентами ценосфер являются оксиды кремния и алюминия. Активной фазой катализатора служил нитрата железа, являющийся предшественником формирования кластеров железа на поверхности ценосфер. Разложение полиэтиленовых отходов и синтез углеродных нанотрубок проводили одностадийно в трубчатом CVD-реакторе в среде азота. Температура синтеза УНТ составляет 800 °С. В результате синтеза, на поверхности ценосфер формируются углеродные нанотрубки с диаметром 15-28 нм, что подтверждается результатами СЭМ-анализа и Раман-спектроскопии.На основании проведенных исследований, авторами предложен метод переработки полиэтиленовых отходов длясинтеза УНТ высокого качества.

Ключевые слова: углеродные нанотрубки, полиэтиленовые отходы, ИК-спектроскопия, электронная микроскопия

Information about authors:

Smagulova G.T. - Doctor PhD,Senior lecturer of the Department of Chemical Physics and Materials Science, Faculty of Chemistry and Chemical Technology, Al-Farabi Kazakh National University; Head of the Laboratory of Functional Nanomaterials, Institute of Combustion Problems, Almaty, Kazakhstan. https://orcid.org/0000-0002-2943-5222

Peter J.F. Harris – Professor, Technical Head of EMLab Research Facility, Technical Head of EMLab Research Facility, member of the Royal Society of Chemistry,Editorial Advisory Board of Carbon and the Editorial Board of "C". https://orcid.org/0000-0003-1598-9686

Mansurov Z.A.- Councilor of the General Directorof the Institute of Combustion Problems, Professor of Al-Farabi Kazakh National University, Editorial-in-Chief of Eurasian Chemico-Technological Journal. https://orcid.org/0000-0002-8956-216X

REFERENCES

[1]Informationontheresultsoftheanalysisofthestateanddevelopmentofthepolymerproductionindustryofthe Member States of the Eurasian Economic Union. Department of Industrial Policy. Eurasian Economic Commission. Moscow, Russia, 2015.53 p. http://www.eurasiancommission.org (In Russian)

[2] Roland G, Jenna RJ, Kara LL. (2017) Production, use, and fate of all plastics ever made, Science Advances, 3(7):5. DOI: 10.1126/sciadv.1700782 (InEng)

[3]An Introduction to Plastic Recycling 2016. Plastic Waste Management Institute Tokyo, Japan 33 p. (InEng)

[4]ZhuoCh, Levendis YA. (2014) Upcycling waste plastics into carbon nanomaterials: a review, Journal applied polymer science, 131(4):14. DOI: 10.1002/app.39931 (InEng)

[5] El Essawy NA, Konsowa AH, Elnouby M, Farag HA. (2017) A novel one-step synthesis for carbon-based nanomaterials from polyethylene terephthalate (PET) bottles waste, Journal of the Air & Waste Management Association, 67(3):358-370. DOI: 10.1080/10962247.2016.1242517 (InEng)

[6]Yangfan Z, Haijun Z, Shengtao G, Jianbo S, Junkai W, Shaowei Z. (2018) Synthesis of carbon nanotube arrays with high aspect ratio via ni-catalyzed pyrolysis of waste polyethylene, Nanomaterials, 8(7):16. DOI:10.3390/nano8070556 (In Eng)

[7]Prikhod′ko NG, Smagulova GT, Rakhymzhan N, Kim S, Lesbaev BT, Nazhipkyzy M, Mansurov ZA. (2017) Comparative investigation of the efficiency of absorption of solar energy by carbon composite materials, Journal of Engineering Physics and Thermophysics, 90(1):117-125. DOI: 10.1007/s10891-017-1546-5. (In Eng)

[8] Smagulova GT, Prikhod′ko NG, Zakhidov AA, Mansurov ZA. (2015) Proceedings of the NAS RK (Series of Chemistry and Technology) [Izvestiya NAN RK (Seriyahimiiitehnologii)] 410(2):29-34. (In Russian)

[9] Kudaybergenov K, Nyssanbayeva G, Ongarbayev Ye, Mansurov Z, Di CapuaR, AlfeM, Gargiulo V. (2019)Sorption ability of modified nano-carbon materials, News of the national academy of sciences of the republic of Kazakhstan. Series chemistry and technology, 3(425):63-70. https://doi.org/10.32014/2019.2518-1491.31

[10] JadhavAS,Mohanraj GT, MayadeviS,GokarnAN. (2018) Rapid method for determinationof nano surface area of arecanut shell derivedactivated carbon by iodine adsorption number, News of the national academy of sciences of the republic of Kazakhstan. Series chemistry and technology, 6(432): 53-56. https://doi.org/10.32014/2018.2518-1491.26

N E W S
OF THE NATIONAL ACADEMY OF SCIENCES OF THE REPUBLIC OF KAZAKHSTAN
SERIES CHEMISTRY AND TECHNOLOGY
ISSN 2224-5286 **https://doi.org/10.32014/2019.2518-1491.68**
Volume 6, Number 438 (2019), 12 – 20

UDC 669.2; 669.85./86; 669.849; 669.864; 546.63

N.S. Ivanov, N.M. Shokobayev, I.Y.Adelbayev, A.Z.Abilmagzhanov, A.E. Nurtazina

JSC "Institute of Fuel, Catalysis and Electrochemistry named after D.V. Sokolsky",
Almaty, Republic of Kazakhstan
E-mail: xumuk777@mail.ru, nurlan.shokobayev@flsmidth.com, clerikc88@mail.ru,
a.abilmagzhanov@ifce.kz, nurtazina.aizhan@bk.ru

INVESTIGATIONOF CONCENTRATION METHOD OF SCANDIUM-CONTAINING SOLUTIONS

Abstract. In current times, enterprises in Kazakhstan that extract uranium by in-situ leaching (ISL) method do not simultaneously recover valuable components. Cardinal problems in this area are the issues of reserves estimation and the availability of effective technology that allows for cost-effective operations. The peculiarities of processing solutions of ISL uranium should also include extremely low contents of valuable components and a complex chemical composition. To solve some of these problems, the authors are working on the development and optimization of technological solutions.

This article presents studies results of further concentration and purification of scandium strippants of the first operations of scandium sorption from uranium sorption filtrates of the ISL cycle. Concentration effect of sodium carbonate on the kinetics and desorption efficiency of scandium from the resin was studied using the example of SE-DEHPA resin under static conditions. Solution's pH influence on second stage operation of sorption on SE-DEHPA resin under static conditions is recognized, and the possibility of subsequent carbonate desorption of scandium was investigated.

As a result of the laboratory studies, a basic technological scheme of scandium associated extraction was developed within the framework of the ISL uranium cycle and the main technological parameters and modes were determined that formed the basis of the basic technical and economic assessment.

Key words: scandium, sorption, desorption, extraction, degree of extraction, exchange capacity, filtrate.

Introduction. Scandium is a rare element and a very expensive metal due to the complex metallurgical processes of its extraction, purification and reduction. General application of scandium oxide is solid oxide fuel cells production. Scandium consumption in light sources production, in nuclear energy, medicine, in the production of refractory materials, phosphors is promising. However, the active use of scandium unique properties is currently constrained by the high cost of its production [1-3].

Due to its low content, scandium is typically recovered as a by-product in the processing of aluminum and rare metal materials. Currently, hydrometallurgical processes, which are mainly associated with leaching, liquid extraction and precipitation, are usually used to extract scandium. One of the major scandium sources is uranium ores, during the processing of which using sulfuric or nitric acid scandium is extracted together with uranium and transferred to leaching solutions. The next time uranium is cleaned, the scandium is separated. When processing uranium-containing leaching solutions, extraction and sorption methods are most often used to extract scandium [4-13].

Separation and purification of scandium is carried out using acidic, alkaline, neutral and chelating extractants. A promising area of extraction chemistry is the use of binary extractants, characterized by high separation and distribution coefficients, a high extraction rate, as well as ease of re-extraction and reagent consumption reduction.Among extractants, the most selective with respect to scandium is di-2-ethylhexylphosphoric acid (DEHPA) [14-22].

The aim of this work is to develop a highly efficient, economically acceptable technology for scandium associated extraction from uranium sorption filtrates.

Experimental procedure

*Consumables.*In our previous investigations, we determined the effectiveness of a binary extractant prepared on the basis of di-(2-ethylhexyl) phosphoric acid (DEHPA) for scandium extraction from uranium sorption filtrates and established the main approaches to desorption.This article discusses the technological issues of further concentration and purification of scandium strippants of the first and second sorption operations.

Table 1 presents the characteristics of DEHPA sorbent used in the work, which underwent preliminary thorough conditioning.

Table1 – Characteristics of the used sorbent DEHPA

Ionite	Functional group	Matrix	Granules size in the air-dry state, mm
SE- DEHPA	$C_{16}H_{35}PO_4$	macroporous, cross-linked polystyrene	0.63÷2.50

Scandium sorption in static conditions.Taking into account the extremely low concentrations of the target components, it is advisable to use a large solution: sorbent phase ratio (L:S) for studies under static conditions.Static sorption was made in a container with a volume of 5 dm^3 using a mixing device with a ratio of L:S 1000:1 (5 dm^3:5 g).Experiment duration was 24 hours. Samples for analysis were taken at certain time intervals without interrupting the experiment. The change in system volume as a result of sampling did not exceed 5%.

The values of the static exchange capacity of the ion exchanger was calculated by the formula:

$$SEC = \frac{C_0 - C_p}{C_0} \cdot \frac{V}{m}, \quad (1)$$

whereC_0andC_p – initial and equilibrium concentrations of the adsorbed component, mg/dm^3 or mmol/dm^3; V – volume of solution, dm^3; m – weight of resin, g.

*Scandium sorption I from a model solution.*Research of the first stage of scandium sorption was carried out on a model solution simulating real solutions composition of the “Irkol” mine.

The composition of model solution with a volume of 60 dm^3 and a scandium concentration of 0.15 mg/dm^3:

- 4.602 mg of scandium oxide Sc_2O_3 with a purity of 99.9%;
- an aqueous solution of sulfuric acid (60%) of "chemical pure" grade 94.6.

Scandium oxide dissolution was done in a hot sulfuric acid solution at a temperature of 80°C for 0.5 hours.

The process of scandium sorption on DEHPA resin in a static mode was conducted research on a laboratory shaker LOIP LS110 at a rotation speed of 190 rpm at room temperature.

ScandiumsorptionIIfromstrippant stage I. Kinetic studies of second stage process of sorption at different pH were carried out in a model solution with a concentration of scandium of 15.81 mg / dm3 simulating stage I strippant.Solution preparation included the dissolution of a selected sample of scandium oxide (99.9%) weighing 0.0153g in 1 cm^3 of concentrated sulfuric acid, followed by dilution of the solution to 1 dm^3.The resulting solution was divided into 5 equal portions of 200 cm^3, which underwent a pH adjustment to the desired value.Solution pH was adjusted to the acidic side with sulfuric acid and alkaline - with sodium carbonate.At sodium carbonate concentration of 200 g/dm^3, the pH was 10.73, while the resin formed large pieces with a diameter of 0.5-1.0 cm, which subsequently stuck together into one large agglomerate.

Studies were carried out at pH values of solutions 1,3,5,10,13.

The process of scandium secondary sorption from the strippant of stage I on resins in the static mode was taken on a laboratory shaker LOIP LS110 at a rotation speed of 190 rpm at room temperature.

*Scandium desorption from saturated DEHPA resin under static conditions.*The processes of primary and secondary desorption of scandium were carried out under static conditions using various concentrations of Na_2CO_3 sodium carbonate desorbing solution:100, 150, 200 and 250 g/dm^3.

In desorption study, the ratio L:S=50:1 (250 cm^3:5 g) was used with a duration of 12 hours.The change in system volume as a result of sampling also did not exceed 5%.

The element content in the resin was calculated based on the material balance taking into account element concentration in the initial solution.

The scandium content in liquid and solid samples was analyzed using plasma atomic emission spectroscopy (Optima 8300 DV, PerkinElmer, LLC).

Resultsanddiscussion

As a result of scandium sorption I from model solutions on DEHPA resin, saturation was established (table2).

Table2 – Results of scandium sorption under static conditions from model solutions on DEHPA resin

Numberofresin'saliquot	Initial Sc concentration, mg/dm^3	Final Sc concentration, mg/dm^3	Estimated Sc concentration on resin, kg/m^3
1	0.12	0.0015	0.118
2	0.12	0.0012	0.119
3	0.12	0.0015	0.118
4	0.12	0.00095	0.119

Scandium I was desorbed from saturated DEHPA resin using a sodium carbonate Na_2CO_3 stripping solution of various concentrations: 100, 150, 200 and 250 g/dm^3 (table3, figure 1).

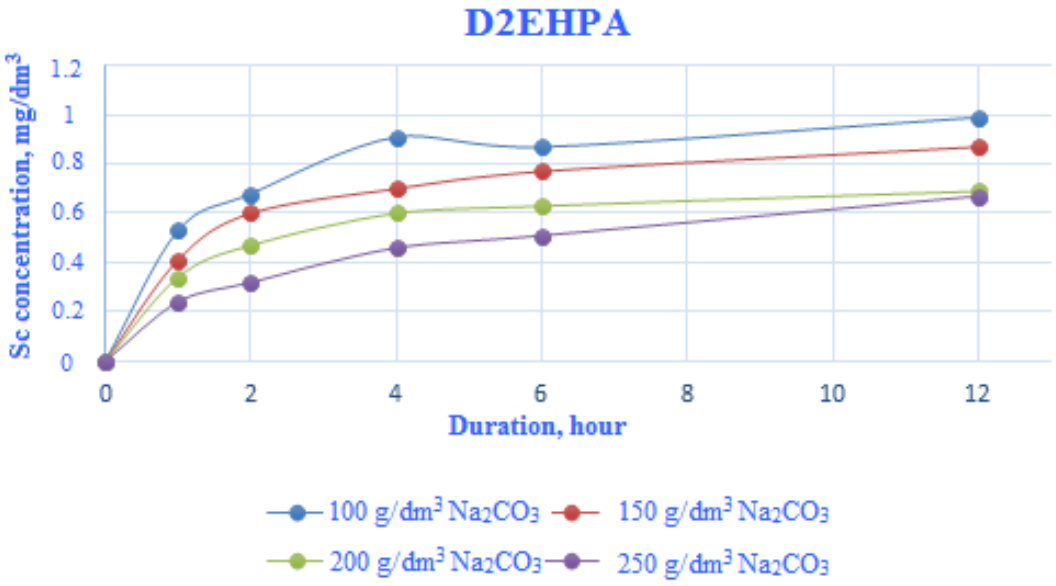

Figure 1 – Scandium desorption I kinetic curves at various concentrations of Na_2CO_3.

Table3 – Researc findings of the kinetics of scandium desorption I at various concentrations of a desorbing agent

Duration	Initial Sc content in DEHPA resin, kg/m^3			
	0.118	0.119	0.118	0.119
	Scandium concentration in solution, mg/dm^3			
	100 g/dm^3 Na_2CO_3	150 g/dm^3 Na_2CO_3	200 g/dm^3 Na_2CO_3	250 g/dm^3 Na_2CO_3
1 hour	0.53	0.41	0.34	0.24
2 hours	0.68	0.60	0.47	0.32
4 hours	0.91	0.70	0.60	0.46
6 hours	0.87	0.77	0.63	0.51
12 hours	0.99	0.87	0.69	0.67
Extraction, %	33.56%	29.24%	23.39%	22.52%

It is seen from table 3, the obtained degree of scandium extraction determined in the static mode, is low and is at the level of 30%, which is probably due to the significant affinity of scandium to the resin and laboratory scale of the tests.The most optimal concentration of a stripping solution providing this extraction degree is 100 g/dm^{3}of Na_2CO_3.

During the second stage of scandium sorption from the strippant of stage I, pH influence of the solution on the kinetic sorption properties of the DEHPA resin was determined. The composition and preparing method of model solutions are described above. The results of testing the operation of scandium sorption II are shown in table 4 and in figure 2.

Table 4 – The results of scandium sorption II kinetics studies with DEHPA resin at various pH solutions

Duration	Scandium concentration in solution, mg/dm^3				
	pH 1	pH 3	pH 5	pH 10	pH 13
1 hour	0.012	0.0012	0.66	7.94	9.42
2 hours	0.020	0.0022	0.95	7.79	8.69
4 hours	0.0072	0.0053	0.79	6.46	10.54
6 hours	0.0037	0.0014	0.56	7.01	10.15
12 hours	<0.00003	<0.00003	0.054	8.01	10.03
24 hours	0.00048	<0.00003	0.0011	7.76	10.05
Extraction, %	100.00%	100.00%	99.99%	50.92%	36.43%
Sc content in resin, kg/m^3	0.474	0.474	0.468	0.400	0.377

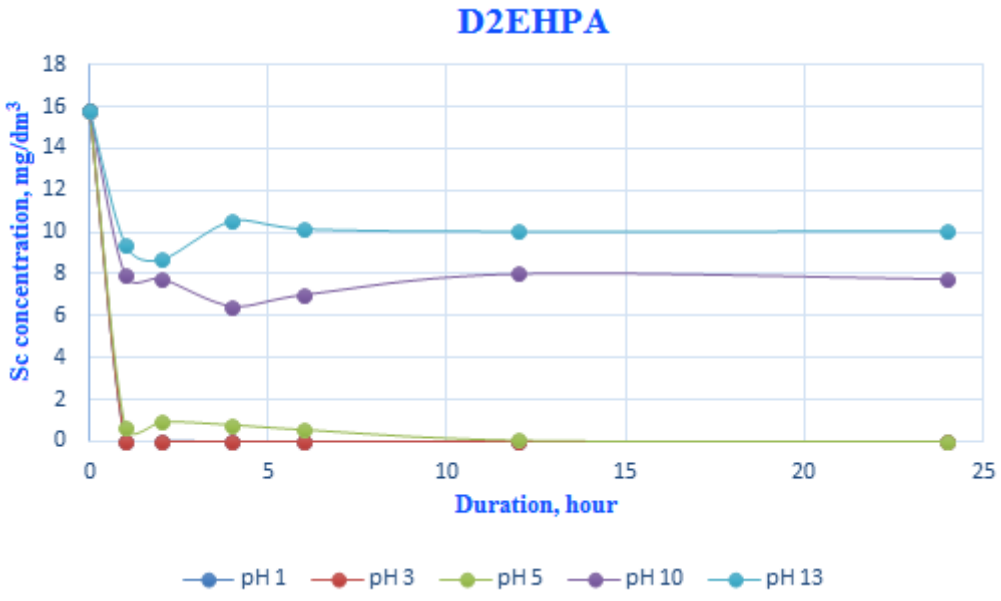

Figure 2 – Kinetic curves of scandium sorption II with DEHPA resin at various pH of the solution

As can be seen from table 4, when the pH of the solution is 5, there is a decrease in the sorption properties of the DEHPA resin and with a further increase in the pH of the solution, the capacity of the resin decreases significantly (up to 70% of the capacity in an acidic environment), which is due to the type of ion-exchange groups.

Studies results confirm the feasibility of carrying out the first operation of solutions desorption using 100 g/dm^3 Na_2CO_3, since in the future, a minimum amount of deoxidizing agent will be required to bring the pH of stage I strippants to 2-3. This solution will allow for efficient sorption extraction in the second stage with the lowest operating cost.

DEHPA resin obtained as a result of scandium sorption II was desorbed in a static mode using 100 g/dm^3 Na_2CO_3. The results of testing scandium desorption operation II are shown in table 5 and figure 3.

Table 5 - Results of kinetics studies of scandium desorption II at 100 g/dm^3 Na_2CO_3

Duration	Scandium concentration in solution, mg/dm^3				
	Resin from pH 1	Resin frompH 3	Resin frompH 5	Resin frompH 10	Resin frompH 13
The initial content of Sc in the resin, kg/m^3	0.474	0.474	0.468	0.400	0.377
1 hour	0.65	1.20	2.03	0.18	0.11
2 hours	1.24	1.47	1.85	0.25	0.11
4 hours	1.90	2.33	2.73	0.30	0.098
6 hours	2.50	2.54	2.41	0.35	0.076
12 hours	3.42	3.09	2.58	0.39	0.1
24 hours	4.99	3.39	3.80	0.42	0.13
Extraction, %	35.66%	25.93%	29.30%	3.89%	1.30%

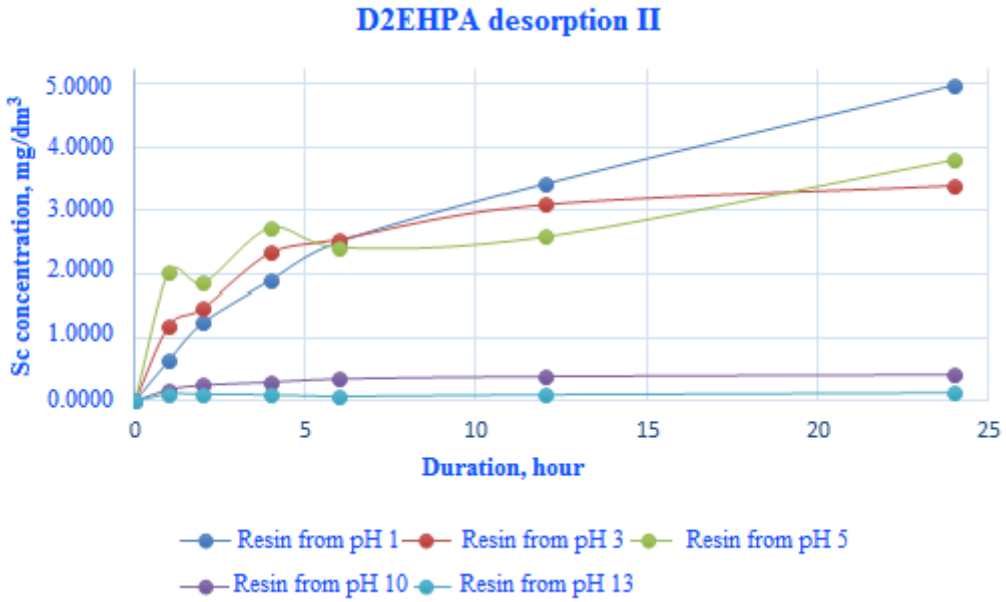

Figure 3 – Kinetic curves of scandium desorption II from DEHPA resin saturated at various pH

As in the case of desorption I, the obtained degree of scandium extraction, determined in static mode, is at the level of 30%, which can be gave a reason by laboratory test scope.It is noteworthy that scandium practically did not desorb from a resin saturated at an alkaline pH.

Derived strippants can be further processed by oxalic acid precipitation.The advantage of this method is scandium precipitation, while calcium (the main impurity element) during oxalic acid deposition remains in solution, which ultimately allows for a cleaner product.

As a result of laboratory studies, a conceptual technological schema was developed for the associated extraction of scandium from uranium sorption filtrates.The main technological parameters and modes, which formed the basis of the base technical and economic assessment, were determined. Indicators given in this assessment are preliminary and cannot be applied directly for project purposes. However, these results will allow giving a sense of feasibility of continuing work in this area.

Considering that the initial and remaining reserves of scandium in the contaminated uranium ore are unknown, at this stage we can assume that scandium equilibrium concentration in solution is 0.22 g/m^3.It makes sense to make an assumption about the feasibility of processing 250 m^3/h of mother liquids for uranium sorption, which is convenient both in hardware design and in terms of minimizing financial risks at an acceptable level of profitability.

The scandium extraction technology is based on sorption I on an impregnated sorbent of the brand SE-DEHPA, carbonate desorption I, neutralization and subsequent sorption II on SE (SE-solid extractant). Desorption II is carried out by sodium carbonate and subsequently scandium oxalate is produced by oxalic deposition in an acidic medium (figure 4).

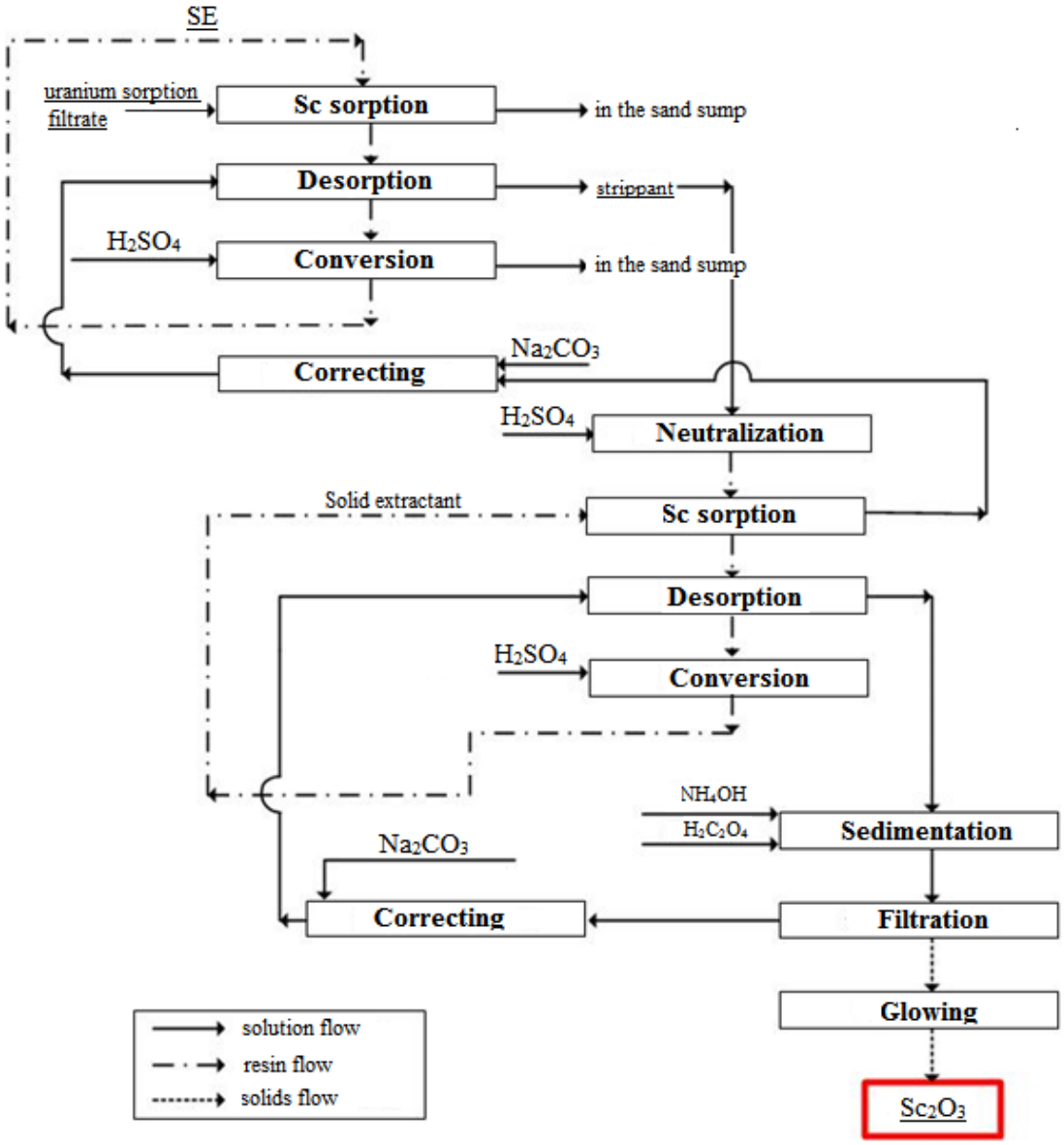

Figure4 – Process flow sheet of scandium extraction from uranium sorption filtrates

The scandium-containing solution (uranium sorption filtrate) is passed through PSC-3m type pressure sorption column filled with SE resin, before the scandium breaks through in the sorption filtrates with a flow of 250 m^3/h.

2 m^3 of scandium-saturated resin is discharged from the column every 24 hours.Sc content in the reloaded resin is 590 g/m^3.Desorption is carried out using sodium carbonate solution with a concentration of 100 g/dm^3 by passing 8 specific volumes of the solution through 2 m^3 of resin in the corresponding column.An extraction degree of 40% sorbed scandium to obtain 16 m^3 of strippant with an average content of 29.7 g/m^3.

The resin is returned to the primary sorption operation. Strippant before subsequent sorption II is deoxidized with sulfuric acid concentrated solution.The conditioned solution is collected in a collection tank and then, with a flow of 0.25 m^3/h, is sent to the sorption of stage II, also carried out on SE in the corresponding column.640 specific volumes (16 m^3) of the stage solution are passed through 0.025 m^3 of the processed resin for 64 hours, after which the scandium content in the resin reaches 18.6 kg/m^3.

At the end of sorption, desorption is carried out in the same column by passing a desorbing solution of 100 g/dm^3 Na_2CO_3.Solution's 8 beats are flowed through 0.025 m^3 of resin with the extraction of at least 50% of the adsorbed scandium.As a result, 0.2 m^3 of solution is formed with an average concentration of 1.13 kg/m^3.The resulting strippant is adjusted in pH to a value of 2÷3 with a solution of ammonia and oxalic acid dihydrate is added.Precipitated sediments are filtered on a nutsche-filter and calcined at a temperature of 900°C to obtain draft quality scandium oxide.

Thus, the productivity of the section will be about 0.214 kg of scandium in 24 hours, or 71.47 kg of scandium per year, which in terms of scandium oxide will be 109.35 kg.

The specified parameters are indicative and require confirmation during conducting semi-industrial tests on real solutions.

Conclusion

Based on the analysis of the obtained experimental data, sorption and desorption processes optimal operating parameters were determined with the simultaneous extraction of scandium from uranium sorption filtrates, which formed the basis of the developed conceptual technological scheme for scandium extraction.A preliminary technical and economic estimate of the process indicates the feasibility of further research on the associated extraction of scandium from real uranium sorption filtrates.

Funding. The research was carried out within the framework of the project AP05133140 "Development and testing of resource-saving technologies for extraction of valuable byproducts during the processing of uranium ores with a comprehensive assessment of its profitability and investment attractiveness" due to scientific projects financing under the of the Scientific Committee of the Ministry of Education and Science of the Republic of Kazakhstan.

УДК 669.2; 669.85./86; 669.849; 669.864; 546.63

Н.С. Иванов, Н.М. Шокобаев, И.Е.Адельбаев,А.З. Абильмагжанов, А.Е. Нуртазина

АҚ "Д.В. Сокольскийатындағыжанармай, катализ және электрохимия институты", Алматы, ҚазақстанРеспубликасы

СКАНДИЙ БАР ЕРІТІНДІЛЕРДІҢ ШОҒЫРЛАНДЫРУ ӘДІСІН ЗЕРТТЕУ

Аннотация. Қазіргі уақытта Қазақстандағы жерастылық ұңғымалық шаймалау әдісімен уран өндіретін кәсіпорындар (ЖҰШ) бір уақытта байланысты компоненттерді шығаруды жүзеге асырмайды. Қорларды бағалау және рентабельдік әрекеттерді жүргізуге мүмкіндік беретін тиімді технология бұл саладағы негізгі мәселелері болып табылады. Уранды ЖҰШ технологиялық ерітінділерінің ерекшеліктеріне пайдалы құрамдастың өте төмен мөлшері және күрделі химиялық құрамы кіруі керек. Осы мәселелердің кейбірін шешу үшін авторлар технологиялық шешімдерді әзірлеу және оңтайландыру бойынша жұмыс жасады.

Бұл мақалада ЖҰШ циклінің уран сорбциялық фильтраттарынан скандий сорбциясының алғашқы операцияларының скандий десорбаттарын әрі қарай шоғырландыру және тазарту зерттеулерінің нәтижелері келтірілген. Статикалық жағдайларда натрий карбонаты концентрациясының кинетикаға әсері және

шайырдан скандийдің десорбциясының тиімділігі ҚЭ-Д2ЭГФҚ шайырының мысалын қолдана отырып зерттелді. Сорбцияның екінші сатысының жұмысына статикалық жағдайда ҚЭ-Д2ЭГФҚ шайырында ерітіндінің pH әсер етуі қарастырылды және де скандийдің кейінгі карбонатты десорбциясы мүмкіндігі зерттелді.

Зертханалық зерттеулердің нәтижесінде ЖҰШ уран циклінің аясында скандийдің ілеспе өндірісінің негізгі технологиялық сызбасы жасалды және негізгі техникалық-экономикалық бағалаудың негізін құрайтын басты технологиялық параметрлер мен режимдер анықталды.

Түйін сөздер: скандий, сорбция, десорбция, экстракция, алудәрежесі, алмасу сыйымдылығы, сүзінді.

УДК 669.2; 669.85./86; 669.849; 669.864; 546.63

Н.С. Иванов, Н.М. Шокобаев, И.Е. Адельбаев, А.З. Абильмагжанов, А.Е. Нуртазина

АО "Институт топлива, катализа и электрохимии им. Д.В. Сокольского", Алматы, Казахстан

ИССЛЕДОВАНИЕ СПОСОБА КОНЦЕНТРИРОВАНИЯ СКАНДИЙСОДЕРЖАЩИХ РАСТВОРОВ

Аннотация. В настоящее время предприятия в Казахстане, добывающие уран методом подземного скважинного выщелачивания (ПСВ), не осуществляют попутное извлечение ценных компонентов. Основными проблемами данного направления являются вопросы подсчета запасов и наличие эффективной технологии, позволяющей вести рентабельную деятельность. К особенностям переработки растворов ПСВ урана следует также отнести крайне низкие содержания ценных компонентов и сложный химический состав. Для решения некоторых из этих проблем авторами ведутся работы по разработке и оптимизации технологических решений.

В данной статье представлены результаты исследований дальнейшего концентрирования и очистки скандиевых десорбатов первой операций сорбции скандия из фильтратов сорбции урана цикла ПСВ. В статических условиях на примере смолы ТВЭКС-Д2ЭГФК изучено влияние концентрации карбоната натрия на кинетику и эффективность десорбции скандия из смолы. Рассмотрено влияние pH раствора на операцию второго этапа сорбции на смоле ТВЭКС-Д2ЭГФК в статических условиях и исследована возможность последующей карбонатной десорбции скандия.

В результате проведенных лабораторных исследований была разработана принципиальная технологическая схема попутного извлечения скандия в рамках цикла ПСВ урана и определены основные технологические параметры и режимы, которые легли в основу базовой технико-экономической оценки.

Ключевые слова: скандий, сорбция, десорбция, экстракция, степень извлечения, обменная емкость, фильтрат.

Informationaboutauthors:

Ivanov Nikolai Sergeevich – Candidate of Chemical Sciences, Leading Researcherin Laboratory of Applied Research, JSC “D.V. Sokolskiy Institute of Fuel, Catalysis and Electrochemistry”,n.ivanov@ifce.kz, https://orcid.org/0000-0002-2153-2802

Shokobayev Nurlan Maratovich – PhD, Junior Researcher in Laboratory of Applied Research, JSC “D.V. Sokolskiy Institute of Fuel, Catalysis and Electrochemistry”, nurlanshokobayev@gmail.com, https://orcid.org/0000-0003-1697-4638

Adelbayev Iskander Yersayanovich – master’s degree, senior engineer in Laboratory of Applied Research of JSC “D.V. Sokolskiy Institute of Fuel, Catalysis and Electrochemistry”, clerikc88@mail.ru, https://orcid.org/0000-0003-1435-8583

Abilmagzhanov Arlan Zainutallaevich – Candidate of Chemical Sciences, head of Applied Research laboratoryof JSC “D.V. Sokolskiy Institute of Fuel, Catalysis and Electrochemistry”, a.abilmagzhanov@ifce.kz, https://orcid.org/0000-0001-8355-8031

Nurtazina Aizhan Erkinbekkyzy – PhD student,master’s degree,senior engineer of Applied Research laboratoryof JSC “D.V. Sokolskiy Institute of Fuel, Catalysis and Electrochemistry”, nurtazina.aizhan@bk.ru, https://orcid.org/0000-0001-7202-5344

REFERENCES

[1] Gupta C.K., Krishnamurthy N. **(2016)** Extractive metallurgy of rare earths, Second edition, ISBN 13:978-1-4665-7638-4 (in Eng).

[2] U.S. Geological Survey **(2017)** Mineral Commodity Summaries. https://minerals.usgs.gov/minerals/pubs/commodity/scandium/mcs-2017-scand.pdf. P. 146–147. (inEng)

[3] YAcenko S.P., Pasechnik L.A. **(2016)** Skandij: nauka i tekhnologiya. Ekaterinburg: Izdatel'stvo Ural. ISBN 978-5-7691-2442-6 (inRussian).

[4] Wang W., Pranolo Y., Cheng C.Y. **(2011)** Metallurgical processes for scandium recovery from various resources.Hydrometallurgy.Volume 108,PP.100-108. https://doi.org/10.1016/j.hydromet.2011.03.001 (in Eng).

[5] Weihua Le., Shengting K., Zhifeng Zh., Guolong Wu., Yanling Li, Chunfa Li., Wuping L. **(2018)** Selective extraction and recovery of scandium from sulfate medium by Cextrant 230. Hydrometallurgy.Volume178, PP.54–59.https://doi.org/10.1016/j.hydromet.2018.04.005 (in Eng).

[6] Yuhua Li, Qinggang Li, Guiqing Zhang, Li Zeng, Zuoying Cao, Wenjuan Guan, Liupei Wang**(2018)** Separation and recovery of scandium and titanium from spent sulfuric acid solution from the titanium dioxide production process.Hydrometallurgy.Volume 178, PP.1-6.https://doi.org/10.1016/j.hydromet.2018.01.019(inEng).

[7] Pirozhenko K.YU. **(2016)** Sorbcionnoe izvlechenie skandiya iz vozvratnyh rastvorov skvazhinnogo podzemnogo vyshchelachivaniya urana: Dis. S.131. (in Russian).

[8] Guanghui *Li*; Qing Ye; Bona Deng; Jun Luo; Mingjun Rao; Zhiwei Peng; Tao Jiang **(2018)** Extraction of scandium from scandium-rich material derived from bauxite ore residues. Hydrometallurgy. Volume 176, PP.62-68.https://doi.org/10.1016/j.hydromet.2018.01.007(in Eng).

[9] Bun'kov G.M. **(2019)** Razrabotka tekhnologii izvlecheniya skandiya iz rastvorov podzemnogo vyshchelachivaniya urana:Dis. S.162. (in Russian).

[10] Guanghui Li, Qing Ye, Bona Deng, Jun Luo, Mingjun Rao, Zhiwei Peng, Tao Jiang. **(2018)** Extraction of scandium from scandium-rich material derived from bauxite ore residues.Hydrometallurgy.Volume 176, PP.62-68.https://doi.org/10.1016/j.hydromet.2018.01.007 (in Eng).

[11] Rodolfo M.R., Brecht U., Ghania O., Koen B., Tom V.G. **(2018)** Extraction of rare earths from bauxite residue (red mud) by dry digestion followed by water leaching. Minerals Engineering. Volume 119, PP.82–92.https://doi.org/10.1016/j.mineng.2018.01.023 (in Eng).

[12] Rodolfo M.R., Buhle X., Ghania O., Koen B., Bernd F., TomV.G. **(2019)** Selective rare earth element extraction using high-pressure acid leaching of slags arising from the smelting of bauxite residue.Hydrometallurgy.Volume 184, PP.162-174.https://doi.org/10.1016/j.hydromet.2019.01.005 (in Eng).

[13] KanggenZh., Chunying T., XuekaiZh., Changhong P., Wei Ch. **(2018)** Enhanced selective leaching of scandium from red mud.Hydrometallurgy.Volume 182, PP.57-63.https://doi.org/10.1016/j.hydromet.2018.10.011 (in Eng).

[14] Huaping N., Yabing W., Yanliang W., ZeyuanZh., Yamin D., Xiaoqi S. **(2017)** Recovery of scandium from leaching solutions of tungsten residue using solvent extraction with Cyanex 572.Hydrometallurgy.Volume 175, PP.117-123.https://doi.org/10.1016/j.hydromet.2017.10.026 (in Eng).

[15] Nghiem V.N., Atsushi I., Etsuro Sh., Takashi N. **(2015)** Study of adsorption behavior of a new synthesized resin containing glycol amic acid group for separation of scandium from aqueous solutions.Hydrometallurgy.Volume 165, PP.51-56.https://doi.org/10.1016/j.hydromet.2015.11.016 (in Eng).

[16] Qing Y., Shunyan N., Wei Zh., Xinpeng W., Yuezhou W. **(2018)** Recovery of scandium from sulfuric acid solution with a macroporous TRPO/SiO_2-P adsorbent.Hydrometallurgy.Volume 181, PP.74-81. https://doi.org/10.1016/j.hydromet.2018.07.025 (in Eng).

[17] Zlobina E.V., Pak L.O. **(2013)**Vestnik KazNU. Seriya himicheskaya. [Bulletin of KazNU.Chemical series] Volume 4, PP.168-176. (in Russian).

[18] P'yae P.A. **(2019)** Sorbciya skandiya iz sernokislyh rastvorov ekstragentsoderzhashchimi materialami: Dis. S.135. (in Russian).

[19] Cherkasov R.A., Garifzyanov A.R., Leont'ev S.V., Davletshin R.R., Koshkin S.A. **(2009)** Extraction of scandium ions by new aminophosphinylextractants. Russ. J. Gen. Chem.Volume 79, PP.2599-2605.https://doi: 10.1134/S107036320912007X(in Eng).

[20] SokolovaY.V. **(2006)**Zhurnal prikladnoj himii [Journal of Applied Chemistry] Volume 79, PP.583-588. (in Russian)

[21] Shokobayev N.M., ZhurinovM.Zh., Zhumabayeva D.S., Ivanov N.S., Abilmagzhanov A.Z.**(2018)** Development of sorption technology of rare-earth metals recovery from uranium in-situ leaching solutions.News of the Academy of Sciences of the Republic of Kazakhstan. Series of geology and technical sciences. Volume 6, Number 432, PP.77-84.https://doi.org/10.32014/2018.2518-170X.37 (in Eng).

[22] Smirnov A.L., Titova S.M., Rychkov V.N., Bunkov G.M., Semenishchev VS, Kirillov EV, Poponin NN, Svirsky IA. **(2017)**Study of scandium and thorium sorption from uranium leach liquors. J. Radioanal. Nucl.Chem. Volume 312, PP.277–283.https://doi.org/10.1007%2Fs10967-017-5234-x (in Eng).

N E W S
OF THE NATIONAL ACADEMY OF SCIENCES OF THE REPUBLIC OF KAZAKHSTAN
SERIES CHEMISTRY AND TECHNOLOGY
ISSN 2224-5286 **https://doi.org/10.32014/2019.2518-1491.69**
Volume 6, Number 438 (2019), 21 – 29

UDC 547.587.11

Zh.B. Satpaeva[1,2], O.A. Nurkenov[2], K.M. Turdybekov[1], L.K. Abulyaissova[1], M.Zh. Burkeev[1], S.D. Fazylov[1,2], S.A. Talipov[3], David Havlicek[4]

[1]Ye.A. Buketov Karaganda State University, Kazakhstan;
[2]Institute of Organic Synthesis and Coal Chemistry of the Republic of Kazakhstan, Karaganda;
[3]A.S. SadykovInstitute of Bioorganic Chemistry of the Academy of Sciences of Republic Uzbekistan, Tashkent, Uzbekistan;
[4]Charles University, Czech Republic
(e-mail: satpaeva_zh@mail.ru, xray-phyto@yandex.kz)

MOLECULAR STRUCTURE AND QUANTUM CHEMICAL CALCULATIONS 4-ETHYL-5-(2-HYDROXYPHENYL)-1,2,4-TRIAZOL-3-THIONE

Abstract. The article is devoted to the study of the spatial structure of 4-ethyl-5-(2-hydroxyphenyl)-1,2,4-triazole-3-thione. The molecular and crystalline structure was determined by x-ray diffraction analysis. Data on the spatial structure and crystal packing of the molecule are presented. It is established that phenyl and triazole rings are flat. Due to hydrogen bonds, the molecules in the crystal form three-dimensional networks. The results of an X-ray diffraction study were deposited at the Cambridge Center for Crystal Structural Data. The structure of the synthesized 1,2,4-triazole was studied by 1H NMR spectroscopy. When analyzing the 1H NMR spectrum of the compound, characteristic signals of the protons of the aromatic ring are observed. The value of the chemical shift and the integrated signal intensity are determined. A quantum chemical study of 4-ethyl-5-(2-hydroxyphenyl)-1,2,4-triazole-3-thione was carried out by the DFT method using the B3LYP exchange-correlation functional in combination with the Danning basic set cc-pVDZ. The molecular characteristics of the compound, such as total electron energy, rotational constants, dipole moment and contributions, and thermodynamic functions, are predicted. The equilibrium geometric parameters of the 4-ethyl-5-(2-hydroxyphenyl)-1,2,4-triazole-3-thione molecule were determined. The performed analysis of the spatial configuration and molecular parameters showed a qualitative correspondence between the crystalline and gas-phase structures of the molecule, while it was noted that the main difference is observed in the relative orientation of six- and five-membered cycles.

Keywords: crystal structure, x-ray diffraction, 1,2,4-triazole, 4-ethyl-5-(2-hydroxyphenyl)-1,2,4-triazole-3-thione, quantum chemical calculations, DFT method, geometric and energy characteristics.

Introduction

Derivatives of 1,2,4-triazole provide great synthetic possibilities for obtaining new effective drugs. A number of 1,2,4-triazole derivatives have been successfully used in medicine as medicines for the treatment of fungal and viral infections, diseases of the cardiovascular system, etc. [1-4]. New derivatives of 1,2,4-triazole are known, which have shown antiviral [5, 6], anti-inflammatory [7, 8], anticonvulsant [9, 10], antitumor [10, 11], antibacterial [12, 13] and other types of activity .Consequently, some of the 1,2,4-triazole derivatives have been approved as drugs, such as anastrazole, letrozole, risatriptan, ribavirin, alprazolam, fluconazole and posaconazole. This leads to intensive studies of both the preparation methods and the properties of the new derivatives of 1,2,4-triazoles.

It is well known that s-triazoles can exist in two tautomeric forms, and most studies have shown that the thion form was dominant in the solid state and in a neutral solution [14–16]. However, there are some studies that describe the presence of a thiol form [17–20].

Nevertheless, it was shown that thiolthionetautomerism plays an important role in several processes related to biological activity, such as proton transfer and hydrogen bonds [21-24].

Currently, X-ray diffraction analysis is one of the most informative, unique and accurate tools for studying the spatial structure of synthesized compounds, which has made a significant and decisive contribution to the study of almost all inorganic and organic classes [25].

Previously, we synthesized a number of 1,2,4-triazoles based on hydrazides of o- and p-hydroxybenzoic acids, which were obtained by interaction with thiosemicarbazides in an aqueous solution of caustic potassium followed by acidification with acetic acid. X-ray diffraction analysis was used to characterize the crystal structure of 4-allyl-3-(4-hydroxyphenyl)-1H-1,2,4-triazole-5(4H)-thione [26-28].In continuation of studies in this direction, we present experimental data on the spatial structure and calculated quantum chemical parameters of 4-ethyl-5-(2-hydroxyphenyl)-1,2,4-triazole-3-thione (1).

Experimentalpart

The NMR^{1}H spectrum was recorded on a Bruker DRX500 spectrometer (500 MHz) in a DMSO-$d_6$solution relative to the internal standard — TMS.

X-ray diffraction analysis of 4-ethyl-5-(2-hydroxyphenyl)-1,2,4-triazole-3-thione (1). Crystals for X-ray diffraction analysis were obtained by double crystallization of compound 1 from 2-propanol.

Cell parameters and intensities of 3461 reflections (1340 independent, R_{int} = 0.0223) were measured on a «Bruker P4»diffractometer (MoK, graphite monochromator, ω scanning, $2.96^o \leq \theta \leq 22.44^o$) at a temperature of 298 K. Monoclinic crystals, a=9.8479(6), b =7.9892(7), c=13.914(1) Å, β=102.616(3)^o, V=1068.3(1) Å^3, Z=4 $C_{14}H_9N_3O_3$, space group $P2_1/c$, $d_{выч}$=1.376 г/см^3,μ = 0.279 мм$^{-1}$. The initial array of the measured intensities was processed and absorption was taken into account using the SAINT and SADABS programs (multi-scan, T_{min} = 0.7072, T_{max} = 0.7448) [29].

The structure is deciphered by the direct method. The positions of non-hydrogen atoms are refined in the anisotropic approximation by full-matrix least squares. Hydrogen atoms of the hydroxyl and amino groups were identified from difference synthesis and their positions were refined in the isotropic approximation, the remaining hydrogen atoms were placed in geometrically calculated positions and their positions were refined in the isotropic approximation with fixed positional and thermal parameters (rider model). In the calculations, 1191 reflections of independent reflections with $I \geq 2\sigma(I)$ were used, the number of refined parameters is 145. Final divergence factors: R_1 0.0301, $_wR_2$ 0.0786(for reflections with $I \geq 2\sigma(I)$), R_1 0.0347, $_wR_2$ 0.0833 (for all reflections), GooF=1.057. Peaks of residual density: Δρ=0.146 and –0.219 *e*/Å3. The structure has been deciphered and refined using the SHELXS [30] and SHELXL-2018/3 [31] programs. PCA data in the form of a CIF file was deposited at the Cambridge Center for Crystal Structural Data (CCDC 1921694).

The quantum chemical calculation for the 4-ethyl-5-(2-hydroxyphenyl)-1,2,4-triazole-3-thione molecule in the gas phase was carried out using the density functional theory method (DFT/B3LYP) [32] using the Gaussian program [33]. In this case, the correlation-consistent Dunning basis set cc-pVDZ was used, which was specially developed to more fully take into account correlation effects.

Resultsanddiscussions

When analyzing the ^{1}H NMR spectrum of compound 1, characteristic signals of the protons of the aromatic ring are observed. So, the signals of the protons of the aromatic ring are recorded at 7.78 ppm. ($J_{H\alpha H\beta}$8.7 Hz), 6.81 ppm ($J_{H\alpha H\beta}$ 8.7 Hz), 7.32 ppm (1H, CH^4_{arom}), 7.02 ppm. (1H, CH^1_{arom}) in the form of doublets, respectively. At 6.95 ppm (1H, CH^2_{arom}), 7.42 ppm. (1H, CH^3_{arom}) signals appear in the form of triplets. In a weak field, signals of protons of aromatic hydroxyl are recorded at 10.33 ppm. and thioamide N-H proton at 13.8 ppm in the form of two small broadened singlets. Signals of methyl group protons resonate at 1.05 ppm. (J_{HH}7.1 Hz) as a triplet and methylene group at 3.85 ppm. (J_{HH}7.2 Hz) as a quartet.

The spatial structure and packaging of the 4-ethyl-5-(2-hydroxyphenyl)-1,2,4-triazole-3-thione molecule (1) are shown in Figures 1 and 2.

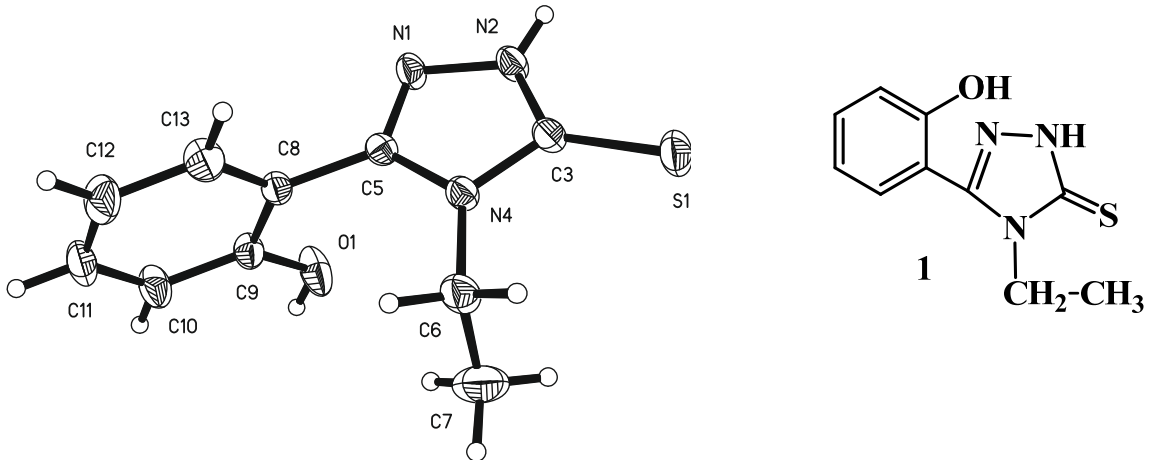

Figure 1 – The molecular structure of the molecule**1**

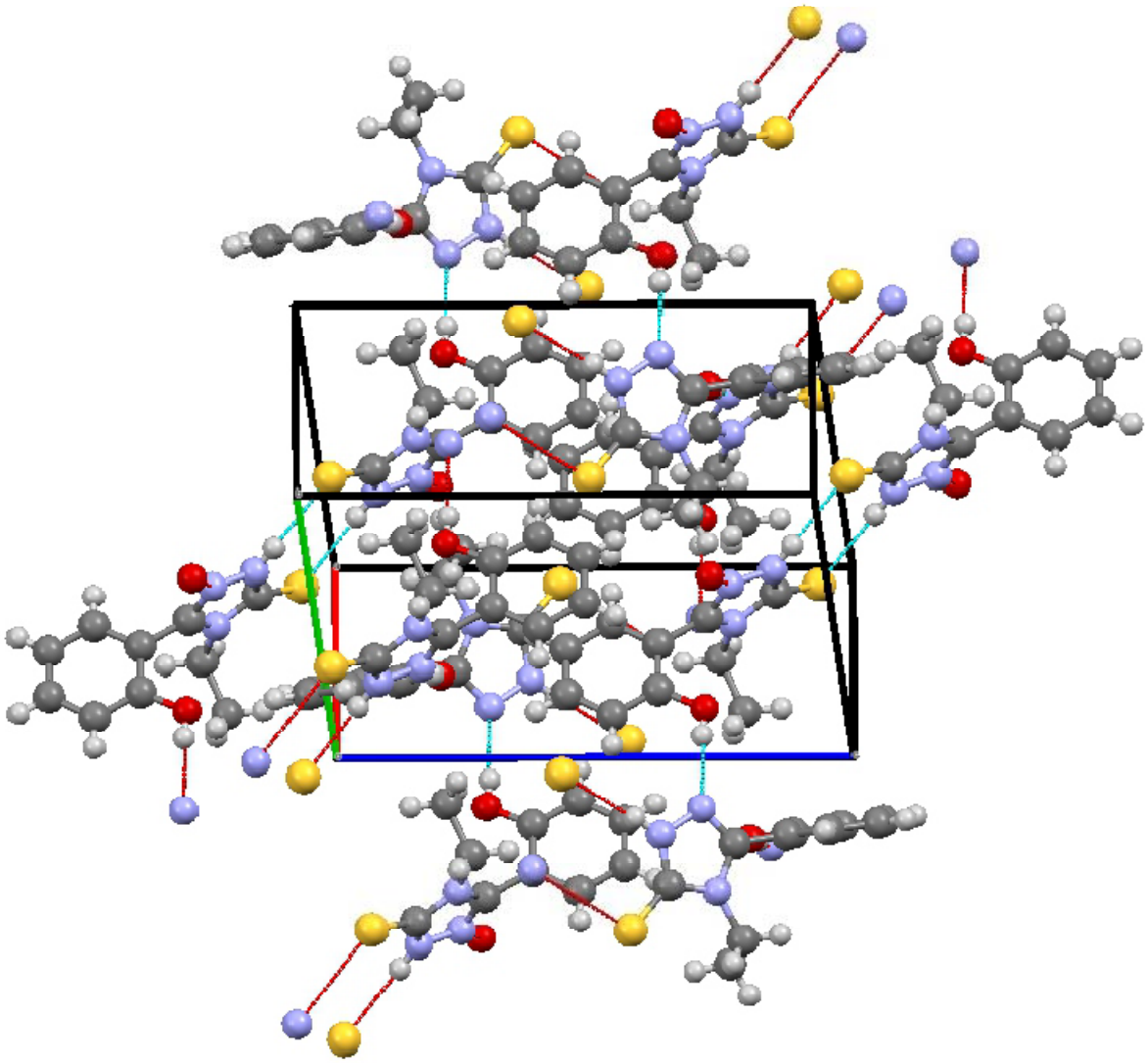

Figure 2 – Packing molecule 1 in the crystal

From the obtained data of X-ray diffraction analysis, it follows that the bond lengths (table 1) and bond angles (table 2) in compounds 1 are close to usual [34]. In molecule 1, the triazole ring is flat; the atoms N1, N2, C3, N4, and C5 are coplanar with an accuracy of ± 0.003 Å. The sulfur atom S1, C6 of the ethyl and C8 phenyl groups slightly leave this plane (by -0.051, 0.053 and -0.035 Å, respectively). The phenyl cycle, flat with an accuracy of ± 0.001 Å, is unfolded relative to the triazole by 85.6°. The O1 atom of the hydroxyl group is practically located in this plane (0.013 Å).

In the crystal, molecules 1 form an intermolecular hydrogen bond N2 H ... S1 (1-x, -y, 1 - z) (distance N ... S 3.299 (2) Å, H ... S 2.44 (2) Å, angle N-H ... S 176 (2)°), linking the triazole moieties of two molecules into dimers. The hydroxyl group forms a hydrogen bond with the N1 atom of another molecule, O1 H ... N1 (1-x, 1/2 - y, 1/2 - z) (distance O ... N 2.853(2) Å, H ... N 2.07(2) E, angle O – H ... N 175(2)°), forming in three-dimensional infinite grids.

A theoretical quantum-chemical approach was used to determine the physicochemical characteristics of 4-ethyl-5-(2-hydroxyphenyl)-1,2,4-triazole-3-thione. In order to find the minimum energy configuration of the molecule in the ground state, the structure is optimized for all independent coordinates. Figure 3 shows an optimized three-dimensional model of the molecule under study (according to quantum chemical calculations). The calculated quantum-chemical structural parameters of the molecule are given (table 1 and table 2) in comparison with the experimental X-ray diffraction data.

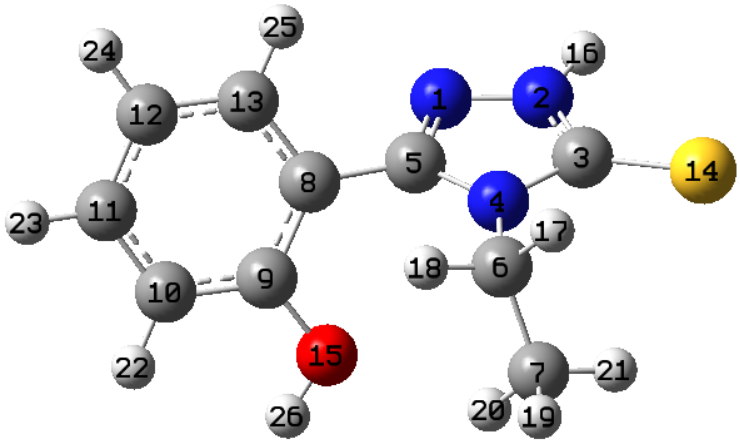

Figure 3 – Optimized Molecule 1 Structure (B3LYP/cc-pVDZ Method)

A comparison of the crystalline and gas-phasestructuresofthemoleculeshowed a qualitativecorrespondencebetweenthem. The main differenceis therelativeorientationofthetwocycles. Inthecrystallinestructure, thetorsionangleis -93.6 °, for a moleculeinthegasphaseitis -54.62 °. Accordingtoquantum-chemicalcalculations, valencebondsbetweenatomsin a gas-phasemoleculearemorestretched (by 0.001-0.106 Å). Onlyfor N(1)-N(2) and N(4)-C(6) areshortenedbondsobserved. Inthecaseof O-H andC-H bonds, thecalculationsgiveclosetostandard (0.96 and 1.09 Å, respectively) values (table 1), while PCA bondsareshorter.

Table 1 - Bond lengths in the molecule of 1

Bond	Length, Å		Angle	Value, deg	
	Exp.	Theor. (B3LYP/cc-pVDZ)		Exp.	Theor. (B3LYP/cc-pVDZ)
S(1)-C(3)	1.6746(19)	1.677	C(3)-N(4)-C(6)	125.18(15)	123.26
O(1)-C(9)	1.358(2)	1.364	C(5)-N(4)-C(6)	126.64(15)	128.39
O(1)-H(01)	0.79(2)	0.969	N(1)-C(5)-N(4)	110.83(15)	111.23
N(1)-C(5)	1.302(2)	1.310	N(1)-C(5)-C(8)	125.76(16)	122.29
N(1)-N(2)	1.378(2)	1.364	N(4)-C(5)-C(8)	123.37(16)	126.32
N(2)-C(3)	1.333(3)	1.362	N(4)-C(6)-C(7)	112.31(17)	113.59

Angle	τ, deg		Angle	τ, deg	
	Exp.	Theor. (B3LYP/cc-pVDZ)		Exp.	Theor. (B3LYP/cc-pVDZ)
N(2)-H(2)	0.87(2)	1.012	N(4)-C(6)-H(6A)	109.1	106.78
C(3)-N(4)	1.371(2)	1.388	C(7)-C(6)-H(6A)	109.1	111.52
N(4)-C(5)	1.375(2)	1.390	N(4)-C(6)-H(6B)	109.1	106.32
N(4)-C(6)	1.468(2)	1.466	C(7)-C(6)-H(6B)	109.1	109.92
C(5)-C(8)	1.477(2)	1.478	H(6A)-C(6)-H(6B)	107.9	108.44
C(6)-C(7)	1.502(3)	1.527	C(6)-C(7)-H(7A)	109.5	110.89
C(6)-H(6A)	0.9700	1.099	C(6)-C(7)-H(7B)	109.5	110.22
C(6)-H(6B)	0.9700	1.101	H(7A)-C(7)-H(7B)	109.5	109.46
C(7)-H(7A)	0.9600	1.098	C(6)-C(7)-H(7C)	109.5	109.15
C(7)-H(7B)	0.9600	1.099	H(7A)-C(7)-H(7C)	109.5	108.77
C(7)-H(7C)	0.9600	1.102	H(7B)-C(7)-H(7C)	109.5	108.29
C(8)-C(13)	1.389(3)	1.404	C(13)-C(8)-C(9)	119.56(17)	118.57
C(8)-C(9)	1.390(3)	1.410	C(13)-C(8)-C(5)	120.09(16)	118.88
C(9)-C(10)	1.383(3)	1.400	C(9)-C(8)-C(5)	120.34(16)	122.45
C(10)-C(11)	1.376(3)	1.396	O(1)-C(9)-C(10)	123.47(17)	122.20
C(10)-H(10)	0.9300	1.094	O(1)-C(9)-C(8)	117.03(16)	117.66
C(11)-C(12)	1.367(3)	1.397	C(10)-C(9)-C(8)	119.50(17)	120.14
C(11)-H(11)	0.9300	1.092	C(11)-C(10)-C(9)	120.15(18)	120.28
C(12)-C(13)	1.382(3)	1.395	C(11)-C(10)-H(10)	119.9	120.34
C(12)-H(12)	0.9300	1.091	C(9)-C(10)-H(10)	119.9	119.37
C(13)-H(13)	0.9300	1.091	C(12)-C(11)-C(10)	120.85(18)	120.25
C(9)-O(1)-H(01)	111.1(16)	109.12	C(12)-C(11)-H(11)	119.6	120.35
C(5)-N(1)-N(2)	104.04(15)	103.95	C(10)-C(11)-H(11)	119.6	119.40
C(3)-N(2)-N(1)	113.35(15)	114.55	C(11)-C(12)-C(13)	119.61(19)	119.36
C(3)-N(2)-H(2)	127.6(14)	124.33	C(11)-C(12)-H(12)	120.2	120.51
N(1)-N(2)-H(2)	118.8(14)	121.11	C(13)-C(12)-H(12)	120.2	120.13
N(2)-C(3)-N(4)	103.64(15)	102.33	C(12)-C(13)-C(8)	120.34(18)	121.40
N(2)-C(3)-S(1)	128.90(14)	128.13	C(12)-C(13)-H(13)	119.8	120.46
N(4)-C(3)-S(1)	127.44(15)	129.51	C(8)-C(13)-H(13)	119.8	118.15
C(3)-N(4)-C(5)	108.13(15)	107.93			

Table 2 - Torsion angles in the molecule of 1

C(5)-N(1)-N(2)-C(3)	-1.0(2)	-0.97	N(1)-C(5)-C(8)-C(13)	-93.6(2)	-54.62
N(1)-N(2)-C(3)-N(4)	0.8(2)	1.46	N(4)-C(5)-C(8)-C(13)	83.8(2)	120.31
N(1)-N(2)-C(3)-S(1)	-177.57(14)	-176.67	N(1)-C(5)-C(8)-C(9)	87.9(2)	121.75
N(2)-C(3)-N(4)-C(5)	-0.29(19)	-1.35	N(4)-C(5)-C(8)-C(9)	-94.7(2)	-63.31
S(1)-C(3)-N(4)-C(5)	178.12(14)	176.75	C(13)-C(8)-C(9)-O(1)	-179.38(18)	177.31
N(2)-C(3)-N(4)-C(6)	177.16(16)	-174.46	C(5)-C(8)-C(9)-O(1)	-0.9(3)	0.93
S(1)-C(3)-N(4)-C(6)	-4.4(3)	3.64	C(13)-C(8)-C(9)-C(10)	0.4(3)	-1.68
N(2)-N(1)-C(5)-N(4)	0.78(19)	0.01	C(5)-C(8)-C(9)-C(10)	178.84(18)	-178.07
N(2)-N(1)-C(5)-C(8)	178.45(16)	175.64	O(1)-C(9)-C(10)-C(11)	179.5(2)	-178.02
C(3)-N(4)-C(5)-N(1)	-0.3(2)	0.88	C(8)-C(9)-C(10)-C(11)	-0.2(3)	0.92
C(6)-N(4)-C(5)-N(1)	-177.73(17)	173.53	C(9)-C(10)-C(11)-C(12)	-0.1(3)	0.20
C(3)-N(4)-C(5)-C(8)	-178.07(16)	-174.52	C(10)-C(11)-C(12)-C(13)	0.3(3)	-0.52
C(6)-N(4)-C(5)-C(8)	4.5(3)	-1.88	C(11)-C(12)-C(13)-C(8)	-0.2(3)	-0.27
C(3)-N(4)-C(6)-C(7)	-88.1(2)	-77.10	C(9)-C(8)-C(13)-C(12)	-0.2(3)	1.37
C(5)-N(4)-C(6)-C(7)	88.8(2)	111.27	C(5)-C(8)-C(13)-C(12)	-178.65(19)	177.89

The deviation of the valence angles from similar experimental ranges from 0.04–3.47°, both in the direction of decreasing and increasing values. For dihedral angles, a larger scatter of values is observed when comparing theoretical and experimental data. Differences in the geometric configuration of the 4-ethyl-5-(2-hydroxyphenyl)-1,2,4-triazole-3-thione molecule in different states of aggregation were expected, because, as you know, the geometry of the molecule in the crystal is determined by packing, in pairs - corresponds to the global minimum of total energy.

Theoretical physico-chemical characteristics, such as total energy, zero-point energy, rotational constants, electric dipole moment and others, are given in table. 3.

Table 3 - Physicochemical parameters of molecule 1 according to calculations by the B3LYP/cc-pVDZ method

Options	B3LYP/ cc-pVDZ
Totalenergy, a.u.	-1025.417093
Rotational Constants, GHz A B C	 1.1483336 0.3421134 0.2921099
Dipole moment and its components, D μ_{total} μ_x μ_y μ_z	 6.265 -6.0563 1.5974 0.1367
E_{B3MO}, a.e.	-0.19583
E_{HCMO}, a.e.	-0.04063
$\Delta E_{B3MO-HCMO}$, эВ	4.223
I, eV	5.329
A, eV	1.106
χ,eV	3.218
η,eV	2.112
S, eV	0.473
C_v, cal/mol·K	51.489
S, cal/mol·K	116.640

Due to the different values of the rotational constants, the molecule is an asymmetric top. Such fundamental properties as the dipole moment, ionization potential, electron affinity, etc., are directly dependent on the geometry of the molecule (table 3). The 4-ethyl-5-(2-hydroxyphenyl)-1,2,4-triazole-3-thione molecule is highly polar. The contributions of the X, Y, and Z components to the total dipole moment are different; the vector of the dipole moment is directed mainly along the X axis.

The most significant orbitals in a molecule are the so-called boundary orbitals: the highest occupied molecular orbital (HOMO) and the lowest free molecular orbital (LUMO). The HOMO energy characterizes the ability to donate an electron, LUMO — to accept an electron, the energy gap between them — the chemical stability of the molecule, with I = - E_{VBMO} and A = -E_{NCMO} (table 3) [35]. The molecule has a rather large ionization potential, electronegativity, and positive electron affinity. The width of the HOMO-LUMO energy gap (ΔE) indicates a sufficiently low polarizability of the molecule, which is consistent with the large value of its constant dipole moment. The high value of the dipole moment is due to the presence of electronegative atoms in the molecule.

Using these data, the molecular characteristics presented in table 3 were theoretically calculated, such as electronegativity χ, chemical rigidity η, and chemical softness S [35]. Absolute electronegativity is calculated as the half-sum of the ionization potential and electron affinity, and absolute chemical rigidity as their half-difference. The stiffness of a substance is considered as a measure of resistance to changes in electronic configuration. Chemical softness is the inverse of stiffness. The table also shows the calculated values of the thermodynamic properties of the compound, such as isochoric heat capacity and entropy.

ӘОЖ 539.19 +548 +547:541.61

Ж.Б. Сэтбаева[1,2*], О.А. Нүркенов[2], К.М. Тұрдыбеков[1], Л.К. Абуляисова[1], М.Ж. Бүркеев[1], С.Д. Фазылов[1,2], С.А. Талипов[3], David Havlicek[4]

[1]Бөкетов атындағы Қарағанды мемлекеттік университеті, Қазақстан;
[2]ҚР Органикалық синтез және көмір химиясы институты, Қарағанды, Қазақстан;
[3] ӨҒА А.С. Садыков атындағы биорганикалық химия институты, Ташкент, Өзбекстан;
[4]Карлов университеті, Чех Республикасы

4-ЭТИЛ-5-(2-ГИДРОКСИФЕНИЛ)-1,2,4-ТРИАЗОЛ-3-ТИОННЫҢ МОЛЕКУЛАЛЫҚ ҚҰРЫЛЫМЫ МЕН КВАНТТЫ-ХИМИЯЛЫҚ ЕСЕПТЕУЛЕРІ

Аннотация. Мақала 4-этил-5-(2-гидроксифенил)-1,2,4-триазол-3-тионның кеңістіктік құрылымын зерттеуге арналған. Қосылыстың молекулалық құрылымы рентген құрылымды әдіс арқылы анықталынды. Молекуланың кристалдық қаптамасы мен құрылымы бойынша мәліметтер келтірілген. Фенилді мен триазолды циклдары жазықтықты екені көрсетілген. Молекуланың сутектік байланысы арқылы кристалда үш өлшемді тордың болатындығы көрсетілген. Рентген құрылымды зерттеу нәтижелері Кембриджтің кристалл құрылымды мәліметтер орталығында тіркелген. Синтезделген 1,2,4-триазолдың құрылымы ЯМР ^{1}H-спектроскопия әдісімен зерттелінді. Қосылыстың ЯМР ^{1}H спектрінде ароматтық сақинаға тән келетін протондардың сигналы байқалады. Химиялық ығысудың мәні және интегралды сигнал қарқындылығы анықталынды. 4-Этил-5-(2-гидроксифенил)-1,2,4-триазол-3-тионды кванттық химиялықз ерттеу DFT әдісімен B3LYP алмасу-корреляциялық функциясын қолданып, Даннингтың негізгі жиынтығы cc-pVDZ жиынтығымен жүргізілді. Толық электронды энергия, айналу константалары, диполь моменті мен қосындылар және термодинамикалық функциялар сияқты қосылыстың молекулалық сипаттамалары болжамдалған. 4-Этил-5-(2-гидроксифенил)-1,2,4-триазол-3-трион молекуласының тепе-тең геометриялық параметрлері анықталды. Кеңістіктік конфигурация мен молекулалық параметрлердің талдауы молекуланың кристалды және газды фазалық құрылымдарының арасындағы сапалы сәйкестікті көрсетілді, алайда басты айырмашылық алты және бес мүшелі циклдердің салыстырмалы бағытында байқалатындығы анықталынды.

Түйін сөздер: кристалдық құрылым, рентген құрылымды анализ, 1,2,4-триазол, 4-этил-5-(2-гидроксифенил)-1,2,4-триазол-3-тион, квантты-химиялық есептеу, DFT әдісі, геометриялық және энергетикалық сипаттамалар.

УДК 539.19 +548 +547:541.61

Ж.Б. Сатпаева[1,2*], О.А. Нуркенов[2], К.М. Турдыбеков[1], Л.К. Абуляисова[1], М.Ж. Буркеев[1], С.Д. Фазылов[1,2], С.А. Талипов[3], DavidHavlicek[4]

[1]Карагандинский государственный университет им. Е.А. Букетова, Казахстан;
[2]Институт органического синтеза и углехимии РК, Караганда, Казахстан;
[3]Институт биорганической химии им. Академика Садыкова, Ташкент, Узбекистан;
[4]Карлов университет, Чешская республика

МОЛЕКУЛЯРНАЯ СТРУКТУРА И КВАНТОВО-ХИМИЧЕСКИЕ РАСЧЕТЫ 4-ЭТИЛ-5-(2-ГИДРОКСИФЕНИЛ)-1,2,4-ТРИАЗОЛ-3-ТИОНА

Аннотация.Статья посвящена исследованию пространственной структуры 4-этил-5-(2-гидроксифенил)-1,2,4-триазол-3-тиона. Молекулярная и кристаллическая структура определена методом рентгеноструктурного анализа. Приведены данные по пространственному строению и кристаллической упаковке молекулы. Установлено, что фенильные и триазольные циклы плоские. За счет водородных связей молекулы в кристалле образуют трехмерные сетки. Результаты рентгеноструктурного исследования депонированы в Кембриджском центре кристаллоструктурных данных. Исследовано строение синтезированного 1,2,4-триазола методом ЯМР ^{1}H-спектроскопии. При анализе спектра ЯМР ^{1}H соединения наблюдаются характерные сигналы протонов ароматического кольца. Определено значение химического сдвига и интегральная интенсивность сигналов. Методом DFT с использованием обменно-корреляционного функционала B3LYP в сочетании с базисным набором Даннингасс-pVDZ проведено квантово-химическое исследование 4-этил-5-(2-гидроксифенил)-1,2,4-триазол-3-тиона. Предсказаны молекулярные характеристики соединения, такие как полная электронная энергия, вращательные постоянные, дипольный момент и

вклады, термодинамические функции. Определены равновесные геометрические параметры молекулы 4-этил-5-(2-гидроксифенил)-1,2,4-триазол-3-тиона. Выполненный анализ пространственной конфигурации и молекулярных параметров показал качественное соответствие кристаллической и газофазной структур молекулы, при этом отмечено, что основное отличие наблюдается в относительной ориентации шести- и пятичленных циклов.

Ключевые слова:кристаллическая структура, рентгеноструктурный анализ, 1,2,4-триазол, 4-этил-5-(2-гидроксифенил)-1,2,4-триазол-3-тион, квантово-химические расчеты, метод DFT, геометрические и энергетические характеристики.

Information about the authors:

Satpaeva Zh.B. – Doctoral student of Buketov Karaganda State University, e-mail: satpaeva_zh@mail.ru, https://publons.com/researcher/P-4887-2017/, https://orcid.org/0000-0003-0962-1148

Nurkenov O.A. – Doctor of chemical sciences, Professor, Institute of Organic Synthesis and Coal Chemistry of the Republic of Kazakhstan, e-mail: nurkenov_oral@mail.ru, https://orcid.org/0000-0002-2771-0411

Turdybekov K.M. – Doctor of chemical sciences, Professor, Department of Physics and Nanotechnology of Buketov Karaganda State University, e-mail: https://orcid.org/0000-0001-9625-0060

Abulyaissova L.K. – Candidate of Chemical Sciences, Professor of the Department of Physical and Analytical Chemistry of Buketov Karaganda State University, e-mail: lyazzat.kz07@mail.ru, https://orcid.org/0000-0002-7530-3378

BurkeevM.Zh. – Acting Dean of the Faculty of Chemistry of Buketov Karaganda State University, e-mail: m_burkeev@mail.ru, https://orcid.org/0000-0001-8084-4825, https://publons.com/researcher/2339931/meyram-z-burkeev/

Fazylov S.D. – corresponding member of NAS RK, Doctor of chemical sciences, Professor, Institute of Organic Synthesis and Coal Chemistry of the Republic of Kazakhstan. e-mail: iosu8990@mail.ru, https://orcid.org/0000-0002-4240-6450

Talipov S.A. – A.S. Sadikov Institute of Bioorganic Chemistry, Uzbekistan Academy of Science, e-mail: samat_talipov@yahoo.com

David Havlicek – Department of Inorganic Chemistry, Charles University in Prague.https://orcid.org/0000-0002-8854-6213; https://publons.com/researcher/B-1376-2017/; Scopus Author ID 6602118880

REFERENCES

[1] Hassan H.Y., El-Shorbagi A.A., El-Koussi N.A., Abdel-Zaher A.O. (1994) Desing and synthesis of some new 1H-1,2,4-triazoles of potential anti-inflammatory and analgesic activities, Bulletin of Pharmaceutical Sciences, 17:27-39. (in Eng)

[2] Turan-Zitouni G., Kaplancikli Z.A., Erol K., Killic F.S. (1999) Synthesis and analgesis activity of some triazoles and triazolothiadiazines, Farmaco, 54:218-223.

[3] Kokil G.R., Rewatkar P.V., Gosain S., Aggarwal S., Verma A., Karla A., et al. (2010) Synthesis and in vitro evaluation of novel 1,2,4-triazole derivatives as antifungal agents, Letters of Drug Desing and Discovery, 7:46-49. DOI: 10.2174/157018010789869415 (in Eng).

[4] Turan-Zitouni G., Kaplancikli Z.A., Yildiz M.T., Chevallet P., Kaya D. (2005) Synthesis and antimicrobial activity of 4-phenyl/cyclohexyl-5-(1-phenoxyethyl)-3-[N-(2-thiazolyl)acetamido]-thio-4H-1,2,4-triazole derivatives, European Journal of Medicinal Chemistry, 40:607-613. DOI: 10.1016/j.ejmech.2005.01.007 (in Eng).

[5] Kritsanida M., Mouroutsou A., Marakos P., Pouli N., Papakonstantinou-Garaufalias S.M., Pannecouque C., et al. (2002) Synthesis and antiviral activity evalution of some new 6-substituted 3-(1-adamantyl)-1,2,4-triazolo[3,4-b][[1,3,4]thiadiazoles, Farmaco, 57:253-357. PMID: 11989804 (in Eng).

[6] Johns B.A., Weatherhead J.G., Allen S.H., Thompson J.B., Garvey E.P., Foster S.A., et al. (2009) The use of axadiazole and triazole substituted naphthyridines as HIV-1 integrase inhibitors. Part 1: Establishing the pharmacophore, Bioorganical and Medicinal Chemistry Letters, 19:1802-1806. DOI: 10.1016/j.bmcl.2009.01.090. PMID: 19217781 (in Eng).

[7] Mathew V., Keshavayya J., Vaidya V.P., Giles D. (2007) Studies on synthesis and pharmacological activities of 3,6-disubstituted-1,2,4-triazolo[3,4-b]-1,3,4-thiadiazoles and their dihydro analogues, European Journal of Medicinal Chemistry, 42(6):823-840. DOI: 10.1016/j.eimech.2006.12.010 (in Eng).

[8] Tozkoparan B., Kupeli E., Yesilada E., Ertan M. (2007) Preparation of 5-aryl-3-alkylthio-1,2,4-triazoles and corresponding sulfones with anti-inflammatory-analgesic activity, Biorganical and Medicinal Chemistry, 15:1808-1814. DOI: 10.1016/j.bmc.2006.11.029. PMID: 17166724 (in Eng).

[9] Kelley J.L., Koble C.S., Davis R.G., McLean E.W., Soroko F.E., Cooper B.R. (1995) 1-(Fluorobenzyl)-4-amino-1H-1,2,3-triazolo[4,5-c]pyridines: Synthesis and anticonvulsant activity, Journal of Medicinal Chemistry, 38:4131-4134. (in Eng)

[10]10 Holla B.S., Poojary K.N., Rao B.S., Shivananda M.K. (2002) New bis-aminomercaptotriazoles and bis-triazolothiadiazoles as possible anticancer agents, European Journal of Medicinal Chemistry, 37(6):511-517. PMID: 12204477 (in Eng).

[11] Sztanke K., Tuzimski T., Rzymowska J., Pasternak K., Kandefer- Szerszen M. (2008) Synthesis, determination of the lipophilicity, anticancer and antimicrobial properties of some fused 1,2,4-triazole derivatives, European Journal of Medicinal Chemistry, 43:404-419. DOI: 10.1016/j.ejmech.2007.03.033 (in Eng).

[12]Bay H.A., Quaddouri B., Guaadaoui A., Touzani R., Benchat N.E., Hamal A., et al. (2010) Synthesis and biological activity of new triazole compounds, Drug Desing and Discovery, 7:737-742. DOI: 10.2174/157018010789869352 (in Eng).

[13] Plech T., Wujec M., Kosikowska U., Malm A., Rajtar B., Polz-Dacewicz B. (2013) Synthesis and in vitro activity of 1,2,4-triazole-ciprofloxacin hybrids against drug-susceptible and drug-resistant bacteria, European Journal of Medicinal Chemistry, 6:128-134. DOI: 10.1016/j.ejmech.2012.11.040 (in Eng).

[14] Roy G., Mugesh G. (2005) Anti-thyroid drugs and thyroid hormone synthesis: Effect of methimazole derivatives on peroxidase-catalyzed reactions, Journal of the American Society, 127:15207-15217. DOI: 10.1021/ja054497u (in Eng).

[15] Wujec M., Pisklak M., Pitucha M., Dobosz M., Siwek A. (2007) The reactions of hydrazide (4-nitroimidazol-1-yl)acetic acid with isothiocyanates, Annals of the Polish Chemical Society, 604-606. (in Eng).

[16] Wujec M., Paneth P. (2008) Mechanism of 4-methyl-1,2,4-triazol-3-thione reaction with formaldehyde, Journal of Physical Organic Chemistry, 20:345-348. DOI: 10.1002/poc.1324 (in Eng).

[17] Plech T., Luszczki J., Wujec M., Flieger J., Pizon M. (2013) Synthesis, characterization and preliminary anticonvulsant evaluation of some 4-alkyl-1,2,4-triazoles, European Journal of Medicinal Chemistry, 60:208-215. DOI: 10.1016/j.ejmech.2012.11.026. PMID: 23291122 (in Eng).

[18] Roy G., Nethaji M., Mugesh G. (2004) Biomimetric studies on anti-thyroid dregs and thyroid hormone synthesis, Journal of the American Society, 126,9:2712-2713. DOI: 10.1021/ja039860g (in Eng).

[19] Zamani K., Faghihi K., Tofighi T., Shariatzadeh M.R. (2004) Synthesis and antimicrobial activity of some pyrydyl and naphthyl substituted 1,2,4-triazole and 1,3,4-thiadiazole derivatives, Turkish Journal of Chemistry, 28:95-100. (in Eng).

[20] Mroczek T., Plech T., Wujec M. (2017) Novel Concept of Discrimination of 1,2,4-triazole-3-thione and 3-thiol tautomers, Journal of Chromatographic Science, 55, 2:117-129. DOI: 10.1093/chromsci/bmw151 (in Eng).

[21] Coyanis E.M., Della Vedova C.O., Haas A., Winter M. (2002) Preparation, characterization and thiol-thionetautomeric studies of 2-thiono-4-mrthyl-5-(2,2,2-trifluoro-1-trifluoromethylethyl)-1,3-thiazoline, Journal of Fluorescence Chemistry, 117(2):185-192. DOI: 10.1016/S0022-1139(02)00186-0 (in Eng).

[22] Anuva S., Bijan K.P., Samiran K., Nihil G. (2011) Excited state lactim to lactam type tautomerization reaction in 5-(4-fluorophenyl)-2-hydroxypyridine: Spectroscopic study and quantum chemical calculation, Journal of Fluorescence, 21:95-104. DOI: 10.1007/s10895-010-0692-3. PMID: 20614169 (in Eng).

[23] Bach A., Tanner C., Manca C., Frey H.M., Leutwyler S. (2003) Ground- and excited state proton transfer and tautomerization in 7-hydroxyquinoline (NH_3)n clusters: Spectroscopic and time resolved investigations, Journal of Chemical Physics, 119(12):5933-5942. DOI: 10.1063/1.1603740 (in Eng).

[24] Douhal A., Kim S.K., Zewail A.H. (1995) Femtosecond molecular dynamics of tautomerization in model base pairs, Nature, 378:260-263. (in Eng).

[25] Bokay G.B., Poray-Koshits M.A. (1964) X-ray analysis. Moskay.

[26] Nurkenov O.A., Fazylov S.D., SatpaevaZh.B., Seilkhanov T.M., KaripovaG.Zh., IsaevaA.Zh. (2014) Synthesis and structure of new derivatives of salicylic acid hydrazide, Russ. J. Gen. Chem.84, 9:1857-1859. DOI: 10.1134/S1070363214090369 (in Eng) .

[27] Nurkenov O.A., Fazylov S.D., Satpaeva Zh.B., Turdybekov K.M., Karipova G.Zh., Isaeva A.Zh., Talipov S.A., Ibragimov B.T. (2015) Synthesis and structure of new 1,2,4 – triazoles derived from *p*-hydroxybenzoic acid hydrazide, Russ. J. Gen. Chem. 85, 1:57-60. DOI: 10.1134/S1070363215010107 (in Eng)

[28] Nurkenov O.A., Fazylov S.D., Zhivotova T.S., Satpayeva Zh.B., Akhmetova S.B., Kurmanbayeva Zh.Zh., Karipova G.Zh., Isayeva A.Zh. (2015) Synthesis, chemical transformations and antimicrobialactivity of somethiosemicarbazidesof o- and p-hydroxybenzoicacid, News of the National academy of sciences of the Republicof Kazakhstan. Ser. chem. andtech. 1, 409:9-14. (inEng)

[29] SMART V5.051 and SAINT V5.00, (1998) Area detector control and integration software, Bruker AXS Inc., Madison, WI-53719, USA.

[30] Sheldrick G.M. (2008). ActaCrystallographica Section A: Foundations of Crystallography. International Union of Crystallography 64:112.

[31] Sheldrick G.M. (2015). ActaCrystallographica Section C: 71:3.

[32] Becke A.D. (1993) J. Chem. Phys., 98, 7:5648.

[33] Frisch M.J., Trucks G.W., Schlegel H.B. et al. (2016) Gaussian 16, Revision A.03, Wallingford CT.

[34] Allen F.H., Kennard O., Watson D.G., Brammer L., Orpen A.G., Taylor R. (1987). Tables of bond lengths deternined by x-ray and neutron diffraction, JournalChemistry Society Perkin Trans. 2, 1.

[35] Fleming I. (1976) Frontier Orbitals and Organic Chemical Reactions. Wiley, London. 249.

N E W S
OF THE NATIONAL ACADEMY OF SCIENCES OF THE REPUBLIC OF KAZAKHSTAN
SERIES CHEMISTRY AND TECHNOLOGY
ISSN 2224-5286 **https://doi.org/10.32014/2019.2518-1491.70**
Volume 6, Number 438 (2019), 30 – 35

UDC 547.99
IRSTI31.23.23

Y.S. Ikhsanov, Y.A. Litvinenko, G.A.Seitimova, G.Sh. Burasheva

Al-Farabi Kazakh National University;
Research Institute of New Technologies and Materials
Republic of Kazakhstan, 050012, Almaty, KarasayBatyr St., 95a
erbol.ih@gmail.com, rumex1978@gmail.com, sitigulnaz@mail.ru, gauharbur@mail.ru

COMPARATIVE ANALYSIS OF CERTAIN MICRONUTRIENTS OF PLANTS OF THE *SUAEDA* GENUS

Abstract. The article presents a comparative analysis of the content of some biologically active micronutrients, namely ascorbic acid, retinol and tocopherol in 6 six representatives of the genus Suaeda of the Amaranthaceae family.

In this paper, we study the micronutrients of the aerial parts of plants of the genus *Suaeda:Suaeda acuminata, Suaeda microphylla, Suaeda altissima, Suaeda spicata, Suaeda vera, Suaeda splendens*.

Species of *Suaeda spicata, Suaeda vera* harvested in the province of Lliedia, Spain. Types of *Suaeda acuminata, Suaeda microphylla, Suaeda altissima, Suaeda splendens* in Ili district, Almaty region

As a result, it was established that in all studied objects, tocopherol is present in the largest quantity (from 10 to 16 mg per 100 g).

The amount of ascorbic acid varies in the range of 3.2-4.5 mg per 100g. The content of retinol in 6 studied species ranges from 1.7 to 3.0 mg per 100g. The highest content of tocopherol is found in the aerial part of *Suaeda microphylla* - 16 mg per 100g. Ascorbic acid is also found in the greatest amount in the aerial part of *Suaeda microphylla* - 4.5 mg per 100g. Retinol is found in the greatest amount in the aerial part of the species Suaeda acuminate - 3.0 mg per 100g.

Keywords: *Suaeda,* ascorbic acid, retinol, tocopherol, aerial parts,*Amaranthaceae.*

Introduction

Micronutrients considered by us belong to the class of biologically active substances known as vitamins.

Vitamins are compounds that cannot be synthesized in the human body, but at the same time are necessary for the functioning of the body, which makes them a necessary part of the diet.

For example, vitamin A deficiency (retinol) is a serious public health problem in developing countries, resulting in 130 million children with an increased risk of morbidity and mortality from infectious diseases [1].

Vitamin-related disorders include blindness (vitamin A), vitamin deficiency (vitamin B1), pellagra (vitamin B3), anemia (vitamin B6), scurvy (vitamin C), and rickets.

Some of the most valuable and essential are vitamins with antioxidant properties, carotenoids (provitamin A), ascorbate (vitamin C) and tochochromanols (vitamin E, including both tocopherols and tocotrienols) [2-6].

For this reason, an important task is to find the sources of these compounds among plants in the interests of health and veterinary medicine.

Swede (from the Arabic “Suwedmullat” or “Suaedabaccata” ”) is a large genus of halophyllous plants of the Mud family (Chenopodiaceae), including about 100 species around the globe, except for the Arctic zone. 25 species are described on the territory of the CIS, 17 of them in Kazakhstan. The main species of

the genus *Suaeda –SuaedaphysophoraPall.,Suaedadendroides (CAM) Moq., Suaedaaltissima (L.) Pall., (Suaedamicrophylla Pall., SuaedaparadoxaBge., Suaedalinifolia Pall., SuaedaeltonicaIjin,). (Kar.Et. Kir) Bge.,Suaedapygmaea (Kar. Et. Kir) Iljin.,Suaedatransoxana (Bge.) Boiss.,SuaedaconfusaIljin., Suaedaacuminata (CAM) MoqSuaedaprostrata Pall., Suaedacorniculata (CAM) Bge., Suaeda salsa (L.) Pall.,SuaedakossinskyiIljin., Suaedaheterophylla (Kar. Et. Kir) Bge.*

Species of the genus *Suaeda* are annuals or perennial grasses, dwarf shrubs and shrubs, mostly with alternate narrow succulent leaves with small flowers. They usually grow in masses in saline places, sea coasts, and coast of saline reservoirs, as well as on depleted steppe and sandy soils. Most representatives of Kazakhstani species of *Suaeda* are valuable winter and autumn forage plants [7].

Representatives of the genus *Suaeda* can serve as a source of flavanoids, alkaloids, polysaccharides, carotenoids, saponins, coumarins, tannins and other biologically active substances [8].

Many types of *Suaeda* in folk medicine have long been used as raw material for the production of potash, from which people used it for cooking the so-called “black” soap, which was used as an anti-inflammatory and wound-healing agent for various skin diseases [9].

According to folk remedies, the aerial part of *Suaedaphysophora* Pall. used as an anthelmintic agent. Broths, dry, water, alcoholic extracts and tinctures have antihypertensive properties. Aqueous extract improves cardiac activity, is less toxic than papaverine, and is proposed as a remedy for the symptomatic treatment of hypertension [10].

According to modern scientific data, herbal medicine based on *Suaedaphysophora*Pall. has a strong hypertensive (for nonadrenaline - 55%, against 37%), antioxidant (for propyl gallate - 89.02%, against 95.5%), antibacterial (*Salmonella typhi*, *Pseudonondsorenogenosa* - for tetracycline - 55%, against 100%) and weak anti-inflammatory (for ibuprofen - 35%, against 65%) activity [11].

Based on the literature on pharmacological agents, the aerial part of *Suaedamaritima* is used in medicine as a means for the complex treatment of hepatitis. Broths, dry, water, alcoholic extracts and tinctures have antiviral, antibacterial, hepatoprotective, laxative and antioxidant activities [12].

From the literature it is known about the presence of antimicrobial activity in Suaedamonoica. The antimicrobial activity of the halophyte Suaedamonoica (Forsst ex Geml) was studied using the extracts of the leaves of this plant on various test microorganisms, including several antibiotic-resistant bacteria and pathogens. Thus, it turned out that the aqueous extract of Suaedamonoica has the highest antimicrobial activity against the following microorganisms: *Rhizopusstolonifer,Mucarrecemosus, Saccharomyces cerevisiae,* and relatively moderate activity against *Bacillus subtilis, Klebsiellapneumoniaea, Bacillus megaterium, Lactobacillus acidophilus,Escherichia coli, Enterobacteraerogenes, Enterobactercloace, Rhizoctoniasolana.*

A high level of antimicrobial activity was also shown by the methanol extract against *Bacillus megaterium* bacteria, and moderate against the microorganism *Lactobacillus acidophilus.* Hexane extract has the highest level of antimicrobial activity against bacteria of the species *Bacillus subtilis, Lactobacillus acidophilus*, and moderate against *Bacillus megaterium, Escherichia coli, Enterobacter aerogenes, Enterobacter cloace, Klebsiella pneumonia*. Chloroform extract is only effective against bacteria *Klebsiella pneumonia* [13].

The study concluded that water, methanol and hexane extracts of *Suaeda monoica* leaves have great potential as antimicrobial agents. As a result, they can be used as inhalation drugs in the treatment of infectious diseases of the respiratory tract and ear canals caused by resistant pathogenic microorganisms, as well as for wastewater treatment of infectious diseases clinics [14].

The methanol and ethanol extracts of the plant *Suaeda monoica* have high antioxidant activity. To detect antioxidant activity, these extracts were tested on various model antioxidant systems. This fact indicates a high value of the potential of the aerial part of Suaeda monoica, which can be used to treat mediated diseases caused by free radicals [15].

In addition, *Suaeda monoica* is used in the complex treatment of hepatitis, as the plant has a pronounced antiviral activity, which is explained by the presence of triterpenoids and styrenes in the phytochemical composition of this plant [16].

Ethanol extract of the plant *Suaeda baccata* and, isolated from this plant, its constituent component, triglinear alkaloid, exhibit pronounced antimicrobial activity against *Staphylococcus aureus* (*Staphylococcus* stamp) [17].

A significant content of biologically active substances in the aerial and underground organs of the medicinal plant *Suaeda japonica* predetermined its use in medicine as a remedy with antioxidant, antidiabetic, and anti-neuroinflammatory activities [18].

Thus, the diversity of biologically active substances in the composition of various species of *Suaeda*, and the associated therapeutic effect cause the need for further research on various species of these plants.

The objects of study were selected aboveground parts of the following representatives of the genus *Suaeda*: *Suaeda acuminata, Suaeda microphylla, Suaeda altissima, Suaeda spicata, Suaeda vera, Suaeda splendens*.

Species of *Suaeda spicata*, *Suaeda vera* harvested in the province of Lliedia, Spain. Types of *Suaeda acuminata, Suaeda microphylla, Suaeda altissima, Suaeda splendens* in Ili district of Almaty region

Herbal raw materials are harvested in accordance with the requirements of the Global Fund of the Republic of Kazakhstan harmonized with the European Pharmacopoeia.

Materials and methods

Determination of the content of vitamin C (ascorbic acid) is carried out as follows: a sample of at least 0.3 g (0.3 ml) is placed in a centrifuge tube, the walls of which are covered with sodium citrate powder. After centrifuging the sample for 30 minutes at 3000 rpm, it is transferred to another tube and an equal amount of bidistilled water and a double amount of freshly prepared 5% solution of metaphosphoric acid are added thereto. The protein precipitate is stirred with a stick and centrifuged for 10 min at 3000 rpm. The amount of the supernatant (0.1-0.5 ml) is introduced into porcelain titration cuvettes (2 parallel samples) and titrated with a 0.001 n-0.0005 n solution of sodium salt 2.6 of a dichlorophenol -indophenol from a special 0.1 ml micropipette.

In parallel, a “blind” experiment is carried out with a 5% solution of metaphosphoric acid and bidistilledwater (1: 1).

To determine the concentration of vitamins A (retinol) and E (tocopherol) using the method of simultaneous fluorometric analysis. To 0.2 ml (g) of the sample, add 1 ml of bidistilled water and shake for 30 seconds. After that add 1 ml of 96% ethanol and shake again for 30 seconds. Then adding 5 ml of hexane, repeat the shaking procedure again (similar measures are carried out with the standard). After the sample is centrifuged for 10 minutes at 1500 rpm. For spectrometry, a clearly separated hexane layer (3 ml) was taken; which can be stored for 2 hours in tightly sealed tubes in a dark place.

In parallel with the experimental samples, standard and control (blank) samples are prepared. In standard samples, 0.2 ml of a standard solution (tocopherol and retinol acetate in ethanol) are taken instead of the test sample. In the control samples instead of prototypes - water.

Spectrofluorimetry (Hitachi Spectrofluorometer, Japan): tocopherol is carried out at an excitation wavelength of 292 nm and a fluorescence of 310 nm; retinol - at 335 and 430 nm, respectively.

The results are shown in Figure 1.

Results and discussion

In the aerial part of the selected representatives of the genus *Suaeda*, we determined the content of the following nutrients: ascorbic acid, retinol and tocopherol.

It has been established that in all samples, tocopherol is the dominant micronutrient, not less than 10 mg per 100 g.

The highest content of tocopherol is observed in the aboveground part of the plant *Suaedamicrophylla* (16 mg per 100g), and the lowest in the aboveground part of *Suaeda acuminate* (10 mg per 100g), these figures are quite high for the aboveground parts of the plant, common in arid areas.

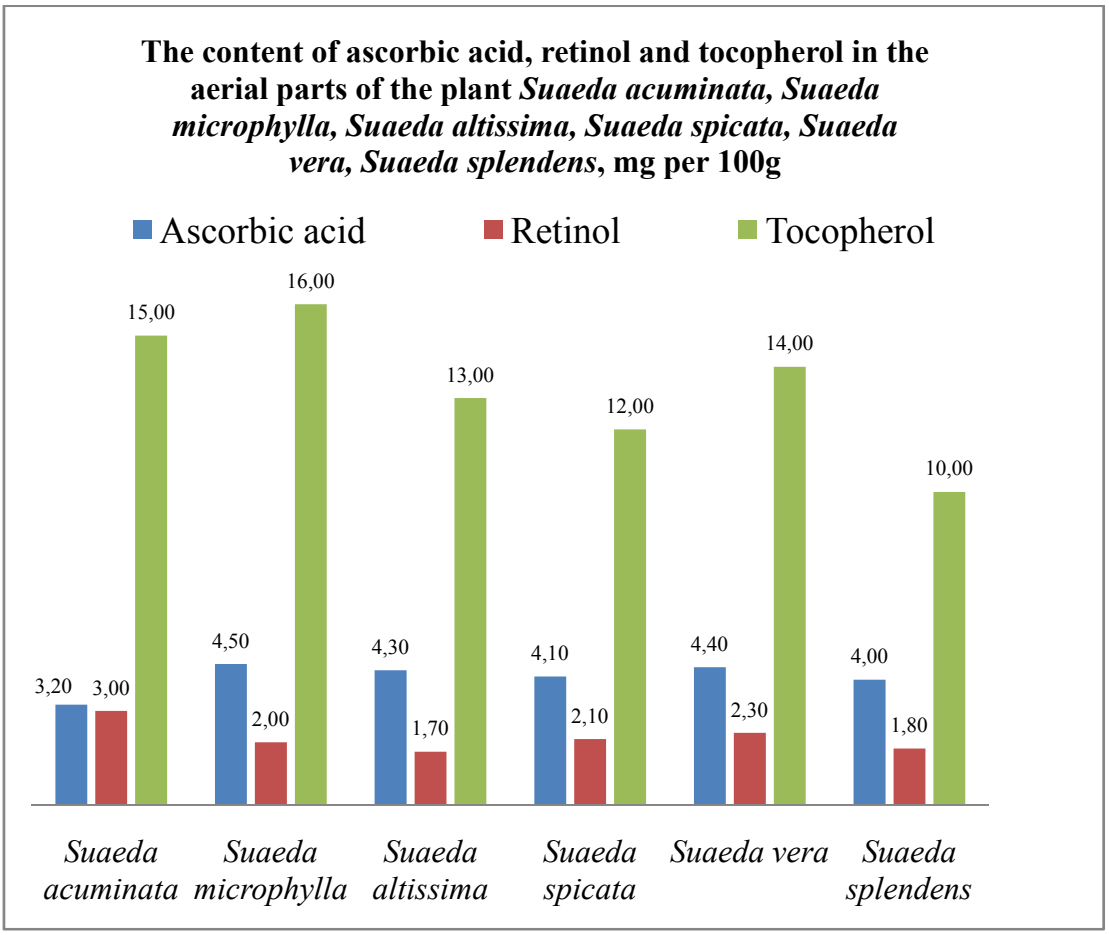

Figure 1 - The content of ascorbic acid, retinol and tocopherol in the aerial parts of the plant *Suaedaacuminata, Suaedamicrophylla, Suaedaaltissima, Suaedaspicata, Suaedavera, Suaedasplendens*, in mg per 100g%

Thus, it was revealed that the above-ground parts of the studied representatives of the genus *Suaeda* can be considered as a source of ascorbic acid, and the seeds and inflorescences are a rich source of tocopherol, based on the fact that the daily human need for vitamin E is 2-6 mg [19-21].

The content of ascorbic acid in the studied species ranges from 3.20 to 4.50 mg per 100g, which is little, but typical for the stems of arid plant species.

Suaedamicrophylla (4.50 mg per 100g) also has the highest content.

Retinol is present in selected species in a relatively small amount, the concentration ranges from 1.80 mg per 100g in *Suaedasplendens* to 3.00 mg per 100g in *Suaeda acuminate.*

Conclusion

In 6 representatives of the genus *Suaeda*: *Suaedaacuminata, Suaedamicrophylla, Suaedaaltissima, Suaedaspicata, Suaedavera, Suaedasplendens*, the following micronutrients were determined: ascorbic acid, retinol and tocopherol. It has been established that in all the objects studied, tocopherol is present in the greatest quantity.

The investigated plant species once again confirmed the importance of the genus *Suaeda*, as a plant requiring attention and careful chemical study, and identifying various types of biological activity.

For the first time, a comparative analysis of the content of ascorbic acid, retinol and tocopherol in the described representatives of the genus *Suaeda.*

УДК 547.99
МРНТИ 31.23.23

Е.С. Ихсанов, Ю.А. Литвиненко, Г.А. Сейтимова, Г.Ш. Бурашева

Казахский национальный университет имени аль-Фараби;
Научно-исследовательский институт новых технологий и материалов
Республика Казахстан, 050012, г.Алматы, ул.Карасай батыра, 95а,

АҚСОРА (SUAEDA) ТЕКТІ ӨСІМДІКТІҢ КЕЙБІР МИКРОНУТРИЕНТТЕРІН САЛЫСТЫРМАЛЫ САРАПТАУ

Аннотация. Келтірілген мақалада *Amaranthaceae* тұқымдасы, (*Suaeda) ақсора* текті алты өсімдіктің құрамындағы кейбір биологиялық белсенді микронутриенттерге, атап айтқанда, аскорбин қышқылы, ретинол және токоферолдың сандық мөлшеріне салыстырмалы сараптау жүргізілген.

Бұл жұмыста (*Suaeda*:) ақсора тегінің, жер беті бөлігінің мына түрлеріне зерттеу жасалған: *Suaeda acuminata*, *Suaeda microphylla*, *Suaedaaltissima*, *Suaedaspicata*, *Suaedavera*, *Suaedasplendens*.

Ақсораның *Suaedaspicata*, *Suaedavera* *түрлері* Испаниядан, Lliedia аймағынан, жазда жиналған. Ал ақсораның *Suaeda acuminata*, *Suaeda microphylla*, *Suaedaaltissima, Suaedasplendens* түрлері Алматы облысы, Іле ауданынан дайындалған.

Зерттеу нәтижесінде барлық ақсора өсімдіктерінде жеткілікті мөлшерде токоферол анықталған (100г-да 10-мг-нан 16-мг-ға дейін). Аскорбин қышқылының мөлшері 100 г-да 3,2-4,5 мг. Ал алты зерттелген өсімдікте ретинолдың 100 г.-да 1,7-3,0 мг. мөлшері белгілі болған.

Suaeda microphylla тегінің жер беті бөлігінде токоферол 100г.-да 16 мг, ал аскорбин қышқылы 100г.-да 4,5мг. анықталған. Ақсораның *Suaeda acuminate* түрінде100г.-да 3,0 мг ретинолдың көп мөлшерде бары белгілі болған.

Түйін сөздер:*Suaeda,* аскорбин қышқылы, ретинол, токоферол, жер беті бөлігінің, *Amaranthaceae*.

УДК 547.99
МРНТИ 31.23.23

Е.С. Ихсанов, Ю.А. Литвиненко, Г.А.Сейтимова, Г.Ш. Бурашева

Казахский национальный университет имени аль-Фараби;
Научно-исследовательский институт новых технологий и материалов
Республика Казахстан, 050012, г.Алматы, ул.Карасай батыра, 95а,

СРАВНИТЕЛЬНЫЙ АНАЛИЗ НЕКОТОРЫХ МИКРОНУТРИЕНТОВ РАСТЕНИЙ РОДА *SUAEDA*

Аннотация. В статье представлен сравнительный анализ содержания некоторых биологически активных микронутриентов, а именно аскорбиновой кислоты, ретинола и токоферола в 6 шести представителях рода *Suaeda* семейства *Amaranthaceae*.

В данной работе изучаются микронутриенты надземных частейрастений рода *Suaeda*: *Suaedaacuminata*, *Suaeda microphylla*, *Suaedaaltissima*, *Suaedaspicata*, *Suaedavera*, *Suaedasplendens*.

Виды *Suaedaspicata*, *Suaedavera* заготовлены в провинции Lliedia, Испания.Виды *Suaeda acuminata*, *Suaeda microphylla*, *Suaedaaltissima, Suaedasplendens* в Илийском районе, Алматинской области

В результате установлено, что во всех изучаемых объектах в наибольшем количестве присутствует токоферол (от 10 до 16 мг в 100г).

Количество аскорбиновой кислоты варьируется в пределах 3,2-4,5 мг в 100г. Содержание ретинола в 6 изучаемых видах колеблется от 1,7 до 3,0 мг в 100г.Наибольшее содержание токоферола установлено в надземной части *Suaeda microphylla* - 16 мг в 100г. Аскорбиновая кислота также в наибольшем количесве выявлена в надземной части *Suaeda microphylla*- 4,5 мг в 100г. Ретинол в наибольшем количестве обнаружен в надземной части вида *Suaedaacuminate*- 3,0 мг в 100г.

Ключевые слова: *Suaeda,* аскорбиновая кислота, ретинол, токоферол, надземная часть, *Amaranthaceae*.

Information about authors:

Ikhsanov Yerbol Saginovich - PhD Department of Chemistry and ChemicalTechnology of theAl-Farabi Kazakh National University, Kazakh National University, e-mail: erbol.ih@gmail.com, mobile number: 87775166526, https://orcid.org/0000-0003-4640-9584

Litvinenko Yuliya Alekseevna - candidate of chemical sciences,Lecturer, Department of Chemistry and Chemical, Technology of theAl-Farabi Kazakh National University, e-mail: yuliya_litvinenk@mail.ru, https://orcid.org/0000-0002-6387-187X

Seitimova Gulnaz Absattarovna - Ph.D. Lecturer at the Faculty Department of Chemistry and ChemicalTechnology of theAl-Farabi Kazakh National University, https://orcid.org/0000-0002-5157-1255

Burasheva Gauhar Shahmanovna - Doctor of Science professor, Department of Chemistry and ChemicalTechnology of theAl-Farabi Kazakh National University, e-mail: gauharbur@mail.ru, https://orcid.org/0000-0003-2935-3531

REFERENCES

[1] Kramer, K. et al. (2008) Are low tolerable upper intake levels for vitamin A undermining effective food fortification efforts? Nutr.Rev. 6:517–525.Doi:10.1111/j.1753-4887.2008.00084.(inEng).

[2] Demmig-Adams, B. and Adams, W.W. (2002) Antioxidants in photosynthesis and human nutrition. Science 298: 2149–2153.Doi:10.1126/science.1078002 (in Eng).

[3] DellaPenna, D. and Pogson, B.J. (2006) Vitamin synthesis in plants: tocopherols and carotenoids. Annu. Rev. Plant Biol. 57: 711–738Doi:10.1146/annurev.arplant.56.032604.14430(in Eng).

[4] Linster, C.L. and Clarke, S.G. (2008) L-Ascorbate biosynthesis in higher plants: the role of VTC2. Trends Plant Sci. 13: 567–573.Doi:10.1016/j.tplants.2008.08.005 (in Eng).

[5] Foyer, C.H. and Noctor, G. (2009) Redox regulation in photosynthetic organisms: signaling, acclimation, and practical implications. Antioxid.Redox Signal. 11: 861–905.Doi:10.1089/ars.2008.2177(in Eng).

[6] Azari, R. et al. (2010) Light signaling genes and their manipulation towards modulation of phytonutrient content in tomato fruits. Biotechnol. Adv. 28: 108–118.Doi:10.1016/j.biotechadv.2009.10.003(in Eng).

[7] Cazzonelli, C.I. and Pogson, B.J. (2010) Source to sink: regulation of carotenoid biosynthesis in plants. Trends Plant Sci. 15: 266–274.Doi:10.1016/j.tplants.2010.02.003 (in Eng).

[8] Falk, J. and Munne´-Bosch, S. (2010) Tocochromanol functions in plants: antioxidation and beyond. J. Exp. Bot. 61: 1549–1566.Doi:10.1093/jxb/erq030

[9]Me`ne-Saffrane´, L. and DellaPenna, D. (2010) Biosynthesis, regulation and functions of tocochromanols in plants. Plant Physiol. Biochem. 48: 301–309.Doi:10.1016/j.plaphy.2009.11.004(in Eng).

[10]Aitkulova RE, Abubakirova AA, Kudasova DE, Kaldybekova GM (2016) Role of medicinal plants from south-kazakhstan region for addition into livestock's fodder.N e w s of the national academy of sciences of the republic of kazakhstan series of biological and medical 314: 155 – 158https://doi.org/10.32014/2018.2518- 1629(in Eng).

[11] TursynovaA., Sunnenova NS, Erezhepova N, Sarsenbayeva NB, Kalekeshov AM, E. MakashevK. (2016)Effect of the feed additive based on bentonite and chlorella body of agricultural animals and birds, News of the national academy of sciences of the republic of Kazakhstan series of biological and medical.3: 27 – 33. https://doi.org/10.32014/2018.2224- 526(in Eng).

[12] Akhani, H., Ghorbanli, M. (1993). A contribution to the halophytic vegetation and flora of Iran.Tasks for Vegetation Science 2: 35–44. Doi:10.1007/978-94-011-1858-3_4 (in Eng).

[13] G. Lakshmanan, C. Rajeshkannan, A. Kavitha, B. Mekala and N. Kamaladevi.(2013) Preliminary screening of biologically active constituents of Suaedamonoica and Sesuviumportulacastrum from palayakayal mangrove forest of Tamilnadu. J. ofPharmacognosy and Phytochem2:149-152.ISSN 2278-4136(in Eng).

[14] Prasanna Lakshmi K and NarasimhaRao GM. Antimicrobial Activity of Suaedamonoica (Forsst ex Geml) against Human and Plant Pathogens(2013). J. of Pharmaceutical, Biological and Chemical Sci. 4: 680-685.ISSN: 0975-8585(in Eng).

[15] A. Nishanthini, A. AgnelRuba, V.R. Mohan (2012). Total phenolic, flavonoid contents and in vitro antioxidant activity of leaf of SuaedamonoicaForssk ex. Gmel (Chenopodiaceae),International J. of Advanced Life Sci. 5:34-43.ISSN 2277 – 758X(in Eng).

[16] Eman A. Al – ImarahLaylaJasim Abbas (2009). The chemical composition and antibacterial activity of Suaeda sp. aqueous and alcoholic extracts.Basrah J. Aagric. Scim 5: 202-219. ISSN: 18175868(in Eng).

[17] Al-Mohammadi S. Suhad, Al-KhateebEkbal, Al-Shamma Ali (2005). Anti-microbial investigation of Suaedabaccata (Chenopodiaceae). AJPS 2: 49-51.ISSN: 18150993(in Eng).

[18] Hyun Kang, SushrutaKoppula, Hoi- Ki Kim and Tae-Kyu Park (2013).Suaeda japonica Makino Attenuates Lipopolysaccharide-Induced Neuro-Inflammatory Responses in BV-2 Microgliavia NF-kappa B Signaling. Tropical J. of Pharm 3: 351-356.Doi:10.4314/tjpr.v12i3.12 (in Eng).

[19] Singh S, Mann R, Sharm SK (2013). Phytochemical investigation of Suaedamaritima (L.).Dumort. Stem. J. of Biological & Sci. Opinion. 1: 297-299.Doi: 10.7897/2321–6328.01402(in Eng)

[20] Bajtenov M.S. (2001) Flora Kazahstana. Rodovojkompleksflory. – Almaty: Gylym. ISBN 9965-07-036-9

[21] OscanovB. S., IkhsanovY. S. ,Litvinenko Yu. A. , AdekenovS. M. ,Burasheva G. Sh., Biologically active substances from plant sudaedavera and their anestizing activity N e w s of the national academy of sciences of the republic of kazakhstan series of biological and medical ISSN 2224-5308 https://doi.org/10.32014/2018.2518-1629.8 Volume 5, Number 329 (2018), 63 – 66(in Eng).

N E W S
OF THE NATIONAL ACADEMY OF SCIENCES OF THE REPUBLIC OF KAZAKHSTAN
SERIES CHEMISTRY AND TECHNOLOGY
ISSN 2224-5286 **https://doi.org/10.32014/2019.2518-1491.71**
Volume 6, Number 438 (2019), 36 – 41

UDC 541.64

Ye.M. Tazhbayev[1], A.A. Bakibaev[2], A.T. Takibayeva[3], T.S. Zhumagalieva[1], L.Zh. Zhaparova[1], A.A. Agdarbek[1], N.Zh. Gazizova[1], O.E. Mukashev[1], A.M. Tazhibay[3]

[1]Academician E.A.Buketov Karaganda State University, Karaganda, Kazakhstan;
[2]Tomsk State University, Tomsk, Russia;
[3]Karaganda State Technical University, Karaganda, Kazakhstan
E-mail: zhumagalieva79@mail.ru, ayaulym_agdarbek@mail.ru

PREPARATION OF POLYMERIC NANOPARTICLES OF ALBUMIN AND IMMOBILIZATION OF THEM WITH THE ANTICANCER DRUG "CYCLOPHOSPHANE"

Abstract. Nanoparticles based on biodegradable and biocompatible polymers allow to attain the targeted drug delivery to the specific organ, without affecting healthy cells of the body and prolonging the therapeutic effect of the drug substance. This study is devoted to the development of the method for the preparation of nanoparticles of human serum albumin (HSA) immobilized with the anticancer drug Cyclophosphamide. Albumin nanoparticles with the sizes of 150-170 nm and narrow particle size distribution (PDI 0.069-0.116) were obtained by coacervation. The yield of nanoparticles is 88.5%. The degree of binding of the drug to polymer nanoparticles was within the range of 54.6% to 92.4%. The drug release was prolonged. After 42 hours 68-77% of the biologically active substance was released from the polymer matrix. It is concluded that the development of HSA-based nanocarrier is promising for the Cyclophosphamide preparation.

Keywords: nanoparticles, drug carriers, human serum albumin, cyclophosphane, cyclophosphamide, anticancer drug.

Introduction

One of the serious diseases leading to death worldwide is cancer. Traditionally, cancer is treated using methods of radiation therapy, chemotherapy and surgery [1]. In order to solve the problems associated with reducing the dosage of the drug and minimize side effects, it is important to use the method of targeted drug delivery using the polymeric nanoparticles and nanocapsules. Nanotechnology-based cancer therapy became one of the promising areas of biomedicine that has been widely studied over the past few decades.[2] The use of nanoparticles in the treatment of cancer overcomes the disadvantages of conventional drug delivery systems, such as nonspecific biodistribution and targeting, insufficient solubility in water, poor oral bioavailability and low therapeutic parameters [3, 4, 5].

Among the main requirements for polymer carriers, the stability and inertness to the blood components should be outlined; also the polymer should protect the drug substance from degradation [6,7]. Human serum albumin was chosen as the polymeric carrier in this work. Albumin is a favorable macromolecular carrier and is widely used in medicine owing to its biodegradability, non-toxicity and non-immunogenicity [8,9]. The incorporation of a drug into albumin nanoparticles is an attempt to carry out the targeted delivery of drug to tumor cells to reduce side effects of the drug. Presently the antitumor drug preparations based on albumin nanoparticles have already been created, but their price is so high that it makes them inaccessible. One of the reasons for the inaccessibility of anticancer drugs created on the basis of nanoparticles is complex synthesis techniques, high energy consumption and instability of nanosystems [10]. To overcome these difficulties, in the framework of this study an attempt was made to develop a relatively simple method for producing albumin nanoparticles, to achieve a high degree of drug immobilization, and to obtain a drug with the potential for prolonged release.

Cyclophosphamide was chosen as a model preparation for immobilization. Cyclophosphamide is a cytostatic antitumor chemotherapeutic drug of an alkylating type of action; a derivative of bis-chloroethylamine and simultaneously a derivative of oxazaphosphorine or a derivative of diamidophosphate (the so-called "phosphoramide mustard"). It is recommended for the treatment of many forms of cancer, including small cell lung cancer, cancer of the ovary, cervix and body of the uterus, breast cancer and others. The drug has many side effects and limitations due to its toxicity and effects on healthy body cells, etc. Thus, ensuring the safety and effectiveness of treatment with this drug is relevant and can be solved using polymeric drug carriers.

Methods

Synthesis of polymer nanoparticles by the incorporation method

Albumin-based nanoparticles of Cyclophosphamide were synthesized using the incorporation method. To an aqueous solution of albumin (2%) was added with a certain speed (not more than 1 ml/min) a solution of the drug in ethanol with concentrations of 2; 4; 8 mg/ml (pH of the solution is 8.0-8.5). The particles formed in this process are small in size (within the range of 50-300 nm). To crosslink the particles glutaraldehyde (6.25% solution) was added to the solution, which stabilized the size and the structure of the particles. Incubation was carried out for 2 hours on a mechanical stirrer (650 rpm). The solution of unreacted serum albumin was purified by washing it three times with deionized water and centrifuging for 15 minutes at 14500 rpm. The obtained nanoparticles were separated by centrifugation (MiniSpin Plus 14500, Eppendorf, Hamburg, Germany). The yield of nanoparticles was determined by gravimetry.

Determination of particle size and polydispersity

The average size of nanoparticles and their polydispersity were determined using photon correlation spectroscopy (FCC) at a Malvern Zetasizer Nano S90 instrument (Malvern Instruments Ltd., UK) at a temperature of 298 K and a scattering angle of 90^0. Each nanoparticle sample was properly diluted with a non-solvent immediately after preparation. The average size and polydispersity index were measured three times for each batch.

Analysis of Nanoparticles Morphology

Nanoparticles' morphology was analyzed by scanning electron microscopy (SEM) using a MIRA 3 LM TESCAN electron microscope (Czech Republic). Carbon was sprayed onto the surface of the samples using magnetron sputtering of carbon fiber to increase conductivity. The measurements were carried out in high vacuum using an SE detector at an accelerating voltage of 4–20 kV.

Investigation of the binding degree of cyclophosphamide with the polymeric nanoparticles

To determine the binding degree of drug to albumin NPs, the obtained particles were separated from the supernatant by ultracentrifugation at 14500 rpm and washed with water. The content of unbound drug was determined spectrophotometrically using a UV-1800 SHIMADZU instrument (Japan) (λ = 247.5 nm).

The Study of Cyclophosphamide Release

The kinetics of drug release from serum albumin NPs was studied using standard methods in phosphate buffered saline at a temperature of 310 K (pH = 7.4). For this, a weighed portion of nanoparticles loaded with cyclophosphamide was dispersed in 10 ml of a phosphate buffer solution. Within 2 days, 2 ml samples were taken from the dispersion at certain time intervals, which were centrifuged at a speed of 14500 rpm. The concentration of the drug in the solution was determined using UV spectroscopy at 247.5 nm [12].

Results and discussion

According to the method described above, an alcoholic drug solution was added to the albumin solution.

The concentration of the drug ranged from 2 to 8 mg/ml. To stabilize the nanoparticles they were crosslinked with glutaraldehyde. The physicochemical characteristics of the particles were determined by photon correlation spectroscopy (PCS). The results of measurements of particle size and polydispersity index are presented in Figure 1 and Table 1. As can be seen from the figure, the obtained nanoparticles have satisfactory physicochemical characteristics: the average particle size was at the range of 148 - 171.5, and the value of polydispersity index is in the interval of 0.0038-0.098. The formation of large particles is not observed in the system, and the particles are uniformly distributed.

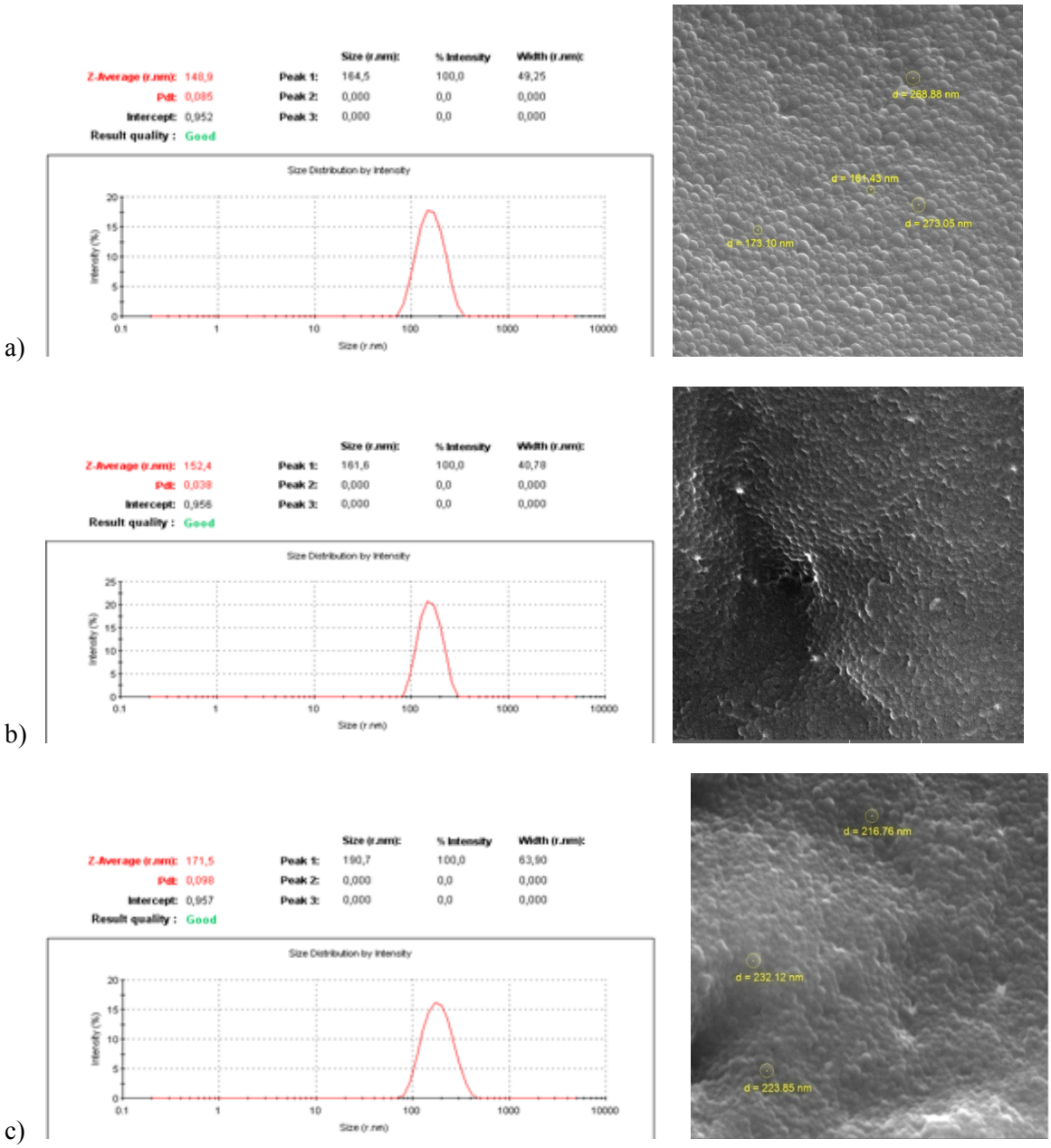

Figure 1 - PCS data and electron microscopic photographs of serum albumin nanoparticles immobilized with cyclophosphamide at concentrations of a) 2 mg / ml; b) 4 mg / ml; c) 8 mg / ml

To confirm the data obtained by the PCS the electron microscopic images of polymeric nanoparticles loaded with cyclophosphamide were made using a scanning electron microscope (Figure 1 a, b, c).

From electron microscopic images (Figure 1), it can be seen that the polymeric nanoparticles have spherical shape and they are uniformly distributed in size and shape: the average particle size of nanoparticles of all concentrations varies from 100 - 300 nm. It was found that with increasing the concentration of the drug the size of the polymeric nanoparticles increases, but their meanings meet the requirements to the nanoparticles for invasive administration. These parameters indicate that the obtained nanoparticles can be used as transporting systems.

The binding degree is an important quantity that characterizes the quantification of the immobilization of a drug substance in a polymer matrix. Therefore, the next step in our study was to determine the binding degree of the cyclophosphamide with albumin nanoparticles. It was found that the binding degree

of cyclophosphamide in the samples reached 92.4% depending on the concentration of the drug (table 1). In this case, the increase in the concentration of the drug in the solution leads to the increase in its content in the polymeric nanoparticles.

Table 1 - Physicochemical characteristics of albumin nanoparticles immobilized with cyclophosphamide

C_{ds}, mg/ml	d, nm	PDI	The yield of the particles with the size up to 1000 nm,%	The binding degree,%	The degree of release,%	The yield of nanoparticles,%
2	140.9	0.154	100	54.6	68.2	70.5
	148.9	0.085	100			
	143.8	0.116	100			
4	152.4	0.038	98.5	79.4	71.5	75.3
	149.1	0.085	100			
	151.2	0.086	99.5			
8	172.6	0.134	100	92.4	77.1	88.5
	171.5	0.098	100			
	168.8	0.116	100			

At the next stage, the release of cyclophosphamide from albumin nanoparticles was studied. The release kinetics was studied under conditions close to physiological (in phosphate-buffered saline at a temperature of 310 K, pH = 7.4) for 2 days. The results of this study are presented in Figure 2.

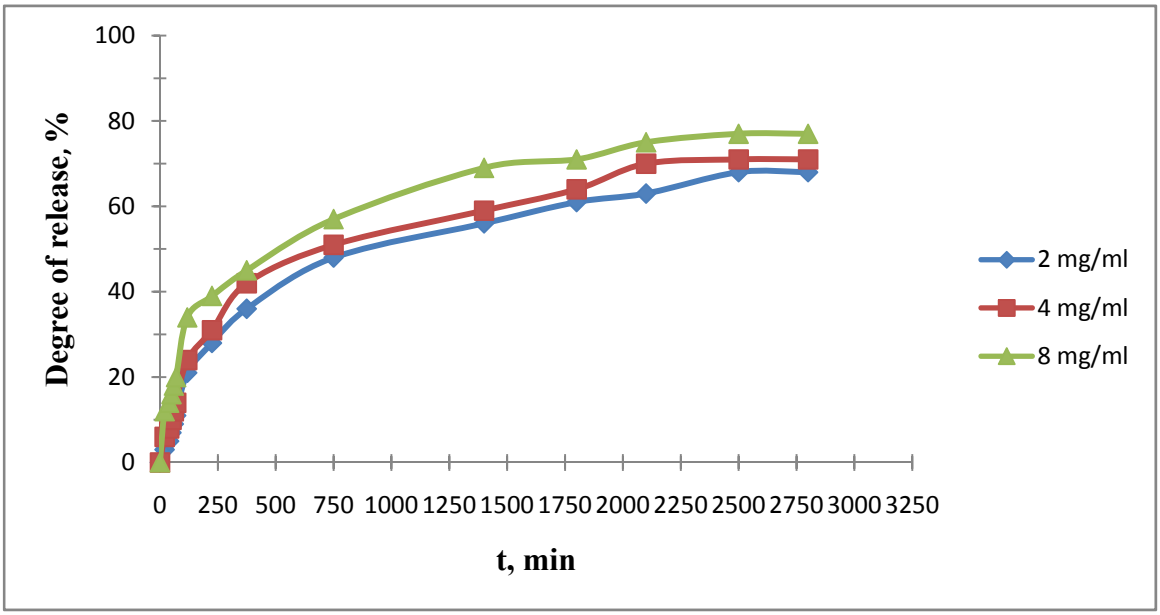

Figure 2 - Kinetics of cyclophosphamide release from NPs

All release curves of cyclophosphamide from the albumin matrix are characterized by the presence of several sites. The first four hours are characterized by the highest speed, when 24-34% of the drug is released which probably characterizes the release of an unbound drug from the surface layer of albumin 1This indicates the retention of the drug in the albumin nanoparticles via non-chemical bonds, possibly via hydrogen, van der Waals, and other bonds. Only after 42 hours the concentration of the drug reaches saturation in solution and its amount is 68-77% depending on the initial concentration. These results point on promising further studies in the field of the creation of prolonged forms of the drug.

Conclusion

It was possible to develop a method for the synthesis of nanometric polymer carriers based on a biocompatible and biodegradable albumin polymer for transporting the anticancer drug Cyclophosphamide. Nanoparticles with satisfactory physicochemical characteristics have been synthesized using incorporaton method. It makes them promising systems for targeted drug delivery. The use of such new dosage forms in the form of nanoparticles will reduce the daily dose of the drug, increase its effectiveness and minimize its side effects.

Е.М. Тажбаев[1], А.А. Бакибаев[2], А.Т. Такибаева[3], Т.С. Жумагалиева[1], Л.Ж. Жапарова[1], А.А. Ағдарбек[1], Н.Ж. Газизова[1], О.Е. Мукашев[1], А.М. Тәжібай[3]

[1]Е.А.Бөкетов атындағы Қарағанды Мемлекеттік Университеті, Қарағанды, Қазақстан
[2]Томский Государственный Университет, Томск, Россия
[3]Қарағанды Мемлекеттік Техникалық Университеті, Қарағанды, Қазақстан

АЛЬБУМИННІҢ ПОЛИМЕРЛІ НАНОБӨЛШЕКТЕРІН АЛУ ЖІНЕ ОЛАРДЫ ҚАТЕРЛІ ІСІККЕ ҚАРСЫ ПРЕПАРАТ «ЦИКЛОФОСФАНМЕН» ИММОБИЛИЗАЦИЯЛАУ

Аннотация. Биоыдырамалы және биоүйлесімді полимерлердің негізіндегі нанобөлшектер дәрілік заттың терапевтикалық әсер ету уақытын ұзарта отырып, сонымен қатар ағзаның сау жасушаларын зақымдамай дәрілік затты мақсатты түрде тікелей нысана ағзаға жеткізуге мүмкіндік береді. Бұл зерттеу қатерлі ісікке қарсы «Циклофосфан» препаратымен иммобилизацияланған адам сарысулы альбуминінің нанобөлшектерін алу жолдарын жасап шығаруға арналған. Коацервация әдісімен 150-170 нм өлшемдегі, полидисперстілік мәні төмен (полидисперстілік индексі 0,069-0,116) альбумин нанобөлшектері алынды. Нанобөлшектердің шығымы 88,5%-ды құрады. Дәрілік заттың полимерлі нанобөлшектермен байланысу дәрежесі 54,6% және 92,4% аралығында болды. Дәрілік заттың босап шығуы пролонгациялық түрде жүрді. 42 сағаттан кейін полимерлі матрицадан биологиялық белсенді заттың 68-77%-ы ортаға босап шықты. «Циклофосфан» препаратына адам сарысулы альбумині негізіндегі нанотасымалдаушыны жасап шығарудың болашағы зор деген қорытынды жасалынды.

Түйін сөздер: нанобөлшектер, дәрі тасымалдаушылар, адам сарысулы альбумині, циклофосфан, циклофосфамид, қатерлі ісікке қарсы препарат.

Е.М. Тажбаев[1], А.А. Бакибаев[2], А.Т. Такибаева[3], Т.С. Жумагалиева[1], Л.Ж. Жапарова[1], А.А. Агдарбек[1], Н.Ж. Газизова[1], О.Е. Мукашев[1], А.М. Тажибай[3]

[1]Карагандинский Государственный Университет им. Е.А.Букетова, Караганда, Казахстан
[2]Томский Государственный Университет, Томск, Россия
[3]Карагандинский Государственный Технический Университет. Караганда, Казахстан

ПОЛУЧЕНИЕ ПОЛИМЕРНЫХ НАНОЧАСТИЦ АЛЬБУМИНА И ИХ ИММОБИЛИЗАЦИЯ ПРОТИВООПУХОЛЕВЫМ ПРЕПАРАТОМ «ЦИКЛОФОСФАН»

Аннотация. Наночастицы на основе биодеградируемых и биосовместимых полимеров дают возможность целенаправленно доставлять лекарственное вещество непосредственно в орган-мишень, при этом не поражая здоровые клетки организма и продлевая срок терапевтического действия лекарственного вещества. Настоящее исследование посвящено разработке способа получения наночастиц человеческого сывороточного альбумина (ЧСА), иммобилизированного противоопухолевым препаратом «Циклофосфан». Методом коацервации получены наночастицы альбумина с размерами 150-170 нм, узкой полидисперстностью (индекс полидисперстности 0,069-0,116). Выход наночастиц составил до 88,5%. Степень связывания лекарства с полимерными наночастицами находилась в пределах 54,6% до 92,4%. Высвобождение препарата происходило пролонгированно. Через 42 часа из полимерной матрицы высвободилось 68-77% биологически-активного вещества. Сделан вывод о перспективности создания наноносителя на основе ЧСА для препарата «Циклофосфан».

Ключевые слова: наночастицы, носители лекарств, человеческий сывороточный альбумин, циклофосфан, циклофосфамид, противоопухолевый препарат.

Information about authors:

Yerkeblan M. Tazhbayev - Academician E.A. Buketov Karaganda State University, Vice Rector for Innovation in Science and Technology, Dr. Chem. Sci., professor, E-mail address: tazhbaev@mail.ru, https://orcid.org/0000-0003-2043-6672

Abdigali A. Bakibaev - Tomsk State University, Leading Researcher, Dr. Chem. Sci., professor, E-mail address: bakibaev@mail.ru, https://orcid.org/0000-0002-3335-3166

Altynarai T.Takibayeva – Karaganda State Technical University, Cand. Chem. Sci., E-mail address: altynarai81@mail.ru, https://orcid.org/0000-0003-0536-0817

Tolkyn S. Zhumagalieva – Academician E.A. Buketov Karaganda State University, Cand. Chem. Sci., E-mail address: zhumagalieva79@mail.ru, https://orcid.org/0000-0003-1765-752X

Lyazzat Zh. Zhaparova – Academician E.A. Buketov Karaganda State University, PhD, E-mail address: lyazzh@mail.ru, https://orcid.org/0000-0003-1894-0255

Ayaulym A. Agdarbek – Academician E.A. Buketov Karaganda State University, 2nd year Master student, E-mail address: ayaulym_agdarbek@mail.ru, https://orcid.org/0000-0001-8808-8315

Nazgul Zh. Gazizova – Academician E.A. Buketov Karaganda State University, 2nd year Master student,, E-mail address: gazizovanz@gmail.com, https://orcid.org/0000-0002-9692-2768

Olzhas E. Mukashev - Academician E.A. Buketov Karaganda State University, 3rd year–PhD Student, E-mail address: mukashevoe@gmail.com, https://orcid.org/0000-0002-8040-6515

Aizhan M. Tazhibay - Karaganda State Technical University, 2nd year Master student, E-mail address: aika_93_16@mail.ru, https://orcid.org/0000-0001-8190-3647

REFERENCES

[1] Urruticoechea A., Alemany R., Balart J., Villanueva A., Vicals F., Capellб G. Recent advances in cancer therapy: An overview. Curr. Pharm. Des. 2010;16:3–10.

[2] Nanotechnology in Medicine and the Biosciences, by Coombs RRH, Robinson DW. 1996, ISBN 2-88449-080-9.

[3] Cai W, Gao T, Hong H, Sun J (2008) Applications of gold nanoparticles in cancer nanotechnology. Nanotechnol Sci Appl 1(1):17–32

[4] Sultana N, Shenoy SB, Sham ME, Keshav S, Kaul R (2012) Nanogoldtechnology-imaging, sensing and target therapy in head and neck cancer. Clin Cancer Investig J 1(1):6–12

[5] Nie, Shuming, Yun Xing, Gloria J. Kim, and Jonathan W. Simmons (2007). «Nanotechnology Applications in Cancer». Annual Review of Biomedical Engineering 9: 257–88. DOI:10.1146/annurev.bioeng.9.060906.152025. PMID 17439359.

[6] I. Vural, H.S. Kas, A.A. Hincal, G. Cavcë, J. Microencapsulation 4 (7) (1990) 511–516.

[7] Mudshinge SR, Deore AB, Patil S, Bhalgat CM. Nanoparticles: emerging carriers for drug delivery. Saudi Pharm J SPJ Off Publ Saudi Pharm Soc. 2011;19(3) :129–41. doi:10.1016/j.jsps.2011.04.001.

[8] Lordick F., Hacker U. In: Chemotherapy and Targeted Therapy, in Imaging of Complications and Toxicity following Tumor Therapy. Kauczor H.-U., Вдuerle T., editors. Springer International Publishing; Cham (ZG, Switzerland): 2015. pp. 3–15.

[9] G.V. Patil, Biopolymer albumin for diagnosis and in drug delivery, Drug Dev. Res. 58 (2003) 219–247.

[10] Kratz F. Albumin as a drug carrier: Design of prodrugs, drug conjugates and nanoparticles // J. Cont. Rel. 2008. 132. P. 171-183.

[11] Bayeshov A., Abijanova D. A., Abduvalieva U. A., Zhurinov M. (2019) Study of electrochemical properties of copper in solution of sulphuric acid with copper (11) ions and titan through potentiodynamic polarized curve //Bulletin of national academy of sciences of the Republic of Kazakhstan. 2019. Vol. 2, N378. P.241-248. ISSN 1991-3494 (Print). https://d0i.org/10.32014/2019.2518-1467.62

[12] E.M. Tazhbaev, M.Zh. Burkeev, L.Zh. Zhaparova, T.S. Zhumagalieva, A.A. Agdarbek (2019) Albumin nanoparticles loaded with the antitumor drug “Hydroxycarbamide” by the incorporation method // Bulletin of the Karaganda University, Chemistry series. 2019. Vol.1 (93), P. 48-53. ISSN 2518-718X. DOI: 10.31489/2019Ch1/54-59

N E W S
OF THE NATIONAL ACADEMY OF SCIENCES OF THE REPUBLIC OF KAZAKHSTAN
SERIES CHEMISTRY AND TECHNOLOGY
ISSN 2224-5286 **https://doi.org/10.32014/2019.2518-1491.72**
Volume 6, Number 438 (2019), 42 – 48

UDK 541.64+678

Zh.B. Rakhimberlinova[1], G.A. Mustafina[2], A.T. Takibayeva[1], I.V. Kulakov[3], A.R. Iskakov[1],O.G. Nazarova[1]

[1]Karaganda State Technical University, Karaganda, Kazakhstan;
[2]LP «KAZ-OPTIMUM», Karaganda, Kazakhstan;
[3]Tyumen State University, Tyumen, Russia
E-mail:kargtu_tss@mail.ru

SYNTHESIZING NITRILE-CONTAINING GLYCONITRILE (CO) POLYMERS

Abstract. The article presents the results of studying the production of new nitrile-containing monomers by acylation of unsaturated N- and N,N′ - α-aminoacetonitrile chlorides (meta) acrylic acids using acrylamide. The initial unsaturated N- and N,N′ - α-aminoacetonitriles were synthesized by interaction of glycolic acid nitrile (glyconitrile) with amines of various classes. The ability of new monomers to radical (co)polymerization was studied, namely, the possibility of producing polyacrylamides based on N,N′ nitrile derivatives of (meta) acrylamide and vinyl ester (N - acetonitrile) monoetholamine (VEEAN) with acrylamide in bulk in the presence of radical initiators and organic solvents with formation of carbochain polymers. The formation of nitrile-containing polyacryamides is confirmed by the data of the elemental analysis, viscometry, IR spectroscopy. Viscometric data [ή] = 0.10 - 0.29 dl/g of polymers indicate low reactivity of the synthesized nitrile acrylamides compared to acrylamide that is associated with the steric effect of the chain length. The synthesized copolymers were studied as modifiers of urea-formaldehyde binders (UFB) used to strengthen unstable rocks. The samples strengthened with UFB solutions without a modifier showed low strength indices for 62 and 77 % concentrations, respectively, while introduction of nitrile-containing copolymers in the amount of 1-5 % wt. improved strength characteristics of the samples by 1.2-1.8 times. The good strength results for mine rocks are explained by the increased flexibility and elasticity of the urea-formaldehyde binder chains with new functional groups responsible for the resin adhesion to the rock.

Keywords:α-aminoacetonitriles, glycolic acid nitrile (glyconitrile), monoethanolamine vinyl ester, acrylamide, polyacrylamide, N,N'- acrylamide nitrile derivatives, copolymers, urea-formaldehyde binder modifiers.

Introduction

Recently the scientific and practical interest in the directed synthesis of nitrile-containing polyfunctional polymers has been steadily growing. This is caused by a wide range of useful properties of these (co)polymers that can be further used as promising flocculants, coagulants, polyelectrolytes, modifiers for urea binders, semi-synthetic soil structures. Great prospects in this direction are opened by studying the interaction of glyconitrile with various compounds cuased by its extremely high reactivity and associated with it rich possibility of obtaining a wide variety of organic compounds. Among the variety of compounds synthesized from glyconitrile, the most interesting are its N- and N,N'-α-amino derivatives, which is associated with the ease of their preparation, the possibility of chemical transformations and their practical significance. Many of them can be proposed as polyfunctional monomers for polymerization or polycondensation, which will allow obtaining new types of interesting polymers both in practical and in scientific terms.

Nitrile-containing polyfunctional polymers described in the article were obtained by joint radical (co)polymerization of monomers of nitrile derivatives N,N'- (meta) acrylamide that were synthesized by acylation of unsaturated N- and N,N'- α-aminoacetonitriles (meta) acrylic acids, acrylates.

The obtained (co)polymers based on derivatives of glycolic acid nitrile are assigned to carbochain polymers of linear structure with long side groups. New nitrile-containing (co)polymers are characterized by a low molecular weight and a significant number of functional groups capable of further transformations and predetermining various fields of their application [1-2].

Experimental Part

Synthesizing α-aminoacetonitriles (I-VI)

Aminoacetonitrile NH_2CH_2CN (I). 16 ml of the 70% aqueous glyconitrile solution (0.2 mol) are added dropwise to 13.6 ml of the 23% aqueous ammonia solution (0.2 mol) with cooling at the temperature of 0-5 °C so that the temperature of the reaction mixture does not exceed 10 °C. After that, the synthesis temperature is raised to the room temperature and held within 1.5 hours. 20 ml of concentrated HCl (0.2 mol) are added to the reaction mixture. The mixture containing aminoacetonitrile in the form of hydrochloric acid salt is evaporated. $HCl{\cdot}NH_2$-CH_2-CN crystals are washed with ester and dried.

N-methylaminoacetonitrile CH_3NHCH_2CN (II). The synthesis is carried out analogously to (I) with 2 moles of amine. At the end of the synthesis, the reaction mixture is saturated with sodium sulfate and extracted repeatedly with diethyl ester. The solvent is distilled off, the residue is subjected to vacuum distillation.

N-allylaminoacetonitrile CH_2=CH-CH_2-NH-CH_2CN (III). To 22.8 ml of the 50 % aqueous solution of allylamine (0.2 mol) there are added dropwise 16 ml of the 70 % aqueous solution of glyconitrile (0.2 mol) while the reaction mixture is cooled to 5 °C. Upon completion of adding the glyconitrile solution, the mixture is heated to 35 °C and kept at this temperature within 2 hours. The separated oil layer of aminonitrile is separated from the aqueous solution using a separatory funnel. An additional amount of aminonitrile is extracted from the aqueous layer with diethyl ester. The ester extract and the organic layer are mixed, dried over anhydrous sodium sulfate, diethyl ester is distilled off, the residue is subjected to vacuum fractional distillation.

*Vinyl ester of (-N-acetonitrile)-ethanolamine CH_2=CH-O-CH_2CH_2NH-CH_2CN (IV).*The synthesis is carried out similarly to (III) with 0.2 moles of amine at 35-40 °C.

N-benzylaminoacetonitrile $C_6H_5CH_2NHCH_2CN$ (V-VI). The synthesis is carried out similarlyto (III) with 0.2 moles of amine at 35-40 °C (Table 1).

Table 1 - Synthesizing α – aminoacetonitrile – $RHNCH_2CN$

Compounds	R	Yield, %	T_{boil}, °C	d_4^{20}	n_D^{20}
I	H	80	T_{mel}165-166	-	-
II	CH_3	65	45/0.4	0.9300	1.4199
III	CH_2═CH─CH_2	78	85-88/0.4	0.9281	1.4486
IV	CH_2═CH─CH─ ─O─CH_2─CH_2	90	91-93/0.4	1.0060	1.4691
V	$C_6H_5CH_2$	90	130-133/0.4	1.0460	1.5388
VI	C_6H_5	50	145/1	-	-

Synthesizing N,N′-derivatives of glycolic acid nitrile (VII-XI)

N,N′-substituted acrylamides: a) a mixture of 200 ml of benzene (diethyl ester or acetone), 7 g of dry K_2CO_3 and 0.2 mol of α-aminoacetonitrile is cooled to 8-10 °C, a solution of 0.2 mol of acrylic acid chloride is added dropwise in 60 ml of benzene (diethyl ester or acetone) at such a rate that the temperature of the reaction mixture does not exceed 10 °C. After 45 minutes, another 7 g of dry $K_2CO_3$are added and stirred within 1 hour at 10 °C, then 1 hour at the room temperature. The inorganic precipitate is filtered off, washed twice with 60 ml of hot benzene (diethyl ester or acetone). The solvent is distilled off, the residue containing nitrile-substituted acrylamide is subjected to fractional vacuum distillation in the presence of the copper chip polymerization inhibitor (Table 2).

b) In the aqueous medium synthesizing N,N′-substituted acrylamides is carried out according to the following procedure: an equimolar amount of acrylic acid chloride in benzene and the 50 % aqueous

NaOH solution are added from two dropping funnels to the reaction mixture of α-aminoacetonitriles obtained by the above procedure II-VI with vigorous stirring and cooling (-5 °C). Then the reaction mixture is kept within 1 hour at the room temperature. The final product is extracted with benzene, the solvent is distilled off, nitrile-substituted acrylamide is subjected to vacuum distillation. Their characteristics are given in Table 2.

Table 2 –Characteristics of N,N′-substituted acrylamides

Compound No.	R	R′	Yield, g	T_{boil}, °C; 0,4 MPa
VII	CH_3	H	15.0 (54)	115-118
VIII	CH_3	CH_3	19.0 (75)	117-120
VIII	CH_3	CH_3	20.3 (80)*	117-120
IX	CH_2=CH-O-CH_2CH_2	H	19.0 (62)	140-142
X	CH_2=CH-O-CH_2CH_2	CH_3	30.6 (90)	147-149
XI	CH_2=CH-O-CH_2CH_2	CH_3	28.0 (85)*	147-149
*-in the aqueous medium				

Homopolymer of N,N′-derivatives of acrylamide (XII)

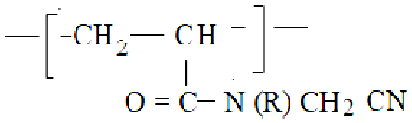

The synthesis is carried out by radical polymerization in bulk or in dimethylformamide (DMF) in the presence of radical initiators: dinitrile azobisisobutyric acid (DAA) or benzoyl peroxide in the amount of 0.5-1 % of the total weight of the monomer at 70 % within 6-10 hours, in argon atmosphere. The copolymers obtained are reprecipitated from solutions in dioxane, acetone, dimethylformamide (DMF), water or methanol and dried at the room temperature in a vacuum oven to the constant weight.

(-N-acetonitrile) ethanolamine vinyl ester copolymers (XIII)

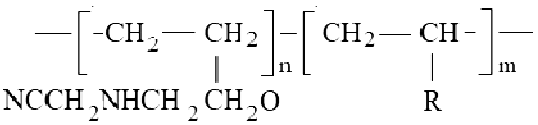

a) with alkyl acrylates (R = -OR ′, where R′-CH_3-; C_2H_5-; C_4H_9-) are obtained in bulk in the presence of 0.5 % DAA at various ratios of monomers, the synthesis temperature is 70 °C, and the duration is 6 hours. The copolymers are reprecipitated according to procedure (1);

b) with acrylamide:

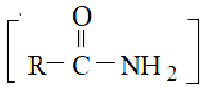

is obtained by copolymerization of components in DMF, in the presence of DAA in the amount of 0.5 % of the monomer weight at the temperature of 70 °C within 6 hours, the ratio of the starting reagents is equimolar. The copolymers are reprecipitated according to procedure (1).

Urea-formaldehyde binders UFB modifications (XIV–XV). Synthesized copolymer (XII) was diluted with water-dioxane (2:1) to the 50 % concentration, the specific gravity of the solution was 1.078 g/cm^3, and copolymer (XIII) was diluted to the 70 % concentration with the specific gravity of 1.073 g/cm^3.

Resultsanddiscussion

The subject of our studies were copolymers and polymers of nitrile derivatives of N,N'(meta) acrylamide with acrylamide that were studied as new modifiers for urea binders used to strengthen unstable rocks, semi-synthetic soil structures, foaming agents in flotation concentration of sulfide copper ores.

Unsaturated N- and N,N'- α-aminoacetonitriles were used as starting monomers for synthesizing the above polymers. The synthesis of α-aminoacetonitriles is based on the reaction of glycolic acid nitrile (glyconitrile) interaction with amines of various classes according to the scheme:

$$RR'NH + HOCH_2CN \rightarrow RR'NCH_2CN + H_2O,$$

where R and R' are alkyl, aryl, alkenyl, heterocycle.

The specific structure of glyconitrile, namely, the close proximity of OH and CN - groups determines the features of its interaction with primary and secondary amines. The synthesis of glyconitrile with amines was studied at the equimolar ratio of the starting reagents, various temperatures, durations, solvents, and the concentration of the starting reagents. The optimum process parameters were found (40-60 °C, 1-2 hours, amine concentration 50-100 %, glyconitrile concentration 50-70 %, water). Above 60 °C side reactions begin to occur with participation of C≡N and NH - groups of products of imines or resins formation. In organic solvents the yield of final products is significantly reduced.

Their structure is confirmed by the data of the elemental analysis, IR and NMR spectra. IR spectra of aminonitriles are characterized by the presence of a number of absorption bands, groups: 2250 - 2240 cm^{-1} - C≡N; 3400 - 3320 cm^{-1} – NH; 1640 cm^{-1} – CH_2═ CH- .

The new N,N' derivatives of acrylamide were synthesized by acylation of unsaturated R-α-aminoacetonitriles obtained by the above procedure with (meta) acrylic acid chlorides:

$$RNHCH_2CN + CH_2 = CR_1\text{-}COCL \longrightarrow CH_2{=}CR_2\text{-}\underset{\underset{O}{\|}}{C}\text{-}\underset{\underset{R'}{|}}{N}CH_2CN \qquad 1)$$

where R = H, - NH-CH_2CH_2OCH═CH_2; R' = H, - CH_3.

The physical-and-chemical constants of the obtained N,N'-derivatives of acrylamide are presented in Table 2. Their composition and structure were confirmed by the elemental analysis, IR and NMR spectra.

The IR spectra of these compounds contain absorption bands in the region of 2300 cm^{-1} (nitrile group), 1650–1680 cm^{-1} (amide group), 1800–1860 cm^{-1} (vinyl group). The NMR spectra show absorption bands of methylene protons of the – CH_2CN group (region 4.26–4.67 ppm) and vinyl protons at 5.9–6.9 ppm and 5.25-6.03 ppm.

We investigated the possibility of producing polymers based on N,N'- nitrile derivatives of (meta) acrylamide and vinyl ester (N - acetonitrile) - monoetholamine (VEEAN) with acryamide with formation of carbochain polymers of the following structure:

- copolymers of N,N'- nitrile derivatives (meta) of acrylamide with acrylamide:

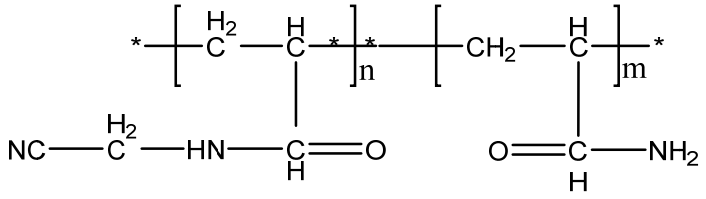

(2)

- copolymer of vinyl ester (N-acetonitrile)-ethanolamine with acrylamide

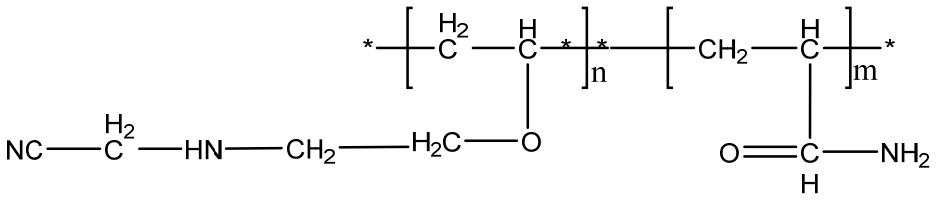

3)

The viscometric data [ή] = 0.10 - 0.29 dl/g of polymers indicate low reactivity of the synthesized nitriacryamides compared to acrylamide that is associated with the steric effect of the long chain and the nature of the R_1 substituent. For the obtained polymers, an anomalous dependence of viscosity on solution concentration is observed, which is associated with the presence of ionogenic groups in the composition. It allows attributing them to polyelectrolytes.

The synthesized copolymers were investigated as modifiers for urea binders (UFB) used to strengthen unstable rocks.

Modification was carried out by combining aqueous solutions of UFB with the copolymers taken in the amount of 1-5 % of the UFB weight. It was noted that copolymers combine well with UFB and do not stratify over time. The presence of active functional groups (CO =, C≡N, NH2, -C-O, $CONH_2$) in the modifiers contributed to increasing the adhesive ability.

In order to establish the modifying effect of the copolymers based on synthesized (co)polymers for compressive strength, the mixtures with a hardener, oxalic acid, and with a filler, ground mine rock, represented by medium strength mudstone, were compiled. The resin to rock ratio was 1: 6, the mixture was loaded into molds and pressed at 10 atm within 3 minutes. Testing the strengthened samples for compressive strength was carried out after 7 and 21 days of storage in the air at 15 °C. The results of testing the rock samples reinforced with modified solutions of UFB depending on the concentration of resin and modifier are presented in Table 3.

Table 3 - The use of polymers based on copolymers of nitrile derivatives of N,N'(meta) acrylamide with acrylamide as bindersfor mine rocks

No.	Modifier	Concentration, %	Modifier concentration %	Compression strength of the samples, kp/cm^2	
				Storage time	days
				7	21
	UFB without a modifier	77	0	18.4	31.1
XIV	(N-acetonitrile)-ethanolamine vinyl ester copolymer with acrylamide	77	1	26.9	41.0
		77	3	-	38.2
		77	5	-	39.6
		62	5	19.8	26.9
XV	Methylacetonitrile acrylamide copolymer with acrylamide	77	-	-	53.8
		77	3	-	56.6
		77	5	-	56.6
		62	5	-	26.2

From the data of Table 3 it follows that the samples strengthened with UFB solutions without a modifier have low strength indicators for 62 and 77 % concentration, respectively. The introduction of nitrile-containing copolymers in the amount of 1-5 % wt. increases the strengthened samples strength by 1.2-1.8 times in comparison with the samples strengthened with unmodified UFB. It has been shown that with decreasing the concentration of UFB in the binder, the samples strength decreases. Increasing the modifier concentration from 1 to 5 % wt. does not lead to a substantial increase in strength properties.

Conclusions

Thus, as a result of studies performed, by the acylation reaction of N- and N,N'- α- aminoacetonitrile chlorides of (meta)acrylic acids with acrylamide, new monomers of (meta)acrylamide were obtained and characterized. The initial unsaturated N- and N,N'- α- aminoacetonitriles were synthesized by the interaction of glycolic acid nitrile (glyconitrile) with amines of various classes. The ability of new monomers to radical (co)polymerization in bulk and in organic solvents with formation of nitrile-containing polyacrylamides has been shown.

According to the results of laboratory tests, the synthesized copolymers have shown that they are good binders for mine rocks, providing relatively high mechanical strength compared to unmodified binders. The strengthening effect of modifiers is caused by increasing the flexibility and elasticity of urea-formaldehyde binder chains (UFB) with the advent of new functional groups CO =; C≡N; CONH2; C-O-C that are responsible for the resin adhesion to the rock.

Ж.Б. Рахимберлинова[1], Г.А. Мустафина[2], А.Т. Такибаева[1],
И.В. Кулаков[3], А. Р. Искаков[1], О.Г. Назарова[1]

[1]Қарағанды мемлекеттік техникалық университеті, Қарағанды, Қазақстан;
[2] ЖШС «KAZ-OPTIMUM», Қарағанды, Қазақстан;
[3]Тюмень мемлекеттік университеті, Тюмень, Ресей

НИТРИЛ ҚҰРАМДЫ ГЛИКОНИТРИЛ СО ПОЛИМЕРЛЕРІНІҢ СИНТЕЗІ

Аннотация. Мақалада N - и N,N′ - α - аминоацетонитрилдерді хлорангидридтермен (мета) акрил қышқылдарымен, акриламидпен ацилдеу жолымен жаңа нитрил бар мономерлерді алуды зерттеу нәтижелері келтірілген. Бастапқы күтпеген N - және N,N′ - α - аминоацетонитрилдер әртүрлі класты аминдермен гликоль қышқылы (гликонитрил) нитрилінің өзара әрекеттесуімен синтезделген. Жаңа мономерлердің радикалды (со)полимерлеуге қабілеттілігі зерттелді, атап айтқанда N,N′ – нитрил туынды (мета) акриламид пен винил эфирі (N – ацетонитрил) моноэтоламин (ВЭЭАН) негізінде радикалды бастамашылардың қатысуымен және карбоцепті полимерлер түзілетін органикалық еріткіштерде акриламидпен полиакриламид алу мүмкіндігі зерттелді. Құрамында нитрил бар полиакриламидтердің түзілуі элементтік талдау, вискозиметрия, ИК – спектроскопия деректерімен расталған. [ή] = 0,10 - 0,29 дл/г полимерлердің вискозиметриялық деректері синтезделген нитрилакриламидтердің акриламидпен салыстырғанда реакциялық қабілетінің төмендігін көрсетеді, бұл тізбек ұзындығының стерильді әсерімен байланысты. Синтезделген сополимерлер тұрақсыз тау жыныстарын нығайту үшін пайдаланылатын мочевино-формальдегидті байланыстырғыш (МФС) модификаторлар ретінде зерттелді. Модификаторсыз МФС ерітіндісімен бекітілген үлгілер 62 және 77% концентрацияға арналған төмен беріктік көрсеткіштерін көрсетті, 1-5% салмақ мөлшерінде нитрил бар сополимерлерді енгізу. үлгілердің беріктігін 1,2-1,8 есеге жақсартты. Шахталық жыныстар үшін беріктік көрсеткіштері бойынша жақсы нәтижелер шайырдың жынысқа адгезиясына жауапты жаңа функционалдық топтармен несепнәрформальдегидті байланыстырушы тізбектерінің икемділігі мен икемділігінің артуымен түсіндіріледі.

Түйін сөздер: α –аминоацетонитрилдер, гликоль қышқылының нитрилі (гликонитрил), моноэтаноламин винил эфирі, акриламид, полиакриламид, N, N' – нитрил туынды акриламид, сополимерлер, мочевин-формальдегидті байланыстырғыштардың модификаторлары.

Ж.Б. Рахимберлинова[1], Г.А. Мустафина[2], А.Т. Такибаева[1],
И.В. Кулаков[3], А. Р. Искаков[1], О.Г. Назарова[1]

[1]Карагандинский государственный технический университет, Караганда, Казахстан;
[2]ТОО «KAZ-OPTIMUM», Караганда, Казахстан;
[3]Тюменский государственный университет, Тюмень, Россия

СИНТЕЗ НИТРИЛСОДЕРЖАЩИХ (СО) ПОЛИМЕРОВ ГЛИКОНИТРИЛА

Аннотация. В статье приведены результаты исследований получения новых нитрилсодержащих мономеров путем ацилирования непредельных N- и N,N′ - α – аминоацетонитрилов хлорангидридами (мета) акриловых кислот, акриламидом. Исходные непредельные N- и N,N′ - α – аминоацетонитрилы синтезированы взаимодействием нитрила гликолевой кислоты (гликонитрила) с аминами различного класса. Изучена способность новых мономеров к радикальной (со)полимеризации, а именно возможность получения полиакриламидов на основе N,N′ – нитрилпроизводных (мета) акриламида и винилового эфира (N – ацетонитрил) моноэтоламина (ВЭЭАН) с акриламидом в массе в присутствии радикальных инициаторов и органических растворителях с образованием карбоцепных полимеров. Образование нитрилсодержащих полиакриамидов подтверждено данными элементного анализа, визкозиметрии, ИК – спектроскопии. Вискозиметрические данные [ή] = 0,10 – 0,29 дл/г полимеров свидетельствуют о невысокой реакционной способности синтезированных нитрилакриламидов по сравнению с акриламидом, что связано с стерическим влиянием длины цепи. Синтезированные сополимеры были исследованы в качестве модификаторов мочевино-формальдегидных связующих (МФС), используемых для укрепления неустойчивых горных пород. Образцы, укрепленные растворами МФС без модификатора, показали низкие прочностные показатели для 62 и 77% концентрации соответственно, введение же нитрилсодержащих сополимеров в количестве 1-5% вес. улучшили прочностные характеристики образцов в 1,2-1,8 раза. Хорошие результаты по прочностным показателям для шахтных пород объясняется увеличением гибкости и эластичности цепей

мочевиноформальдегидных связующих новыми функциональными группами, ответственных за адгезию смолы к породе.

Ключевые слова: α – аминоацетонитрилы, нитрил гликолевой кислоты (гликонитрил), виниловый эфир моноэтаноламина, акриламид, полиакриламид, N,N' – нитрилпроизводные акриламида, сополимеры, модификаторы мочевин-формальдегидных связующих.

Information about the authors:

Rakhimberlinova Zh.B. – Candidate of Chemical Sciences, Karaganda State Technical University, e-mail:kargtu_tss@mail.ru, orcid.org/0000-0002-3326-0998

Mustafina G.A. - Candidate of Chemical Sciences, LTD «KAZ-OPTIMUM», e-mail: gmustafina@list.ru, orcid.org/0000-0001-7265-2524

Takibayeva A.T. – Candidate of Chemical Sciences, Karaganda State Technical University, e-mail: altynarai81@mail.ru, orcid.org/0000-0003-0536-0817

Kulakov I.V. – Candidate of Chemical Sciences,Tyumen State University, e-mail:ivanku1@mail.ru, orcid.org/0000-0001-5772-2096.

Iskakov A.R. – Master student, Karaganda State Technical University, e-mail:arnur2397@mail.ru, orcid.org/0000-0003-4303-0894

Nazarova O.G. - Master student, Karaganda State Technical University, e-mail:nazarova_olga_pochta@mail.ru, orcid.org/0000-0003-4166-0905

REFERENCES

[1] Dukjoon Kim. Swelling and mechanical properties of superporous hydrogels of poly(acrylamide-co-acrylic acid)/polyethylenimine interpenetrating polymer networks / Dukjoon Kim., Kinam Park // J. Polymer. 2004. Vol. 45. Issue 1. P. 189–196.

[2] Patent 8080595B2 USA. Process for grinding in an aqueous medium of mineral matter and binders using a reverse emulsion of a polymer acrylamide with an acrylic monomer / atrickGane, Rothrist (CH), Philipp Hunziker, Joachim Schoellkopf, Killwangen (CH).20.12.2011.

[3] Terekhov I.V. Obtaining a copolymer of acrylonitrile and acrylic acid under conditions of living radical polymerization / I.V. Terekhov, N.V. Timoshenko, V.V. Kireyev, S.N. Filatov // Advances in Chemistry and Chemical Technology. 2010. V. 24, No. 4. P. 95.

[4] Timoshenko N.V. Nitrile-containing imid-forming acrylic copolymers: Diss. for the degree of Cand. Chem.: specialty 02.00.06 "High molecular compounds" / N.V. Tymoshenko. Moscow, 2013. 17 p.

[5] TakibayevaA.T., KulakovI.V., SydykovaD.M., KapbassovaA.S., RakhimberlinovaZh.B. Selecting optimal modes of knotweed raw materials pressing out and developing technology for obtaining dry extract // News of the Academy of sciences of the Republic of Kazakhstan, series chemistry and technology. 2019. № 5. P. 82-87. https://doi.org/10.32014/2019.2518-1491.57.

[6] TakibayevaA.T., KulakovI.V., KapbassovaA.S., SydykovaD.M., RakhimberlinovaZh.B.Optimization of methods of quantitative determiningflavanoids in knotweed raw material// News of the Academy of sciences of the Republic of Kazakhstan, series chemistry and technology. 2019. № 5. P. 88-91. https://doi.org/10.32014/2019.2518-1491.58.

[7] NurkenovO. A., Ibraev M.K., Seilkhanov T.M., Shulgau Z.T., Fazylov S.D., TakibayevaA.T. Synthesis, structure and anti-radical activity of 6-methyl-4-oxo-4н-chromen-3-acylhydrazones // News of the Academy of sciences of the Republic of Kazakhstan, series chemistry and technology. 2019. № 4. P. 25-31.https://doi.org/10.32014/2019.2518-1491.38.

N E W S
OF THE NATIONAL ACADEMY OF SCIENCES OF THE REPUBLIC OF KAZAKHSTAN
SERIES CHEMISTRY AND TECHNOLOGY
ISSN 2224-5286 **https://doi.org/10.32014/2019.2518-1491.73**
Volume 6, Number 438 (2019), 49 – 54

UDC 547.918:547.926

D. Usmanov[1], N.Sh. Ramazanov[1], U. Yusupova[1], K.Dzh. Kucherbayev[2,3]

[1]Institute of Chemistry of Plant Substances AS RUz, Tashkent, Uzbekistan;
[2]Regional Social-Innovational University, Shymkent, Kazakhstan;
[3]JSC «South-Kazakhstan Medical Academy», Shymkent, Kazakhstan

IRIDOIDS FROM *PHLOMIS SEVERTZOVII* AND ITS IMMUNOSTIMULATING AND ANTITOXIC ACTIVITY

Abstract. From the aerial parts of *Phlomis severtzovii* (*Lamiaceae*) growing in Uzbekistan, five known iridoid glycosides were isolated for the first time. On basis of UV, IR, ^{1}H and ^{12}C NMR spectroscopy the isolated substances were identified as 6β-hydroxypolamid (1), loganin (2), pulchelloside (3), shanshiside methyl ester (4) and phlorigidoside C (5). Additionally, noticeable immunostimulating and antitoxic activity of the sum of iridoids and 6β-hydroxypolamid (1) were revealed.

Keywords: *Phlomis severtzovii*, iridoid, 6β-hydroxypolamid, loganin, pulchelloside, shanshiside methyl ester, phlorigidoside C, immunostimulating activity, antitoxic effect.

Introduction. Among the various low-molecular biologically active substances synthesized by plants, iridoids occupy a prominent place. At present time, it is clear, that this type of compounds are widespread in plant world [1]. Presence of important biological activities (antitumor activity, antimicrobial activity, etc.) of these compounds is main perspective practical reason for further investigation [2].

Iridoid glycosides have great theoretical importance as in terms of chemistry and due to their participation as precursors in alkaloid biosynthesis [3].

Therefore search of novel iridoidcontaining plant sources, development of rational scheme of isolation of these compounds, determination their chemical structure, revealing of physical, chemical parameters and useful properties of novel compounds are actual problems of the modern bioorganic chemistry [4].

The aim of our study is investigation of iridoids from *Phlomis severtzovii* (*Lamiaceae*) and their biological activity.

Materials and methods. *Phlomis severtzovii* (*Lamiaceae*) growing in Middle Asia, Tashkent and Fergana regions.

NMR spectra were acquired on a Bruker, 500 MHz, spectrometer using standard pulse sequence at ambient temperature. Chemical shifts are given in δ (ppm), and coupling constants are reported in Hz. The samples for NMR analysis were diluted in C_5D_5N.

Results and discussion. Five known iridoid glycosides were isolated from the aerial parts of *Phlomis severtzovii* collected during vegetation phase. Their chemical structure were determined on basis of analysis of UV, IR, ^{1}H and ^{13}C NMR spectra and identified as 6β-hydroxypolamid **1**, loganin **2**, pulchelloside **3**, shanshiside methyl ester **4** and phlorigidoside C **5** (Fig.1).

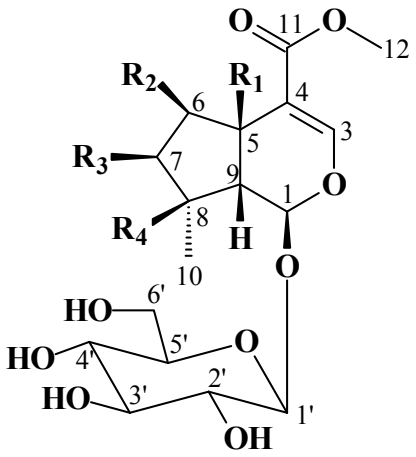

1: R_1 = OH, R_2 = OH, R_3 = H, R_4 = OH
2: R_1 = H, R_2 = H, R_3 = OH, R_4 = H
3: R_1 = OH, R_2 = OH, R_3 = OH, R_4 = H
4: R_1 = H, R_2 = OH, R_3 = H, R_4 = OH
5: R_1 = H, R_2 = OH, $R_3 + R_4$ = O

Figure 1 – Chemical structures of iridoid glycosides isolated from the aerial parts of *Phlomis severtzovii*

6β-Hydroxypolamid (1). Compound **1** was isolated as pale yellow crystals, $C_{17}H_{26}O_{12}$, ESI-MS *m/z* 445.15 $[M + Na]^+$, mp 76°C, UV (C_2H_5OH) λ_{max} 235.5 nm. IR (KBr) ν_{max} 3388 (OH), 1639 (C=O), 1551 (C=C). Yield 0.031 %.

^{1}H NMR (Bruker 500 MHz, C_5D_5N): 6.05 (1H, s, H-1), 7.77 (1H, s, H-3), 5.55 (1H, d, H-6), 2.19 (1H, d, Ha-7), 2.55 (1H, d, Hb-7), 2.99 (1H, d, H-9), 1.44 (3H, s, H-10), 3.68 (3H, s, H-12), 5.67 (1H, d, H-1`), 4.34 (1H, t, H-2`), 4.29 (1H, t, H-3`),4.22 (1H, t, H-4`), 4.45 (1H, ddd, H-5`), 4.37 (1H, dd, , Ha-6`), 4.28 (1H, dd, Hb-6`), 6.52 (H, br.s., OH);

^{13}C NMR (126 MHz, C_5D_5N: 93.91 (C-1), 154.92 (C-3), 115.73 (C-4), 74.4 (C-5), 72.39 (C-6), 48.58 (C-7), 73.88 (C-8), 57.59 (C-9), 26.82 (C-10), 168.64 (C-11), 52.04 (C-12), 99.01 (C-1`), 74.49 (C-2`), 78.18 (C-3`), 71.81 (C-4`), 78.67 (C-5`), 63.65 (C-6`) [6].

Loganin (2). Compound 2 was isolated as white crystals. $C_{17}H_{26}O_{10}$, ESI-MS *m/z* 413.39 $[M + Na]^+$, mp 222.2°C, UV (C_2H_5OH) λ_{max} 234.72 nm. IR (KBr) ν_{max} 3440 (OH), 1642 (C=O), 1446 (C=C). Yield 0.021 %.

^{1}H NMR (Bruker 500 MHz, C_5D_5N): 5.87 (1H, d, H-1), 7.72 (1H, s, H-3), 3.59 (1H, dd, H-5), 2.07(1H, dd, Ha-6), 2.35 (1H, dd, Hb-6), 4.04 (1H, ddd, H-7), 2.59 (1H, m, H-8), 3.13 (1H, dd, H-9), 1.16 (3H, s, H-10), 3.60 (3H, s, H-12), 5.69 (1H, d, H-1`), 4.27 (1H, t, H-2`), 4.33 (1H, t, H-3`), 4.22 (1H, t, H-4`), 4.11 (1H, ddd, H-5`), 4.19 (1H, dd, Ha-6`), 4.34 (1H, dd, Hb-6`), 6.82 (H, br.s., OH);

^{13}C NMR (126 MHz, C_5D_5N): 96.04 (C-1), 151.64 (C-3), 111.46 (C-4), 32.71 (C-5), 37.71 (C-6), 74.57 (C-7), 40.42 (C-8), 43.36 (C-9), 14.18 (C-10), 168.69 (C-11), 51.73 (C-12), 100.72 (C-1`), 75.07 (C-2`), 78.60 (C-3`), 71.81 (C-4`), 78.40 (C-5`), 63.65 (C-6`) [7].

Pulchelloside (3). Compound **3** was isolated as yellow crystals. $C_{17}H_{26}O_{12}$, ESI-MS *m/z* 445.13 $[M + Na]^+$, mp. 124,6°C, UV (C_2H_5OH) λ_{max} 235.76 nm. IR (KBr) ν_{max} 3437 (OH), 1640 (C=O), 1443 (C=C). Yield 0.073 %.

^{1}H NMR (Bruker 500 MHz, C_5D_5N): 5.86 (1H, s, H-1), 7.77 (1H, s, H-3), 4.48 (1H, d, H-6), 3.72 (1H, dd, H-7), 2.41 (1H, dd, H-8), 2.90 (1H, dd, H-9), 1.22 (3H, d, H-10), 3.72 (3H, s, H-12), 5.70 (1H, d, H-1`), 4.32 (1H, dd, H-2`), 4.32 (1H, d, H-3`), 4.22 (1H, dd, H-4`), 4.46 (1H, ddd, H-5`), 4.36 (1H, dd, Ha-6`), 4.21 (1H, dd, Hb-6`), 6.57 (H, br.s., OH);

^{13}C NMR (126 MHz, C_5D_5N): 97.29 (C-1), 152.93 (C-3), 112.78 (C-4), 73.54 (C-5), 77.19 (C-6), 75.39 (C-7), 38.22 (C-8), 51.35 (C-9), 14.44 (C-10), 168.84 (C-11), 52.35 (C-12), 100.91 (C-1`), 74.94 (C-2`), 78.55 (C-3`), 71.81 (C-4`), 78.38 (C-5`), 63.65 (C-6`) [8].

Shanshiside methyl ester (4). White crystals, $C_{17}H_{26}O_{11}$, ESI-MS *m/z* 429.38 $[M + Na]^+$, mp 94.8°C, UV (C_2H_5OH) λ_{max} 236.97 nm. IR (KBr) ν_{max} 3437 (OH), 1642 (C=O), 1438 (C=C). Yield 0.013 %.

^1H NMR (Bruker 500 MHz, C_5D_5N) 6.28 (1H, s, H-1), 7.81 (1H, s, H-3), 3.33 (1H, dd, 6.48, H-5), 4.51 (1H, ddd, H-6), 2.20 (1H, dd, Ha-7), 1.80 (1H, dd, Hb-7), 2.64 (1H, dd, H-9), 1.51 (3H, s, H-10), 3.60 (3H, s, H-12), 5.77 (1H, d, H-1`), 4.30 (1H, dd, H-2`), 4.28 (1H, t, H-3`), 4.22 (1H, t, H-4`), 4.44 (1H, ddd, H-5`), 4.30 (1H, dd, Ha-6`), 4.38 (1H, dd, Hb-6`), 6.28 (1H, br.s., 6-OH);

^{13}C NMR (126 MHz, C_5D_5N) 93.62 (C-1), 152.48 (C-3), 111.72 (C-4), 41.08 (C-5), 70.95 (C-6), 48.65 (C-7), 78.79 (C-8), 49.87 (C-9), 26.95 (C-10), 168.69 (C-11), 51.78 (C-12), 100.92 (C-1`), 74.81 (C-2`), 78.54 (C-3`), 71.81 (C-4`), 78.35 (C-5`), 63.65 (C-6`) [9].

Phlorigidoside C (5). Colourless, $C_{17}H_{24}O_{11}$, ESI-MS *m/z* 427.11 $[M + Na]^+$, mp 66°C, UV (C_2H_5OH) λ_{max} 238.3 nm. IR (KBr) ν_{max} 3418 (OH), 1637 (C=O), 1549 (C=C). Yield 0.028 %.

^1H NMR (Bruker 500 MHz, C_5D_5N) 6.08 (1H, d, H-1), 7.83 (1H, s, H-3), 2.81 (1H, dd, H-5), 4.17 (1H, dd, H-6), 3.48 (1H, s, H-7), 2.43 (1H, dd, H-9), 1.49 (3H, s, H-10), 3.60 (3H, s, H-12), 5.45 (1H, d, H-1`), 4.28 (1H, d, H-2`), 4.29 (1H, dd, H-3`), 4.19 (1H, dd, H-4`), 4.44 (1H, ddd, H-5`), 4.28 (1H, dd, Ha-6`), 4.38 (1H, dd, Hb-6`), 6.08 (1H, br.s., OH);

^{13}C NMR (126 MHz, C_5D_5N) 93.07 (C-1), 152.55 (C-3), 106.18 (C-4), 38.20 (C-5), 73.09 (C-6), 64.23 (C-7), 65.05 (C-8), 46.80 (C-9), 16.67 (C-10), 168.47 (C-11), 51.92 (C-12), 101.46 (C-1`), 74.78 (C-2`), 78.45 (C-3`), 71.81 (C-4`), 78.35 (C-5`), 63.65 (C-6`) [10].

Investigation of the biological activity. Experiments were set on white outbred mice (18-20 g). Reaction of Jerne, Nordin was used for evaluation of the preparation influence to the humoral immunity [11]. Mice were immunized with red blood cells (RBCS) of sheep and in the same day of immunization, in biological active dose the water-alcohol solutions of the iridoids sum were injected intragastric (10 мг/кг. Mice of the control group received the water-alcohol solution in the same volume. On the 5th day after immunization, the number of antibody-producing cells (APC) was determined in the spleens of mice.

Studies were performed on intact mice and mice subjected to stress. The state of stress was caused by the N. Selye “swim stress” model. To do this, mice for 45 min were placed in a tank with water, so that the water level did not allow mice to jump out.

The research results are presented in table 1.

The table shows that the SI in mice causes a pronounced ($p<0.001$) enhancement of the process of antibody formation in response to sheep RBCS.

In the control group of immunized mice, 11,800 ± 928.08 APC accumulate on the spleen and 132.8 ± 2.49 APC per 1 million nucleated spleen cells (NSC). The SI increases the number of APC on the spleen to 21,400 ± 1,369.18, the number of APC per 1 million of NSC - to 242.0 ± 2.83.

Table 1 – The effect of sum of iridoids from the plant *Phlomis severtzovii* on immunity indicators

Group	Control	SI
Immunized mice		
APC on spleen	11800±928,08	21400± 1369,18
APC on 1 million of NSC	132,8±2,49	242,0±2,83
Immunized mice + stress		
APC on spleen	6400±314,11	13200±461,88
APC on 1 million of NSC	75,7±3,33	151,0±2,67

Under the influence of “swimming” stress, the sum of APC in mice decreases to 6400 ± 314.11 per spleen and to 75.7 ± 3.33 per 1 million NSC. The sum of iridoids increases the number of APC per spleen to 13,200 ± 461.88, by 1 million splenic cells - to 151.0 ± 2.67.

Under the influence of the SI, there is a tendency to increase the mass and cellularity (total cell content) of the spleen, the mass of the thymus and lymph nodes, a significant increase in the cellularity of the thymus and lymph nodes.

As a result, it was shown that the SI obtained from the plant *Phlomis severtzovii* possesses immunostimulating activity, and is not immunotoxic.

It was previously established, that iridoids obtained from the aerial part of *Phlomis severtzovii* have hepatoprotective properties and a positive effect on the functional state of the liver [12]. Given this fact,

we investigated the effect of the SI and iridoid 6β-hydroxypolamide on acute alcohol intoxication. Experiments were performed on white outbred mice - females weighing 20-22 g. Ethanol in the form of a 24% solution was injected intraperitoneally at a narcotic dose (4.8 g/kg). The test substances were administered orally using an atraumatic metal probe at doses of 10-25-50 mg/kg 60-70 minutes before the introduction of ethanol. Evaluation of the effectiveness of the compounds was determined by the duration of the lateral position of the animals. The control group of animals under similar conditions of experience instead of the drug was injected with sterile distilled water. The results of the research are presented in table 2.

Table 2 – The results of the influence of drugs on the narcotic action of ethanol

No	Name of preparations	dose	The duration of the lateral position in minutes	Effect in %
1	Control EtOH	4,8 g/kg	110	100%
2	SI +EtOH	10 mg/kg 4,8 g/kg	85	22,8%
3	SI + EtOH	25 mg/kg 4,8 g/kg	62,7	43%
4	SI + EtOH	50 mg/kg 4,8 g/kg	63,8	42%
5	6β-hydroxypolamid + EtOH	10 mg/kg 4,8 g/kg	72,4	34,2%
6	6β-hydroxypolamid + EtOH	25 mg/kg 4,8 g/kg	53,9	51%
7	6β-hydroxypolamid + EtOH	50 mg/kg 4,8 g/kg	60,5	45%

The results of the studies (table 2) showed that in the control group of animals after applying EtOH at a dose of 4.8 g/kg in all mice came the state of anesthesia (lateral position) with an average duration of 110 minutes. Preliminary application of the SI and 6β-hydroxypolamide at doses of 10-25-50 mg/kg shortened the state of the lateral position of the experimental mice by 22.8%-43%-42% and 34.2% -51%-45%, respectively, compared to with a control group of animals.

Consequently, the compounds studied, depending on the dose administered, have an antitoxic effect during acute alcohol intoxication.

Experimental. Air-dried and grinded plant material was extracted with MeOH three times at room temperature. After filtration, the solvent was partly removed by rotary evaporation and the extract residue was diluted with equal quantity of water. The formed precipitate in the extract was filtered. Residues of MeOH were removed by rotary evaporation. The obtained water part of the extract was extracted in consecutive order with $CHCl_3$ and *n*-BuOH. *n*-BuOH extract was evaporated on rotary evaporator and the *n*-BuOH fraction was obtained. The *n*-BuOH was set to column with silica gel and obtained several fractions. Re-chromatography isolation of these fractions by elution with solvent systems $CHCl_3$÷MeOH: 1) 100÷1; 2) 50÷1; 3) 40÷1; 4) 30÷1; 5) 20÷1; 6) 15÷1; 7) 9÷1 and 8) 4÷1 yield the individual compounds: 6β-hydroxypolamid **1**, loganin **2**, pulcheloside **3**, shanshiside methyl ester **4** and florigidoside C **5**.

In order to get novel immunomodulating preparations dried aerial parts of *Phlomis severtzovii* were extracted with EtOH at room temperature. EtOH extract was filtered and the solvent was removed on rotary evaporator. The obtained extract was diluted with water and the water mixture was treated at first with $CHCl_3$, then with *n*-BuOH five times. The solvents were removed on rotary evaporator. Yellow powder were get in yield. Enriched SI were obtained from *n*-BuOH fraction by treating with the solvent system $CHCl_3$ - EtOH 6÷1.

Conclusion. In this study, we investigated the iridoid constituent of *Phlomis severtzovii* growing in Uzbekistan and for first time we have isolated known iridoids identified on basis of UV, IR, ^{1}H and ^{13}C

NMR spectra as 6β-hydroxypolamid **1**, loganin **2**, pulchelloside **3**, shanshiside methyl ester **4** and phlorigidoside C **5**.

Immunostimulating activity of the sum of iridoids obtained from *Phlomis severtzovii* was revealed.

It was determined that the sum of iridoids and iridoid 6β-hydroxypolamide have an antitoxic effect during acute alcohol intoxication.

Acknowledgments - Authors would like to thank the ICPS (Uzbek Academy of Sciences) for providing all necessary equipment, chemicals and animals for the study.

Д. Усманов[1], Н.Ш. Рамазанов[1], У. Юсупова[1], К.Дж. Кучербаев[2,3]

[1]ӨР ҒА Өсімдік затларының химиясы институты, Ташкент, Өзбекстан;
[2]Аймақтық әлеуметтік-инновациялық университет, Шымкент, Қазақстан;
[3]«Оңтүстік-Қазақстан медицина академиясы» АҚ, Шымкент, Қазақстан

PHLOMIS SEVERTZOVII ИРИДОИДТАРЫ ЖӘНЕ ОЛАРДЫҢ ИМУНИТЕТТІ ЫНТАЛАНДЫРУШЫ ЖӘНЕ УЫТТЫЛЫҚҚА ҚАРСЫ БЕЛСЕНДІЛІКТЕРІ

Аннотация. Өзбекстанда өсетін *Phlomis severtzovii* (*Lamiaceae*) жер үсті бөліктерінен бірінші рет бес иридоид гликозидтері бөліп алынды. УК, ИҚ, ^{1}Н және ^{12}С ЯМР спектроскопия көмегімен олар 6β-гидроксиполамид (1), логанин (2), пулчелозид (3), шаншизид метил эфирі (4) және флоригидозид С (5) екендігі анықталды. Қосымша иридоидтар жыйынтығы және 6β-гидроксиполамидтың иммунитетті ынталандырушы және уыттылыққа қарсы белсенділіктері анықталды.

Түйін сөздер: *Phlomis severtzovii*, иридоид, 6β-гидроксиполамид, логанин, пулчелозид, шаншизид метил эфирі, флоригидозид С, иммунитетті ынталандырушы белсендік, уыттылыққа қарсы белсенділік.

Д.Усманов[1], Н.Ш.Рамазанов[1], У.Юсупова[1], К.Дж.Кучербаев[2,3]

[1] Институт химии растительных веществ АН РУз, Ташкент, Узбекистан;
[2]Региональный социально-инновационный университет, Шымкент, Казахстан;
[3]АО «Южно-Казахстанская медицинская академия», Шымкент, Казахстан

ИРИДОИДЫ ИЗ *PHLOMIS SEVERTZOVII* И ИХ ИММУНОСТИМУЛИРУЮЩАЯ И АНТИТОКСИЧЕСКАЯ АКТИВНОСТЬ

Аннотация. Впервые из надземных частей *Phlomis severtzovii* (*Lamiaceae*) произрастающей в Узбекистане выделены пять ранее известных иридоидных гликозидов. На основе УФ, ИК, ^{1}Н и ^{12}С ЯМР спектроскопии выделенные вещества были идентифицированы с 6β-гидроксиполамидом (1), логанин (2), пулчеллозид (3), метиловый эфир шаншизида (4) и флоригидозид С (5). Дополнительно, выявлены значительная иммуностимулирующая и антитоксическая активность суммы иридоидов и 6β-гидроксиполамида (1).

Ключевые слова: *Phlomis severtzovii*, иридоид, 6β-гидроксиполамид, логанин, пулчелозид, метиловый эфир шаншизида, флоригидозид С, иммуностимулирующая активность, антитоксический эффект.

Information about the authors:

Durbek Usmanov - Institute of Chemistry of Plant Substances AS RUz, Tashkent, Uzbekistan, durbekusmanov@bk.ru, https://orcid.org/0000-0002-7349-377X;

Ugiloy Yusupova - Institute of Chemistry of Plant Substances AS RUz, Tashkent, Uzbekistan, yusupovauyu@gmail.com , https://orcid.org/0000-0003-3401-2379;

Nurmurod Sheralievich Ramazanov - Institute of Chemistry of Plant Substances AS RUz, Tashkent, Uzbekistan, ramazonovn@list.ru, https://orcid.org/0000-0003-2563-626X;

Kamal Dzhamalovich Kucherbayev - Regional Social-Innovational University, Shymkent, Kazakhstan, JSC «South-Kazakhstan Medical Academy», Shymkent, Kazakhstan, kkamaljsci@gmail.com, https://orcid.org/0000-0003-1981-1260

REFERENCES

[1] Galves M, Martin-Cordero C, Houghton PJ, Jesus Ayoso M. (**2005**) Antioxidant activity of methanol extracts from Plantago species. *Agricultural and food chemistry*, **53**, 1927-1933.

[2] Yang L, Jia Z–J, Su B–N. (**1997**) Neolignan, phenylpropanoid and iridoid glycosides from Pedicularis verticillata. *Phytochemistry*, **45**, No 6, 1271-1273.

[3] Lucjan Swigtek. Glukozydy iridoidowe w rodzinie Scrophullariaceae (**1973**) *Acta Polon Pharm.* **XXX**, No2, 203-212.

[4] Povodish MN. (**2006**) Diversity of iridoids in Lamiaceae family and their biological activity. *Plant resources* [In Russian], **42**, 2, 131-149.

[5] Maksudov MS. (**1996**) Iridoids from plants of Scrophulariaceae, Bignoniaceae and Lamiaceae family. *Dissertation of PhD on chemistry* [In Russian], Tashkent, 127.

[6] Stermitz FR, Abdel-Kader MS, Foderaro TA, Pomeroy M. (**1994**) Iridoid glycosides from some butterflies and their larval food plants. *Phytochemistry*, **37**, 4, 997-9.

[7] Taguchi, H, Yokokawa Y, Endo T. (**1973**) Constituents of Patrinia villosa. *Yakugaku Zasshi*, **93**, 5, 607-11.

[8] Milz S, Rimpler H. (**1978**) Pulchelloside I, a new iridoid from Verbena pulchella Sweet. *Tetrahedron Letters*, **10**, 895-8. CODEN:TELEAY ISSN:0040-4039.

[9] Yoshio T, Hiroshi N, Hiroyuki I. (**1977**) Two new iridoid glucosides from Messaenda parviflora and Mussaenda shikokiana. *Phytochemistry*, **16**, 9, 1401-1404.

[10] Kobayashi S, Mima A, Kihara M, Imakura Y. (**1986**) *Chem.Pharm.Bull.*, **34**, 876.

[11] Jerne NK, Nordin AA. (**1963**) Plague formation in agar by single antibody producing cells. *Science*. **140**, 405.

[12] Nabiev AN, Khushbaktova ZA, Zakhidov UV, etc. (**1999**) Hepatoprotective properties of iridoid glycosides in acute toxic liver damage by heliotrin in mice. *Chemical-pharm. Journ.*, **8**, 11.

[13] A.Zh. Kaldybekova, A.T. Amangazyeva, Z.B. Halmenova, A.K. Umbetova. Development of technology for the complex isolation of biological active substances from plants of the genus haplophyllum A.juss., News of NAS RK. Series of Chemistry and technology. Volume 5, Number 431 (2018), 74 – 81 https://doi.org/10.32014/2018. 2518-1491.10 ISSN 2518-1491 (Online), ISSN 2224-5286 (Print).

[14] A.A. Janibekov, T.X. Naubeev, N.Sh. Ramazanov, G.A. Sabirova, K.Dzh. Kucherbayev. Determination of chemical structure of cyclolehmanoside A from *Astragalus lehmannianus.* News of NAS RK. Series of Chemistry and technology. Volume 2, Number 434 (2019), 50 – 54 https://doi.org/10.32014/2019.2518-1491.18 ISSN 2224-5286 (Online), ISSN 2224-5286 (Print).

N E W S
OF THE NATIONAL ACADEMY OF SCIENCES OF THE REPUBLIC OF KAZAKHSTAN
SERIES CHEMISTRY AND TECHNOLOGY
ISSN 2224-5286 **https://doi.org/10.32014/2019.2518-1491.74**
Volume 6, Number 438 (2019), 55 – 60

UDC 66.047.2: 66.047.1

B. T. Abdizhapparova[1], N. S. Khanzharov[2], B. O. Ospanov[1], I. A. Pankina[3], D.K. Kamalbek[1], Zh. M. Akhmetov[1]

[1]M. Auezov South Kazakhstan State University, Shymkent, Kazakhstan;
[2]International Humanitarian-Technical University, Shymkent, Kazakhstan;
[3]Peter the Great St. Petersburg Polytechnic University, St. Petersburg, Russia
e-mail: bahyt_04@mail.ru

INVESTIGATION OF VACUUM-ATMOSPHERIC DRYING OF CAMEL AND MARE'S MILK

Abstract. The relevant problem of dehydration of dairy products is a subject of research in this issue. Camel and mare's milk are of interest in this regard. Actually, for these products energy-intensive methods of vacuum and vacuum-sublimation drying are usually used, that is explained by high preservation of biochemical composition of dried materials. It causes the problem of further study and improvement of various aspects of drying processes. A method of vacuum-atmospheric drying of camel and mare's milk is proposed, based on their dehydration in a drying plant where these processes are carried out in a parallel way. Combining processes should be based on the selection of modes of the above-mentioned drying methods. Experimental studies of vacuum-atmospheric drying of camel and mare's milk depending on pressure and temperature of heating the medium in the vacuum chamber, as well as the speed and temperature of drying agent in the device for atmospheric drying have been conducted. Empirical equations allowing describing quite adequately processes of heat and mass transfer at vacuum-atmospheric drying of dairy products are received.

Keywords: vacuum, drying, camel, mare, milk, method, atmospheric.

Introduction

The issue in developing of new and innovative drying techniques is still actual one [1, 2]. Main reasons to accelerate attempts for development of advanced drying techniques are: making the process cost effective, reducing the energy consumption, intensifying the drying rates, improving the quality of dried food products, increasing safety in operation and making the drying process easy to control [3, 4]. Particularly relevant in this aspect is solution of problem of dehydration of dairy products. Camel and mare's milk are of interest in this regard. In practice, for these products energy-intensive methods of vacuum and vacuum-sublimation drying are usually used, that is explained by high preservation of biochemical composition of final product. It causes the problem of further study and improvement of various aspects of drying processes. In the aspect of solving this problem, a method of vacuum-atmospheric drying of camel and mare's milk is proposed, based on their dehydration in a drying plant in which these processes are carried out in a parallel way.

The essence of the developed process of vacuum-atmospheric drying of liquid materials is consists of combination into a single process of separate experimentally obtained processes of vacuum and atmospheric drying. The developed method includes vacuum drying of milk to a certain intermediate humidity and its atmospheric drying to the final humidity. In this case, the drying process is accelerated due to the parallel implementation of vacuum and atmospheric drying processes. Since atmospheric drying is carried out by using the condensation heat of the working substance of a refrigeration machine included in the drying plant according to heat pump scheme. A moderate temperature difference is created, equivalent to temperature head during vacuum drying. Also, by using condensation heat of refrigerant to heat the dried material, a gentle mode of milk drying in the vacuum chamber is achieved. Drying of the

material is carried out by air heated by waste heat of condensation of refrigerant, which saves the energy of heating the drying agent.

The developed experimental drying plant implementing the developed method of vacuum-atmospheric drying of dairy materials includes units of vacuum drying, heat pump and atmospheric drying [5]. In the installation, the vacuum drying unit provides the drying process of materials in a rarefied medium from the initial moisture content to the intermediate one. The heat pump unit provides high-potential heat to the atmospheric drying unit and low-potential heat to the moisture defroster of the drying unit. The unit of atmospheric drying of materials provides the process of atmospheric drying of thermolabile materials from the intermediate humidity of the material to the final one, regulated by technical requirements for the finished product.

Experimental methods

The study of vacuum and atmospheric drying processes in order to further combination them into a single process of vacuum-atmospheric drying was carried out under the following conditions:

- vacuum drying: pressure of medium – (6÷10) kPa; temperature of heating of medium - (35÷45) ^{0}C; height of dried layer is 0.01 m.

- atmospheric drying: drying agent temperature - (36÷40) ^{0}C; drying agent velocity - (0,35÷0,45) m/s.

Selection of temperature and pressure intervals during vacuum drying was substantiated by necessity for maximum preservation of biochemical composition of investigated drying materials at a sufficiently high intensity of drying process. The choice of temperature intervals and drying agent velocities during atmospheric drying of materials was determined by the same reasons.

The necessary of combination and selection of optimal modes of vacuum and atmospheric drying was carried out in such a way as to ensure a uniform character of the drying process of the material, which would take place only in vacuum or only in atmospheric drying. In practice, the combination of drying modes was carried out by studying the nature or kinetics of vacuum and atmospheric drying processes, the selection of humidity and temperature of material in the process of dehydration, as well as selection of material moisture to which it is advisable to carry out the vacuum drying process. Accordingly, when the dried material reaches that humidity level, the process of atmospheric drying begins.

Processing of results of experimental studies of vacuum and atmospheric drying showed that for the developed vacuum-atmospheric process it is recommended to combine the following drying modes:

- vacuum drying at pressure of medium 6 kPa and heating temperature of medium 40 ^{0}C with atmospheric drying at air temperature 40 ^{0}C;

- vacuum drying at pressure medium 10 kPa and a heating temperature of medium 40 ^{0}C with atmospheric drying at air temperature 36 ^{0}C;

- vacuum drying at pressure medium 8 kPa and a heating temperature of medium 45 ^{0}C with atmospheric drying at air temperature 38^{0}C.

Under these conditions, there is not only a high intensity of the drying process, but also the absence of kick of milk from a container. Also, the optimal velocity of the drying agent in the atmospheric drying device was determined experimentally, which was equal to 0.35 m/s at heating temperatures (36÷40) ^{0}C.

Experimental studies of vacuum-atmospheric drying of camel and mare's milk depending on pressure and temperature of heating the medium in the vacuum chamber, as well as the velocity and temperature of drying agent in the device of atmospheric drying have been conducted. As it known, drying is a complex operation involving simultaneous heat and mass transfer processes [3].The results of experimental studies, processed in the form of heat and mass transfer coefficients for camel and mare´s milk are shown in figures 1-4.

Results and discussions

The figure 1 shows that when the heating temperature of medium increases from 35 to 45 ^{0}C, the values of heat transfer coefficients increase by 11.4÷14.2 %. At the heating temperature of vacuumed medium 45 ^{0}C with a deepening of rarefaction of medium from 10 to 6 kPa, the values of the heat transfer coefficients increase from 3.55 to 4.89 W/(m^{2}K), i.e. by 27.4 %. With deepening of rarefaction of medium, the values of mass transfer coefficients, as well as the heat transfer coefficients, increase (figure 2). The greatest break is observed when the degree of rarefaction of medium decreases from 10 to 6 kPa at

temperature of heating 45 ^{0}C, when values of mass transfer coefficients increase from 0.11 to 0.17 s/m or by 35.3 %. At 40 ^{0}C this figure is increased b 26.4%, at 35 ^{0}C by 32.9%.

A similar change in heat and mass transfer coefficients from the drying modes is observed during vacuum drying of mare's milk.

In view of the above, the optimal mode of vacuum drying of camel and mare's milk should be considered as medium pressure 6 kPa and heating temperature 45 ^{0}C.

For atmospheric drying (figures 3 and 4), it can be concluded that in the temperature range (36÷40) ^{0}C, the nature of change in heat and mass transfer coefficients for camel and mare's milk is almost identical. Thus, the value of heat transfer coefficient increases from 3.10 to 4.75 W/(m^{2}K) and the mass transfer coefficient from 0.10 to 0.15 s/m, which is 34.7 and 33.3% for each case.

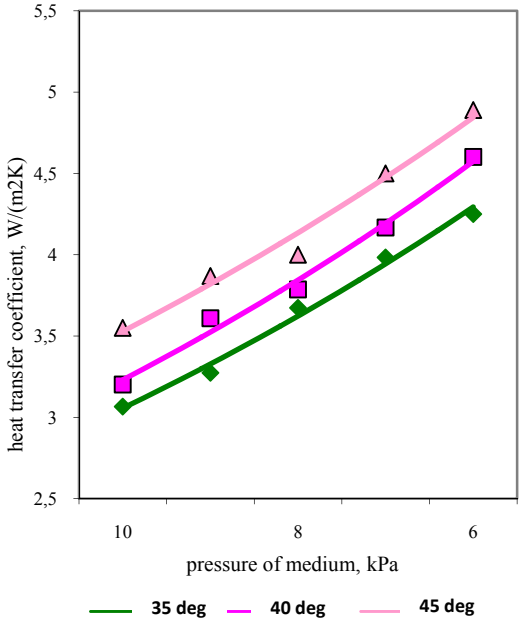

Figure 1 – Dependence of heat transfer coefficient from pressure at various temperatures of heating of medium at vacuum drying of camel milk.

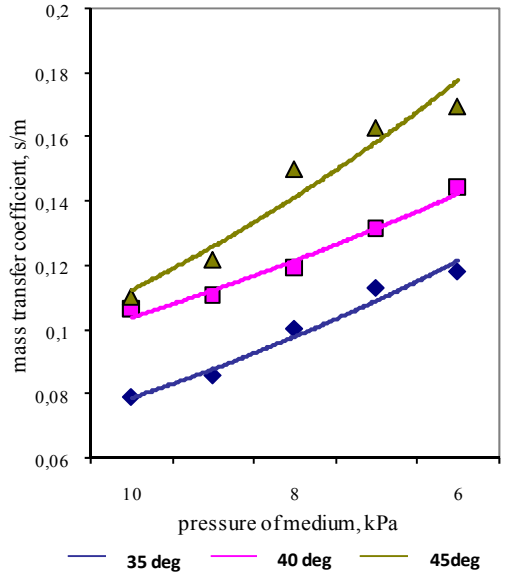

Figure 2 - Dependence of mass transfer coefficient from pressure at various temperatures of heating of medium at vacuum drying of camel milk.

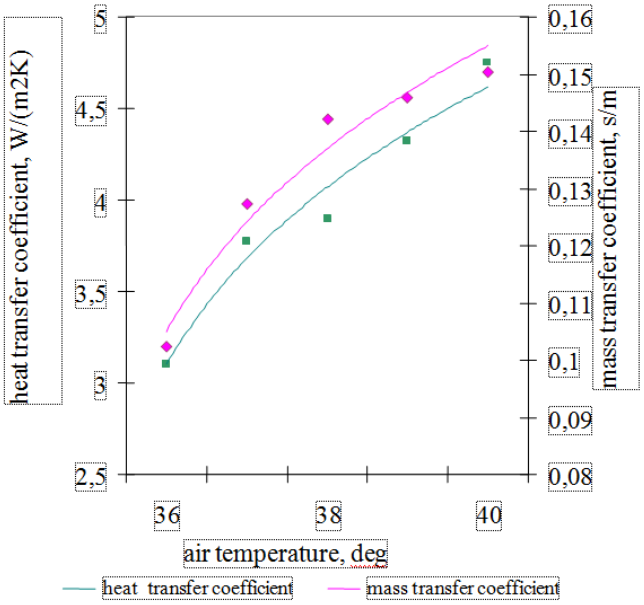

Figure 3 – Dependencies of heat and mass transfer coefficients from temperature of drying agent at air velocity 0.35 m/s at atmospheric drying of camel milk

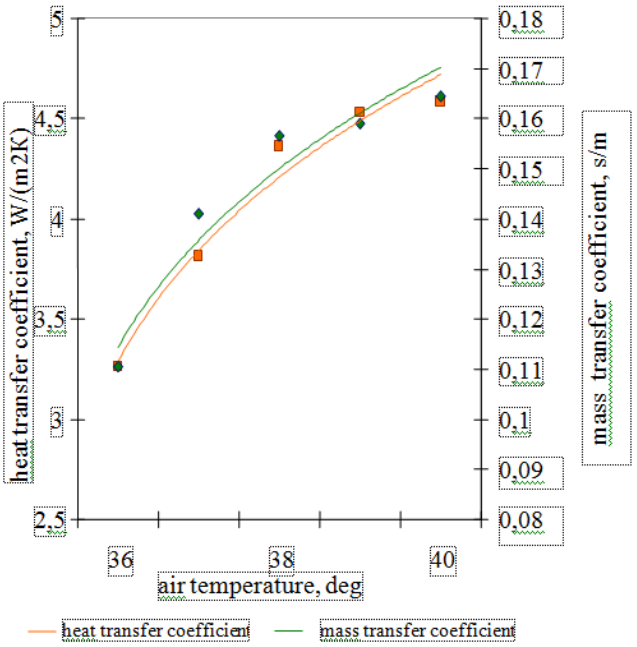

Figure 4 – Dependencies of heat and mass transfer coefficients from temperature of drying agent at air velocity 0.35 m/s at atmospheric drying of mare´s milk

For mare's milk in a given temperature range, the heat transfer coefficient increases from 3.35 to 4.52 W/(m^{2}K) or 25.9%, and the mass transfer coefficient – from 0.11 to 0.16 s/m or 31%. Analyzing figures 3 and 4, it can be concluded that the optimal mode of atmospheric drying should be considered the temperature range of the drying agent (38÷40) ^{0}C.

Based on analysis of experimental data on heat and mass transfer during vacuum - atmospheric drying of camel and mare's milk for the vacuum drying process, the equations of thermal Nu and diffusion Num of the Nusselt criteria are obtained:

$$Nu=5,25\ Pr^{0,33}\ Re^{0,025}\ Gu^{0,47},$$

$$Nu_m=0,056\ Pr_m^{\ 0,33}Re^{0,61}Gu^{\ 0,16}.$$

Also, on the basis of experimental data on heat and mass transfer during vacuum - atmospheric drying of these dairy products, the equations of thermal Nu and diffusion Nu_m of the Nusselt criteria for the atmospheric drying process are obtained:

$$Nu=0,638\ Pr^{0,33}\ Re^{0,16}Gu^{0,26},$$

$$Nu_m=0,71Pr_m^{\ 0,33}Re^{0,18}\ Gu^{0,14}.$$

Conclusion

So, the method of vacuum-atmospheric drying of camel and mare's milk is developed; it includes vacuum drying of material to intermediate humidity and atmospheric drying till final one. It allows achieving good quality of the product and promotes significant decreasing of energy consumption for drying. Also empirical equations are obtained allowing describing the processes of heat and mass transfer at vacuum-atmospheric drying of dairy products.

Б.Т. Абдижаппарова[1], Н.С.Ханжаров[2], Б.О. Оспанов[1], И.А.Панкина[3], Д.К. Камалбек[1], Ж.М. Ахметов[1]

[1]М.Әуезов ат. Оңтүстік Қазақстан мемлекеттік университеті (Қазақстан);
[2]Халықаралық гуманитарлы-техникалық университеті (Қазақстан);
[3]Ұлы Петр ат.Санкт-Петербург мемлекеттік политехникалық университеті (Ресей)

ТҮЙЕ ЖӘНЕ БИЕ СҮТТЕРІН ВАКУУМДЫ-АТМОСФЕРАЛЫҚ КЕПТІРУДІ ЗЕРТТЕУ

Аннотация. Берілген мақалада зерттеу нысаны сүтті өнімдерді ылғалсыздандыру өзекті мәселе болып табылады. Осы орайда түйе және бие сүттері қызығушылық тудырады. Тәжірибеде бұл өнімдер үшін әдетте энергия шығыны көп кептірудің вакуумды және вакуум-сублимациялық әдістері пайдаланылады, бұл кептірілуші материалдардың биохимиялық құрамының толық сақталуымен түсіндіріледі. Бұл кептіру процесстерінің түрлі аспекттерін әрі қарай зерделеу және жетілдіру мәселесін қозғайды. Түйе және бие сүттерін кептіру қондырғысында ылғалсыздандыруға негізделген әрі бұл процесстер параллельді жүретін вакуумды-атмосфералық кептіру тәсілі ұсынылды. Процесстерді қиюластыру жоғарыда көрсетілген кептіру түрлерінің режимдерін таңдауға негізделуі тиіс. Температура мен қысым тәуелділігіне байланысты вакуумды камерадағы ортаны қыздыру, сондай-ақ атмосфералық кептіруге арналған құрылғыдағы кептіргіш агенттің жылдамдығы мен температурасы арасындағы тәуелділікке сәйкес түйе және бие сүттерін вакуумды-атмосфералық кептіру бойынша эксперименттік зерттеулер жүргізілді. Сүтті өнімдерді вакуумды-атмосфералық кептіру кезіндегі жылумассаалмасу процесстерін жеткілікті түрде дәл өрнектеуге мүмкіндік беретін эмпирикалық теңдеулер алынды.

Түйін сөздер: вакуум, кептіру, түйенің, биенің, сүт, әдіс, атмосфералық.

Б.Т. Абдижаппарова[1], Н.С.Ханжаров[2], Б.О. Оспанов[1], И.А.Панкина[3], Д.К. Камалбек[1], Ж.М. Ахметов[1]

[1]Южно-Казахстанский государственный университет им.М.Ауэзова (Казахстан);
[2]Международный гуманитарно-технический университет (Казахстан);
[3]Санкт-Петербургский государственный политехнический университет им.Петра Великого (Россия)

ИССЛЕДОВАНИЕ ВАКУУМНО-АТМОСФЕРНОЙ СУШКИ ВЕРБЛЮЖЬЕГО И КОБЫЛЬЕГО МОЛОКА

Аннотация. Предметом исследования в данной статье является актуальная проблема обезвоживания молочных продуктов. В этом аспекте интерес представляют верблюжье и кобылье молоко. На практике для

этих продуктов обычно используются энергоемкие методы вакуумной и вакуум-сублимационной сушки, что объясняется высокой сохранностью биохимического состава высушиваемых материалов. Это вызывает проблему дальнейшего изучения и совершенствования различных аспектов процессов сушки. Предложен способ вакуумно-атмосферной сушки верблюжьего и кобыльего молока, основанный на их обезвоживании в сушильной установке, где эти процессы осуществляются параллельно. Комбинирование процессов должно основываться на выборе режимов вышеуказанных способов сушки. Проведены экспериментальные исследования вакуумно-атмосферной сушки верблюжьего и кобыльего молока в зависимости от давления и температуры нагрева среды в вакуумной камере, а также скорости и температуры сушильного агента в устройстве для атмосферной сушки. Получены эмпирические уравнения, позволяющие достаточно адекватно описывать процессы тепломассообмена при вакуумно-атмосферной сушке молочных продуктов.

Ключевые слова: вакуум, сушка, верблюжье, кобылье, молоко, метод, атмосферный.

Information about the authors:

Abdizhapparova Bakhytkul Telkhozhaevna - M. Auezov South Kazakhstan State University, Shymkent, Kazakhstan, https://orcid.org/0000-0001-8277-8243;

Khanzharov Nurlan Serikbayevich - International Humanitarian-Technical University, Shymkent, Kazakhstan, https://orcid.org/0000-0002-7406-0386;

Ospanov Bakhytzhan Orazalievich - M. Auezov South Kazakhstan State University, Shymkent, Kazakhstan, https://orcid.org/0000-0002-6437-5579;

Pankina Ilona Anatol'evna - Peter the Great St. Petersburg Polytechnic University, St. Petersburg, Russia;

Kamalbek Dinmukhammed Kuanyshbekuly - M. Auezov South Kazakhstan State University, Shymkent, Kazakhstan;

Akhmetov Zhasurbek Mansurbekovich - M. Auezov South Kazakhstan State University, Shymkent, Kazakhstan

REFERENCES

[1] Kudra T., Mujumdar A.S. *Advanced Drying Technologies*, 2nd ed. CRC Press, Taylor and Francis, Quebec, 2009. 438 p.

[2] Mujumdar A.S., Wu Z. *Thermal drying technologies-Cost-effective innovation aided by mathematical modeling approach*. Drying technology, 2008, Vol. 26, pp. 146-154.

[3] Sachin V. Jangam, Lim Law Chung, Mujumdar A. S. Drying of Foods, Vegetables and Fruits, Mechanical Engineering Department & M3TC National University of Singapore, Singapore, Vol. 1, 2010. 232 p.

[4] Hanzharov N.S., Abdizhapparova B.T. Razrabotka processa vakuumno-atmosfernoj sushki pishhevyh materialov // Materialy mezhdunar. nauchno-praktich. konf. «Strategija razvitija pishhevoj i legkoj promyshlennosti». Almaty: ATU. 2004, T.1. - S.371-373. [Khanzharov N.S., Abdizhapparova B.T. Development of processes of vacuum-atmospheric drying of food materials // Proceedings of international scient.-practical conference “Strategy of development of food and light industry”. Almaty: ATU. 2004, vol.1. P. 371-373].

[5] Abdizhapparova B.T., Khanzharov N.S., Ospanov B.O., Baranenko A.V., Dosmakanbetova A.A. (2018) Stage vacuum drying of camel milk and shubat, NEWS OF THE ACADEMY OF SCIENCES OF THE REPUBLIC OF KAZAKHSTAN, series of agricultural sciences, 5(47): 73–80. https://doi.org/10.32014/2018.2224-526X.10

N E W S
OF THE NATIONAL ACADEMY OF SCIENCES OF THE REPUBLIC OF KAZAKHSTAN
SERIES CHEMISTRY AND TECHNOLOGY
ISSN 2224-5286 **https://doi.org/10.32014/2019.2518-1491.75**
Volume 6, Number 438 (2019), 61 – 69

UDC 66.047.2: 66.047.1

B. T.Abdizhapparova[1], N. S. Khanzharov[2], B. O. Ospanov[1], I. A. Pankina[3], S. Kumisbekov[1], K. S. Islam[1]

[1]M. Auezov South Kazakhstan State University, Shymkent, Kazakhstan;
[2]International Humanitarian-Technical University, Shymkent, Kazakhstan;
[3]Peter the Great St. Petersburg Polytechnic University, St. Petersburg, Russia
e-mail: bahyt_04@mail.ru

RESULTS OF VACUUM-ATMOSPHERIC DRYING OF LARGE-DISPERSED FOOD MATERIALS

Abstract. In the given article the results of researches of heat and mass transfer for vacuum-atmospheric drying of large-dispersed food materials as crushed tubers of topinambour, potato, apple and peas are considered. Optimal regimes of vacuum-atmospheric drying of the given materials are developed. Results of vacuum and atmospheric drying of large-dispersed materials are studied. Depending on height of layer of drying material, pressure of medium into vacuum camera, temperature level of drying the numerical values of coefficients of heat and mass transfer and equations of heat and diffusion Nusselt criterions are received. Comparison on adequacy to real conditions is conducted in order to check the criterion equations. Meanings of experimental and calculated data of heat and mass transfer coefficients have satisfied convergence.

Keywords: vacuum, drying, large-dispersed, method, heat, mass, transfer, atmospheric.

Introduction

Currently, advanced areas for development of technology of food drying are: study of heat and mass transfer in drying, development and improvement of existing designs of drying plants and optimization of technological parameters of drying [1].

The analysis of results of modern researches shows that the most preferable method of dehydration of large-dispersed food materials is vacuum sublimation from the point of view of maximum preservation of biochemical composition and useful properties of dried material. However, along with high quality, finished product dried in a vacuum freeze dryer has an increased cost associated with high energy consumption for implementation of drying process.

Experimental methods

Development of dryers for large-dispersed food materials which implement a method of vacuum-atmospheric drying is assigned to improve efficiency and reduce energy consumption of dryers.

Vacuum-atmospheric drying includes combination of separate processes of vacuum and atmospheric drying. Combination of the processes is carried out in such a way as to ensure a uniform nature of drying process of studied material, i.e. implemented method of vacuum-atmospheric drying includes vacuum drying the material to certain intermediate moisture content and its atmospheric final drying to final moisture content. The processes of vacuum and atmospheric dehydration in drying plant are carried out simultaneously by including a heat pump in it scheme. In this case, the drying modes are selected by such way that identical drying curves should be peculiar to dried material at the moment of its transition from vacuum to atmospheric dehydration.

The developed experimental vacuum-atmospheric dryer includes the following units [2]: unit of vacuum drying, in which the process of vacuum dehydration from initial moisture content of the material to intermediate one is conducted; unit of atmospheric drying - for drying the material from intermediate

humidity to the final one; heat pump [3-5] unit on the basis of a single-stage refrigeration machine designed for heating and cooling the elements of drying plant and reduce the load on a vacuum pump.

Studies on vacuum and atmospheric drying of large-dispersed food materials were carried out on the experimental dryer. Crushed topinambour (Jerusalem artichoke) tubers, potato tubers, apples and green peas were selected as materials for investigation.

It is revealed that intensity of drying mainly depends on the height of bulk layer of dried material. Generalization of research results of influence of height of bulk layer of material being dried on drying kinetics during vacuum dehydration shows that changing the layer height from 0.01 m to 0.04 m leads to a decrease in the rate of drying of apples by 175 %, potatoes - by 195 %, topinambour tubers – by 205 %, and green peas - approximately 210 %. Analysis of drying curves obtained in the process of atmospheric drying at the heights of bulk layer of material 0.01; 0.02; 0.03 and 0.04 m shows that they have a drying kinetics similar to drying curves with same heights of bulk layer during vacuum dehydration. Therefore, it is concluded that during vacuum-atmospheric drying of large-dispersed material, the optimal height of the bulk layer should be 0.01-0.02 m.

Results and discussions

As experimental data show, the pressure in vacuum chamber is also one of the main factors determining the drying rate of large-dispersed materials. Changing the pressure in vacuum chamber leads to a corresponding change in drying rate of the materials. Thus, when the pressure increases from 2 to 10 kPa, the drying time of Jerusalem artichoke tubers increases from 3.5 to 10 hours. At the same time, reducing the pressure in vacuum chamber from 4 to 2 kPa leads to less significant increase in drying rate than with other pressure changes. Therefore, it can be recognized that the most optimal for vacuum drying are the pressure interval from 4 to 6 kPa.

The temperature level of vacuum drying process also directly affects the drying rate. In this regard, taking in mind analysis of experimental results on quality of finished product and duration of vacuum drying process, the recommended temperature intervals for heating the vacuumed medium were determined. The recommended lower limit for heating the medium in a vacuum chamber, which provides a sufficiently high drying intensity, is 40 ^{0}C. Drying of materials at a temperature 60 ^{0}C and above leads to deterioration sensory characteristics, and therefore, the offered upper limit of medium heating is 55 ^{0}C. Results of experimental studies of atmospheric drying show that there is a significant gap between the drying curves at 40 and 35 ^{0}C. This temperature range can be called a boundary, which separates the areas of intensive (temperature of medium in the chamber above 40 ^{0}C) and low-intensive (temperature of medium below 35 ^{0}C) drying. Also the optimal rate of drying agent in the device for final atmospheric drying was determined. It is established that the optimal speed of drying agent having the optimal heating temperature (36 ÷ 40) ^{0}C should be within (0.25 ÷ 0.4) m/s.

Drying is a complex operation involving simultaneous heat and mass transfer processes [6]. Study of heat and mass transfer processes in drying plants, both vacuum and atmospheric, is based on the determination of heat and mass transfer coefficients.

Experimental studies of heat and mass transfer for vacuum-atmospheric drying were carried out depending on pressure and temperature of medium during vacuum drying and temperature and air rate during atmospheric drying. Figures 1-6 show the dependences of heat and mass transfer coefficients for the above mentioned parameters. From the data shown in figures 1 and 2 it can be seen that heat and mass transfer coefficients have the highest values at heating temperature of vacuum medium 55 ^{0}C. This means that compare to heating temperatures 35 and 45 ^{0}C the intensity of heat and mass transfer is higher when it is heated at 55 ^{0}C. The analysis of experimental data shows that during vacuum drying, the change in the height of the bulk layer of the material has a much greater impact on heat transfer intensity than change in pressure or temperature of vacuum medium (figures 5 and 6). At the same time, the change in height of bulk layer of material has a slightly smaller effect on values of mass transfer coefficients. Thus, the change in height of bulk layer of topinambour tubers from 0.01 to 0.04 m leads to decreasing meanings of heat transfer coefficients from 10.23 to 5.81 W/(m^{2}K) that is by 1.76 times. Accordingly, potato tubers - from 10.01 to 5.54 W/(m^{2}K) – 1.81 times; apples – from 9.14 to 4.4 W/(m^{2}K) - 2.08 times, and green peas - decrease in values of heat transfer coefficients occurs from 4.96 to 2.65 W/(m^{2}K) that is 1.87 times. The values of heat and mass transfer coefficients during atmospheric at height of bulk layer of material 0.02 m drying are calculated depending on air temperatures (figures 7 and 8). It can be seen that the highest heat

and mass transfer intensities are observed at air temperatures 40 ^{0}C. At this temperature, the numerical values of heat transfer coefficients of Jerusalem artichoke tubers 8.78; potatoes – 8.43; apples -7.09 and green peas - 4.16 W/(m^{2}K). The corresponding values of mass transfer coefficients are: 0.0169; 0.015; 0.0089 and 0.0081 s/m. That is, at this pressure, values of heat transfer coefficients of topinambour tubers are 1.04; 1.24 and 2.11, and mass transfer coefficients are 1.13; 1.9 and 2.09 times, respectively, higher than compared products. Comparison of ratios of numerical values of coefficients of heat and mass transfer of the materials received in processes of their vacuum and atmospheric drying shows their rather satisfactory coincidence.

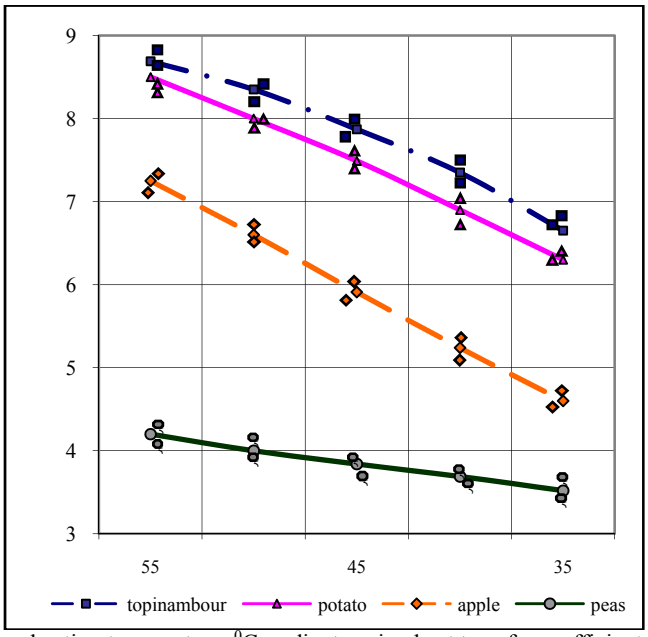

abscissa axis - heating temperature, ^{0}C; ordinate axis - heat transfer coefficient, W / (m^{2}K).

Figure 1 - Dependences of heat transfer coefficients of dried materials on heating temperature at a medium pressure 4 kPa and height of material layer 0.02 m.

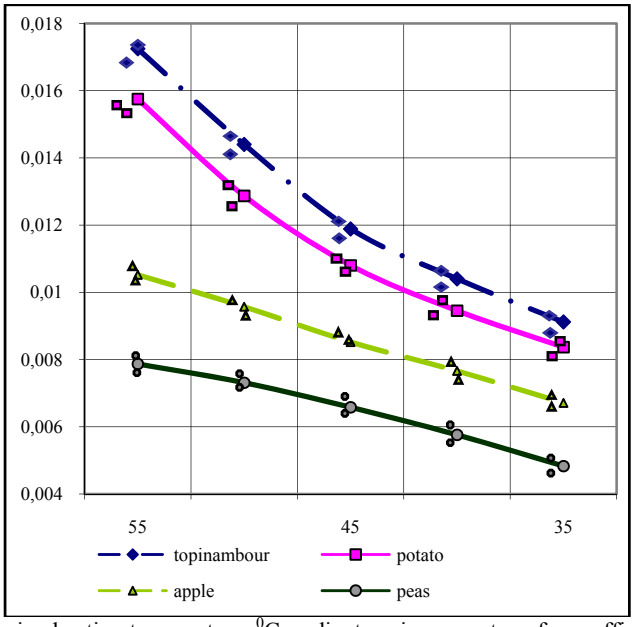

abscissa axis - heating temperature, ^{0}C; ordinate axis - mass transfer coefficient, s/m.

Figure 2 - Dependence of material mass transfer coefficients on heating temperature at medium pressure of 4 kPa and layer height of material 0.02 m.

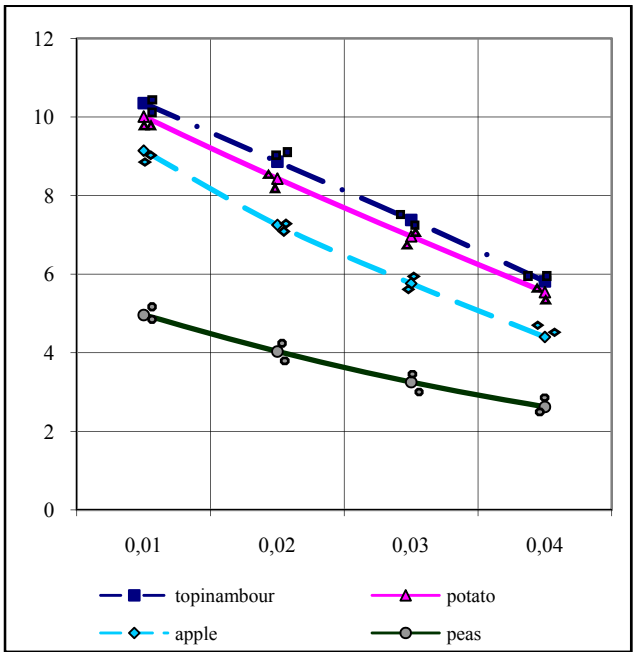

abscissa axis - layer height, ^{0}C; ordinate axis - heat transfer coefficient, W / (m^{2}K).

Figure 3 - Dependences of heat transfer coefficients on height of layer of dried materials at pressure of medium pressure 4 kPa and temperature of medium 55 ^{0}C.

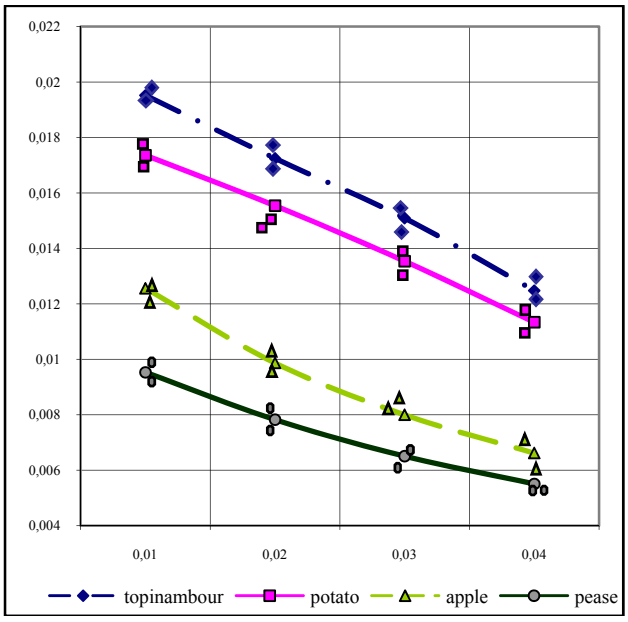

abscissa axis - layer height, m; ordinate axis - coefficient of mass transfer, s/m.

Figure 4 - Dependences of mass transfer coefficients on height layer at pressure of medium 4 kPa and temperature of medium 55 ^{0}C

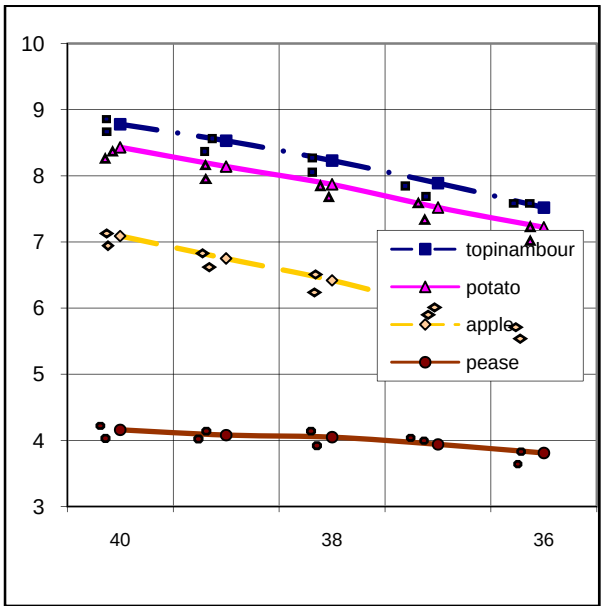

abscissa axis – air temperature, ^{0}C; ordinate axis - heat transfer coefficient, W / (m^{2}K).

Figure 5 - Dependences of heat transfer coefficients of the dried materials
on the air temperature at air velocity 0.4 m/s and layer height of material 0.02 m during atmospheric drying

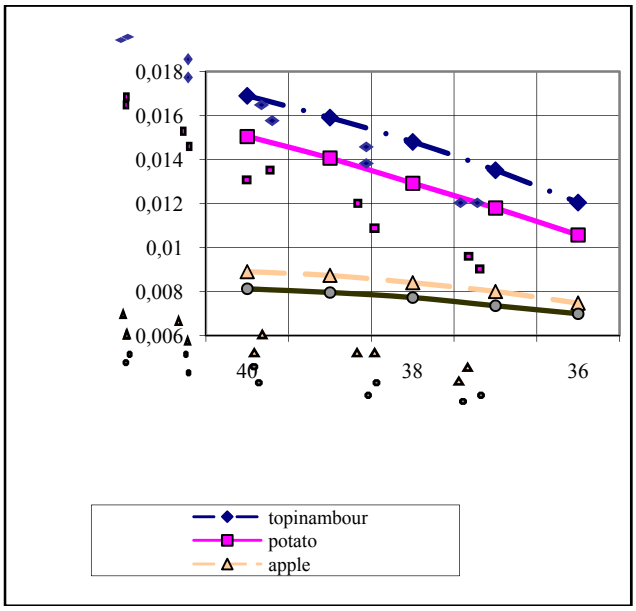

abscissa axis – air temperature, ^{0}C; ordinate axis - mass transfer coefficient, s/m.

Figure 6 - Dependences of mass transfer coefficients on air temperature
at air rate 0.4 m/s and height layer 0.02 m during atmospheric drying.

On the base of analysis of experimental data on heat and mass transfer drying of large-dispersed materials for processes of vacuum drying the following equations of heat and diffusion Nusselt criteria are obtained:

$$Nu=1,21Re^{0,154}Gu^{0,21}Pr^{0,33}\Gamma^{0,135},$$

$$Nu_m=0,29Re^{0,85}Gu^{0,16}Pr^{0,33}\Gamma^{0,045},$$

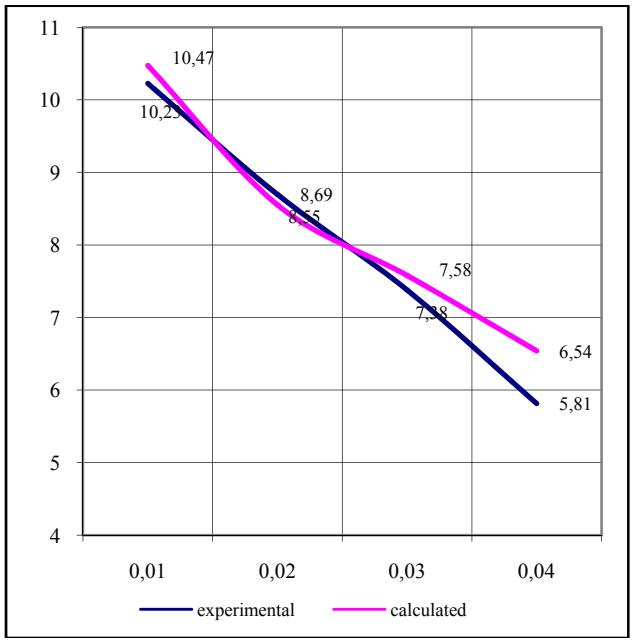

abscissa axis – height layer, m; ordinate axis - heat transfer coefficient, W/(m^{2}K).

Figure 7 - Dependences of experimental and calculated coefficients of heat transfer on height layer of dried material at pressure of medium 4 kPa and temperature of heating 55 ^{0}C

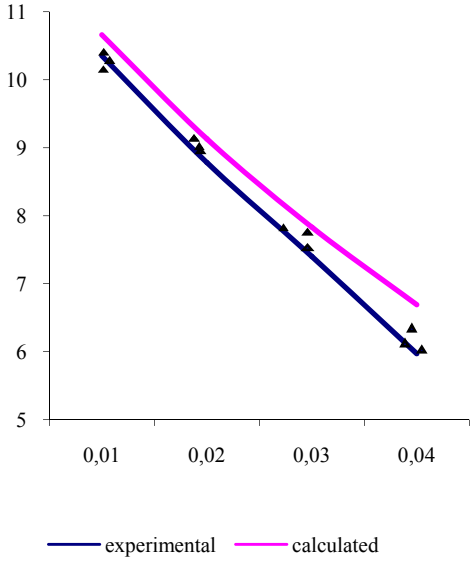

abscissa axis – height layer, m; ordinate axis - heat transfer coefficient, W/(m^{2}K).

Figure 8 - Dependences of experimental and calculated coefficients of heat transfer on height layer of dried material at air temperature 40^{0}C and air rate 0.4 m/s.

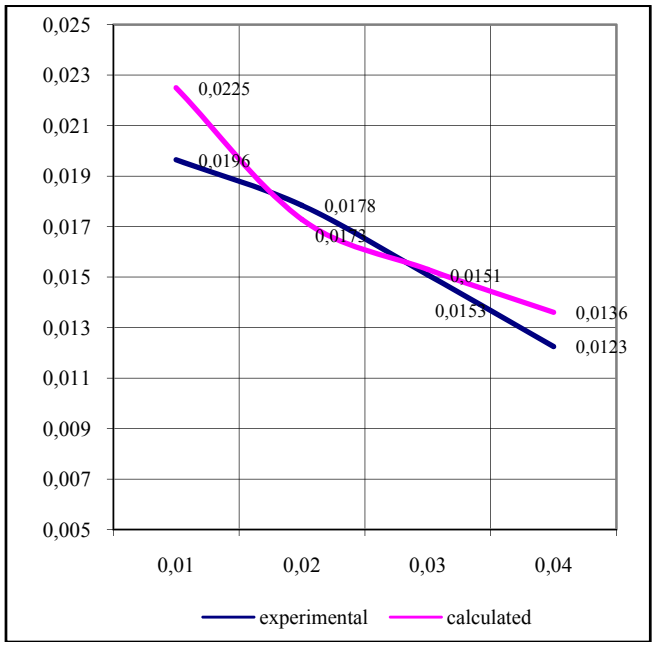

abscissa axis – height layer, m; ordinate axis - mass transfer coefficient, m/s.

Figure 9 - Dependences of experimental and calculated coefficients of mass transfer on height layer of dried material at pressure of medium 4 kPa and temperature of heating 55 ^{0}C

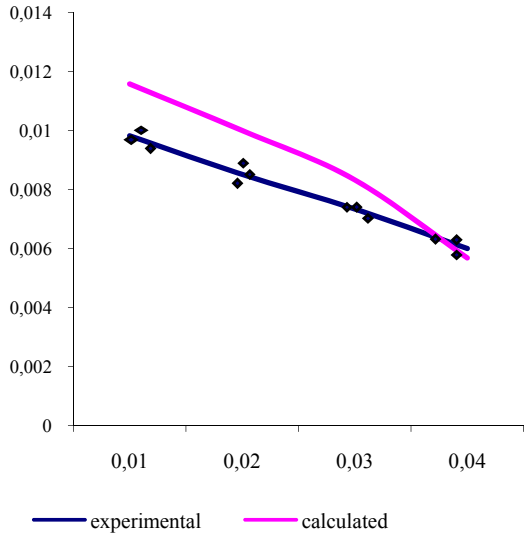

abscissa axis – height layer, m; ordinate axis - mass transfer coefficient, m/s.

Figure 10 - Dependences of experimental and calculated coefficients of mass transfer on height layer of dried material at air temperature 40 ^{0}C and height layer 0.02 m.

Also on base of experimental data the following equations of heat and diffusion Nusselt criteria for atmospheric drying are obtained:

$$Nu = 0{,}54\, Pr^{0{,}33}\, Re^{0{,}35}\, Gu^{0{,}17},$$

$$Nu_m = 0{,}34\, Pr_m^{0{,}33}\, Re^{0{,}35}\, Gu^{0{,}17}.$$

Conclusion

Comparison on adequacy to real conditions is conducted in order to check the criterion equations. Numerical meanings of experimental and calculated coefficients of heat and mass transfer at vacuum drying depending on height layer of dried material at pressure of medium 4 kPa and heating temperature 55 ^{0}C are given in figures 7 and 8. Meanings of heat and mass transfer coefficients depending on air rate at air temperature 40 ^{0}C and height layer 0.02 m at atmospheric drying are shown in figures 9 and 10.

As it seen from the figures, meanings of experimental and calculated data of heat and mass transfer coefficients have satisfied convergence. Divergence of experimental and calculated mass transfer coefficients does not exceed 17.5%.

Б.Т. Әбдіжаппарова[1], Н.С.Ханжаров[2], Б.О. Оспанов[1], И.А.Панкина[3], С.А. Күмісбеков[1], Қ.С. Ислам[1]

[1]М.Әуезов ат. Оңтүстік Қазақстан мемлекеттік университеті (Қазақстан),
[2]Халықаралық гуманитарлы-техникалық университеті (Қазақстан),
[3]Ұлы Петр ат. Санкт-Петербург мемлекеттік политехникалық университеті (Ресей)

ІРІДИСПЕРСТІ ТАҒАМДЫҚ МАТЕРИАЛДАРДЫ ВАКУУМДЫ-АТМОСФЕРАЛЫҚ КЕПТІРУДІҢ НӘТИЖЕЛЕРІ

Аннотация. Ұсынылған мақалада асбұршақ, ұсақталған жер алмұрты, картофель және алма сияқты ірідисперсті тағамдық материалдарды вакуумды-атмосфералық кептіру кезіндегі жылумассаалмасуды зерттеу нәтижелері қарастырылған. Осы оңтайлы вакуумды-атмосфералық кептірудің режимдері әзірленді. Ірі дисперсті материалдарды вакуумды және атмосфералық кептірудің нәтижелері зерделенді. В зависимости от высоты слоя высушиваемого кептірілуші материал қабатының биіктігіне, вакуумды камерадағы ортаның қысымына, кептірудің температуралық деңгейіне тәуелділігіне байланысты Нуссельттің жылу- және массаалмасу критерийлерінің теңдеулері және жылу- және массатасымалдау коэффициенттерінің сандық мәндері алынды. Критериальді теңдеулерді тексеру мақсатында оларды нақты жағдайларға ұқсастығын сараптау үшін талдау жүргізілді. Жылу- және массатасымалдау коэффициенттерінің эксперименталды және есептік мәліметтерінің мәндері олардың қанағаттанарлық сәйкестігін көрсетеді.

Түйін сөздер: оңтайлы, жер алмұрты, эксперимент, зерттеу, массаалмасу, режим.

Б.Т. Абдижаппарова[1], Н.С.Ханжаров[2], Б.О. Оспанов[1], И.А.Панкина[3], С.А. Кумисбеков[1], К.С. Ислам[1]

[1]Южно-Казахстанский государственный университет им.М.Ауэзова (Казахстан),
[2]Международный гуманитарно-технический университет (Казахстан),
[3]Санкт-Петербургский государственный политехнический университет им.Петра Великого (Россия)

РЕЗУЛЬТАТЫ ВАКУУМНО-АТМОСФЕРНОЙ СУШКИ КРУПНОДИСПЕРСНЫХ ПИЩЕВЫХ МАТЕРИАЛОВ

Аннотация. В данной статье рассмотрены результаты исследований тепломассообмена при вакуумно-атмосферной сушки крупнодисперсных пищевых материалов, таких как горох, измельченные клубни топинамбура, картофеля и яблок. Разработаны оптимальные режимы вакуумно-атмосферной сушки данных материалов. Изучены результаты вакуумной и атмосферной сушки крупнодисперсных материалов. В зависимости от высоты слоя высушиваемого материала, давления среды в вакуумной камере, температурного уровня сушки получены численные значения коэффициентов тепло- и массопереноса и уравнения тепло- и массобменных критериев Нуссельта. С целью проверки критериальных уравнений проведен анализ сходимости их реальным условиям. Значения экспериментальных и расчетных данных коэффициентов тепло- и массопереноса показывают их удовлетворительное совпадение.

Ключевые слова: оптимальный, топинамбур, эксперимент, исследование, массообмен, режим.

Information about the authors:

Abdizhapparova Bakhytkul Telkhozhaevna - M. Auezov South Kazakhstan State University, Shymkent, Kazakhstan, https://orcid.org/0000-0001-8277-8243;

Khanzharov Nurlan Serikbayevich -International Humanitarian-Technical University, Shymkent, Kazakhstan, https://orcid.org/0000-0002-7406-0386;

Ospanov Bakhytzhan Orazalievich - M. Auezov South Kazakhstan State University, Shymkent, Kazakhstan, https://orcid.org/0000-0002-6437-5579;

Pankina Ilona Anatolyevna - Peter the Great St. Petersburg Polytechnic University, St. Petersburg, Russia;

Kumisbekov Serik - M. Auezov South Kazakhstan State University, Shymkent, Kazakhstan;

Islam Karlygash Sapibullakyzy - M. Auezov South Kazakhstan State University, Shymkent, Kazakhstan

REFERENCES

[1] Hanzharov N.S., Balabekov O.S., Abdizhapparova B.T. Issledovanie teplomassoobmena pri vakuumno-atmosfernoj sushke krupnodispersnyh pishhevyh materialov // Pishhevaja tehnologija i servis. - 2004, № 2. - S.58-64. [Khanzharov N.S., Balabekov O.S., Abdizhapparova B.T. Investigation of heat and mass exchange at vacuum-atmospheric drying of large-dispersed food materials // Food technology and service. 2004, №2. P.58-64].

[2] Khanzharov N.S., Abdizhapparova B.T., Ospanov B.O., Dosmakanbetova A.A., Baranenko A.V., Kumisbekov S.A., Serikuly Zh. Designs of dryers based on combination of vacuum and atmospheric drying of food products (2018), NEWS OF THE ACADEMY OF SCIENCES OF THE REPUBLIC OF KAZAKHSTAN, series of geology and technical sciences, 5(431):141 – 149(in Eng).

[3] Nathakaranakule A., Kraiwanichkul W., Soponronnarit S. Comparative Study of Different Combined Superheated-steam Drying Techniques for Chicken Meat. Journal of Food Engineering, 2007, Vol. 80(4). pp.1023-1030.

[4] Perera C.O., Rahman M.S. Heat pump drying. Trends Food Sci. Technol., 1997, №8(3), p. 75

[5] Lee K.H., Kim O.J. Investigation on Drying Performance and Energy Savings of the Batch-Type Heat Pump Dryer. Drying Technology, 2009, Vol. 27, pp. 565–573.

[6] Jangam Sachin V., Lim Law Chung, Mujumdar A.S.. Drying of Foods. Vegetables and Fruits, 2010, Vol. 1, 232 p.

N E W S
OF THE NATIONAL ACADEMY OF SCIENCES OF THE REPUBLIC OF KAZAKHSTAN
SERIES CHEMISTRY AND TECHNOLOGY
ISSN 2224-5286 **https://doi.org/10.32014/2019.2518-1491.76**
Volume 6, Number 438 (2019), 70 – 78

Y.Y. Nurmakanov, G.D. Zakumbaeva, S.S. Itkulova, and L.V. Komashko

[1]D.V. Sokolsky Institute of Fuel, Catalysis and Electrochemistry, Almaty, Kazakhstan
e-mail: s.itkulova@ifce.kz

METHANE CONVERSION OVER Mo/Al_2O_3 – CATALYSTS MODIFIED WITH ADDITIVES OF ZEOLITE AND PHOSPHOROUS

Abstract. Mo-containing catalysts supported on a matrix consisting of alumina modified with additives of both zeolite – HZSM and phosphorus were synthesized. The molybdenum content was varied within a range of 1-5 mas.%. The physicochemical properties of the catalysts were studied by BET, XRD, electron microscopy, and microdiffraction analysis. The catalytic properties of the synthesized catalysts were tested in the processes of dry and combined steam-dry conversion of methane. It was shown that the synthesized catalysts are the nanosystems with particle sizes are 3-50 nm depending on the amount of molybdenum and the processing methods of the catalysts. The activity of the catalysts grows with increasing of both molybdenum content and temperature. The main product of methane conversion is synthesis gas. The H_2/CO ratio increases at adding steam to an initial feed. In dry reforming of methane the reaction products also contain C_2, C_6 hydrocarbons and alcohols.

Key words: Dry and Combined Dry-Steam Conversion of Methane, Syngas, Molybdenum, Zeolite, Phosphorus.

1. INTRODUCTION

In recent years, the processing of gaseous hydrocarbons into value-added products has attracted attention. Conversion of methane, the primary constituent of natural gas, associated petroleum gas, biogas is considered to be the promising one. Biogas is considered as a renewable source of energy [1].

One of the ways of conversion methane-containing feedstock to chemicals is production of synthesis gas [2]. There are three reforming reactions that allow converting methane into syngas with different H_2/CO ratio: partial oxidation, steam reforming, and dry reforming [3]. The last one has gained a lot of attention due to possibility to reduce the emissions of two main greenhouse gases like carbon dioxide and methane [4]. The ratio of H_2/CO produced in the dry reforming of methane is ~ 1 which preferable as a feed for production long chain hydrocarbons and oxygenates [5, 6].

The main challenge is that the reaction is highly endothermic and high temperatures are required to reach considerable extent of conversion as well as surpass side reactions [7, 8]. Lack of stable catalysts against quick deactivation because of coking and active sites sintering is another disadvantage [2,9]. To reduce the undesirable carbon deposition process, it is necessary to create an active catalyst and technology capable of involving the surface C_{ads} formed as a result of the destructive decomposition of methane into interaction with CO_2 (Eq.1). Surface adsorbed carbon is the product of the complete dehydrogenation of a methane molecule during its carbon dioxide conversion at the metal-containing active center of the catalyst.

$$CO_2 + C_{ads} \rightarrow 2CO \qquad \text{(Eq.1)}$$

Therefore more efforts are being expended in the development of new catalysts that will represent activity, resistance to coking, as well as, long-term stability. Non-noble metals like Ni, Co, Fe and noble metals including Pt, Rh, Ir, Pd and etc. have been studied as a catalyst in the dry reforming of methane [10-13]. Non-noble-based catalysts are preferable over noble metals because of the availability and low cost. Noble metals are usually applied as a promoter in polymetallic catalysts due to their high activity and greater resistance to coke formation compared to non-noble metals [14]. It allows overcoming the

deactivation of non-noble catalysts caused by excessive coke deposition, while simultaneously reducing total cost. Other benefits of this approach are it increases the dispersion of the metal, decreases the size of the metal particle and thus retain a good catalytic activity and stability.

Supported transition metals (or their carbides) are another type of catalysts that have attracted attention due to their comparable activity and stability to noble metals [8,15-16]. The performance of a catalyst does not depend not only on active metal and promoter, but also on the support. Main role of supports is in provision of certain textural and physicochemical properties [17]. These properties give possibility to a catalyst to stay well-dispersed and resistant to carbon deposition. Single-metal support such as γ-alumina performs very well in the reforming of methane, but it is apparent that mixed and/or structured supports have properties that make them attractive to use in methane reforming [11]. Zeolites with a high Si/Al ratio are considered to give better conversions, which are more basic. Their good performance is due to the confinement of active metal particles inside their pores, providing a higher resistance to sintering, as well as their basic character that decreases carbon deposition [18].

In this work, the new Mo-containing catalysts supported on alumina modified with additives of zeolite (HZSM-5) and phosphorus were synthesized and tested in dry and combined steam-dry reforming of methane.

2. EXPERIMENTAL

Catalysts were prepared by mixing $Al(OH)_3$ with HZSM-5 zeolite followed by drying and forming of the granules and their calcination. The ratio Al_2O_3:HZSM=7:3. The prepared by such a way matrix was impregnated by molybdenum salt and phosphoric acid. The molybdenum content varied from 1 to 5 mas.% by weight of the catalyst, the phosphorus content – 1.0 mas. %.

The model feed corresponding to biogas composed of CH_4 – 53.5 vol. %, CO_2 – 46.5 vol. % was used for dry reforming of methane (DRM). For combined steam-dry conversion of methane or so-called bireforming of methane (BRM), 20 vol.% of steam was added to an initial feed. The ratio (vol.) of the components in the feedstock was: CH_4:CO_2:H_2O=1.15:1.0:0.2. The process was carried out in a laboratory flow quarts reactor operated under atmospheric pressure at varying temperature within 500-1000°C and the gas hourly space velocity (GHSV) was varied from 500 to 1000 h^{-1}.

The physicochemical properties of the catalysts were studied by XRD, BET, TEM, and microdiffraction analysis.

The initial and final reaction products were analyzed by on-line GC. The conversion degrees of carbon dioxide (X_{CO2}) and the methane (X_{CH4}) were calculated according to formulas (1, 2) respectively. Thus, the activity of catalysts was compared.

$$X_{CO2} = ([CO_2]_{in} - [CO_2]_{out}) \cdot 100\% / [CO_2]_{in} \quad (1)$$

$$X_{CH4} = ([CH_4]_{in} - [CH_4]_{out}) \cdot 100\% / [CH_4]_{in} \quad (2)$$

where $[CH_4]_{in}$ and $[CO_2]_{in}$ – mole fraction of CH_4 and CO_2 in inlet stream, $[CH_4]_{out}$ and $[CO_2]_{out}$ – mole fraction of CH_4 and CO_2 in outlet stream.

Conversion of water was not calculated.

Yields of reaction products: hydrogen, carbon oxide and hydrocarbons (Y_{H2}, Y_{CO} and Y_{Cn} respectively) expressed as its amount (μmol) formed by gram of the catalyst per second (μmol/(g·s)).

3. RESULTS AND DISCUSSION

3.1 Catalyst characterization

The specific surface area (BET) and pore volume of both fresh and spent samples of the Mo catalysts in the dry conversion of methane were determined. The fresh catalyst samples with varied Mo content have the same characteristics. The difference was observed between the fresh and spent samples of 2% Mo/Al_2O_3-HZSM-P, which was long-term tested (for 30 hours) in BRM. Specific surface area was decreased from 307.1 to 201.7 m^2/g, while pore volume was not significantly changed: 296.8 and 290.8 ml/g for fresh and spent samples respectively (Table 1).

Table 1 – The specific surface of 2%Mo/Al_2O_3-HZSM-P catalysts (BET)

S,m^2/g		V, ml/g	
fresh	spent (30 h)	fresh	spent (30 h)
307.1	201.7	296.8	290.8

The XRD method did not show the presence of any structures except alumina in the catalysts due to possibly high dispersed state of the catalysts and therefore they are X-ray amorphous. Other reason may be a low metal content, the determination of which is outside the sensitivity range of the equipment.

Studies of the 2%Mo/Al_2O_3-HZSM-P catalyst (fresh) by TEM showed an accumulation of dense particles of a prismatic shape and translucent laminated particles with sizes of 30-70 nm (Fig. 1). The microdiffraction pattern is represented by a small number of rings composed of reflections assigned to a mixture of phases: Mo_3Si (JCPDS, 4-814) and $AlMo_3$ (JCPDS 11-18).

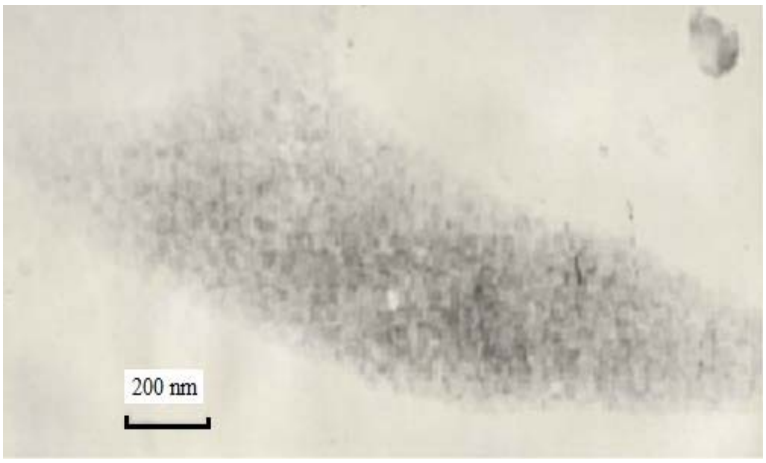

Figure 1 – TEM image of the fresh sample 2%Mo /Al_2O_3-HZSM-1%P catalyst

Also, the particles with a size of 30–50 nm were observed. Their microdiffraction pattern can be attributed to Mo_3Si (JCPDS, 4-814). The small particles with a size of 8-10 nm give the microdiffraction pattern, which corresponds to SiP structure (JCPDS, 27-608). The presence of Mo_3Si and SiP structures in the catalyst indicates the entry of Mo and phosphorus into the zeolite framework.

A large aggregate composed of translucent lamellar particles of predominantly 10-30 nm correspond to $AlPO_4$ (JCPDS, 31-28). At low magnification, the translucent lamellar particles were detected. The microdiffraction pattern is represented by reflections located in rings and separate reflexes and can be assigned to a mixture of phases: $AlPO_4$ in the modification (JCPDS, 20-45) and $MoOPO_4$ (JCPDS, 18-942). The presence of two modifications of $AlPO_4$ may be explained by the interaction of phosphorus with aluminum in zeolite framework and aluminum in Al_2O_3.

3.2 Dry reforming of methane on Mo/HZSM-P-Al_2O_3 catalyst

The effect of temperature on the performance of the 1%Mo/HZSM-P-Al_2O_3 catalyst in dry reforming of methane (DRM) has been studied under conditions: CH_4/CO_2=1.15, P=0.1MPa, GHSV=1000h^{-1} and varying temperature within 775-1000°C. The degrees of methane and carbon dioxide conversion grow from 1.7 to 31.1 and 21.3 to 65.2% respectively with an increase in temperature from 775 to 1000°C.

In the entire temperature range studied, the main product of DRM over the 1%Mo/HZSM-P-Al_2O_3 catalyst is synthesis gas. Traces of C_2, C_6 hydrocarbons and traces of oxygenates are also formed. Increasing temperature leads to growing the hydrogen content in the synthesis gas formed. Thus, an increase in temperature from 775 to 1000°C causes an increase in the H_2/CO ratio from 0.5 to 1.1. At high temperatures of 900-1000°C traces of oxygenates (C_1-C_2 alcohols) are formed. In the temperature range of

800-900°C, traces of C_2 and C_6 hydrocarbons are detected. At 1000°C, ethylene is formed in an amount of 0.2% (Table 2). The formation of these products occurs due to the interaction of alkyl and methylene surface-adsorbed fragments of incomplete methane destruction. The ability of Mo/HZSM catalysts to convert methane to benzene is well-known [19].

Table 2 – The effect of the process temperature on DRM over the 1%Mo/HZSM-P-Al_2O_3 at CH_4:CO_2=1.15:1, GHSV=1000h^{-1}, P=0.1MPa

t,°C	Conversion, %		H_2/CO	Yield of products	
	X_{CH4}	X_{CO2}		hydrocarbons	oxygenates
800	8.2	21.5	0.5	C_6 (traces)	-
900	19.6	42.1	0.8	C_2 (traces)	alcohols (traces)
1000	31.1	65.2	1.1	C_2H_4 - 0.2%	alcohols (traces)

It is known that in the process of methane dehydrocyclization over the Mo/HZSM catalyst along with the formation of benzene, significant carbonization of the catalytic surface occurs. Microdiffraction and TEM data on Mo/HZSM-P-Al_2O_3 studied confirm the formation of a nanosystem containing the various surface structures due to interaction molybdenum with zeolite and alumina to form Mo_3Si and Al_2Mo_3. Modification of the Mo/HZSM-P-Al_2O_3 catalyst with phosphorus leads to formation of $MoOPO_4$ structure. Phosphorus also can be included into the zeolite framework as SiP and $AlPO_4$. Interaction between phosphorus and alumina with formation of $AlPO_4$ was previously shown [20]. The multicomponent chemical composition of the catalytic surface due to modification by phosphorus leads to the suppression of the formation of benzene and C_2- hydrocarbons. The formation of synthesis gas becomes the main direction of carbon dioxide conversion of methane over the Mo-P-HZSM composed catalyst.

The catalytic processing of methane and other hydrocarbons is accompanied by the appearance of carbon deposits on the active catalyst sites. The effect of C_{ads} on the catalyst activity will depend on the nature of metal. Mo is able to form carbides with C_{ads}.

With an increase in the temperature of DRM from 800°C to 1000°C the reaction products mainly contain synthesis gas, the H_2/CO ratio increases from 0.5 to 1.2, which is associated with prevailing destructive decomposition of methane on Mo containing centers. In this case, the C_{ads} formed can interact with CO_2, but at a low concentration of CO_2 the C_{ads} can be introduced into the molybdenum structure with the formation of carbide – Mo_2C.

Comparative analysis of data [19,21-22] and results of this study allows to conclude that the formation and destruction of molybdenum carbide depend on the carbon dioxide content in the reaction zone. At a low concentration of CO_2 in the feedstock C_{ads} formed can interact with molybdenum to form carbides at high temperatures. At high CO_2 concentrations in the feed, carbide is destructed as a result of the reaction (Eq.2) [21-22]. Molybdenum carbide is an active catalyst for dry reforming of methane.

$$Mo_2C + CO_2 \rightarrow 2CO + MoO_2 \quad \text{(Eq.2)}$$

3.3 Bireforming of methane on Mo/HZSM-P-Al_2O_3 catalysts

To enrich the synthesis gas with hydrogen, the steam additives (20 vol.%) were introduced into the feed CH_4-CO_2. The combined dry-steam reforming of methane or bireforming of methane (BRM) was carried out over the 1%Mo/HZSM-P-Al_2O_3 catalyst under P=0.1MPa, GHSV=1000h^{-1}, CH_4:CO_2:H_2O=1.15:1.0:0.2 and varying temperature within a range of 500-1000°C.

At a temperature of 1000°C, the degree of conversion of methane and carbon dioxide reaches 43.7 and 78.2% respectively (Fig.2). Conversion of carbon dioxide is higher because its content in initial feed is less. The main product of BRM is synthesis gas. H_2/CO ratio is increased from 0.6 to 1.2 at growing temperature from 800 to 1000°C. The addition of steam into the reaction mixture inhibits the formation of hydrocarbons. C_2 and C_6 hydrocarbons and oxygenates presented in small amounts at relatively low temperature – 780°C and completely disappeared at higher temperatures (Table 3).

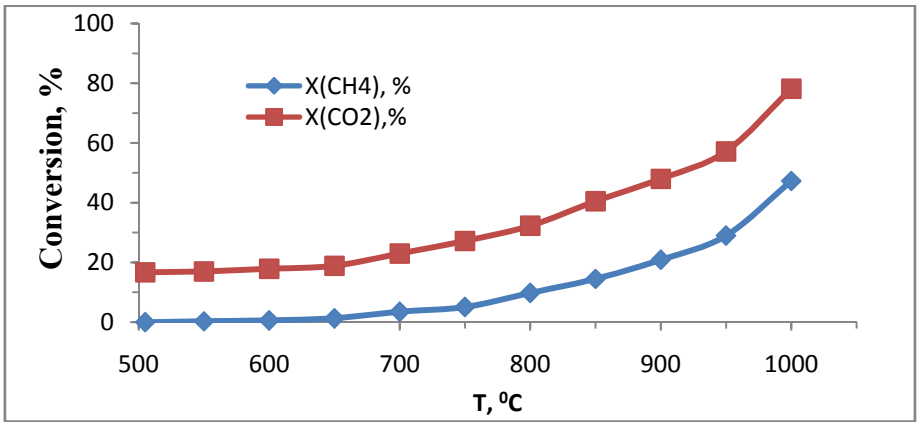

Figure 2 – The effect of temperature on BRM over the 1% Mo/HZSM-P-Al_2O_3 catalyst at CH_4:CO_2:H_2O=1.15:1:0.2, P=0.1 MPa, GHSV=1000h^{-1}

Table 3 – Effect of temperature on the products composition in BRM over the 1%Mo/HZSM-P-Al_2O_3 catalyst at CH_4:CO_2:H_2O=1.15:1:0.2, P=0.1 MPa, GHSV=1000h^{-1}

t, °C	Conversion, %		H_2/CO	Product yield	
	X_{CH4}	X_{CO2}		Hydrocarbons	Oxygenates
780	9.1	29.0	0.6	C_2H_4, C_6 (traces)	traces
800	9.8	32.3	0.6	-	traces
900	20.9	48.0	0.8	-	traces
1000	47.3	78.2	1.2	-	traces

The analysis of Tables 2 and 3 shows that the participation of steam in methane conversion leads to increase in conversion both of methane and carbon dioxide as well as to enrich synthesis gas with hydrogen. Consumption of carbon dioxide is higher than methane i.e. CO_2 may actively reacts with C_{ads} with formation of CO at the Mo-containing centers.

Mainly, the optimal amount of the active component of the catalyst is experimentally determined. In this work, the Mo content ranged from 1 to 5 mas. % weight. Figure 3 shows the effect of temperature on the conversion of CH_4 and CO_2 in BRM over the 2%Mo/HZSM-P-Al_2O_3 catalyst. The high activity of the catalyst in BRM is observed at a temperature region of 800-1000°C: methane conversion was 72.4 and carbon dioxide – 86% at 960°C. The main reaction product over the 2%Mo/HZSM-P-Al_2O_3 catalyst is synthesis gas, the H_2/CO ratio is 1.3.

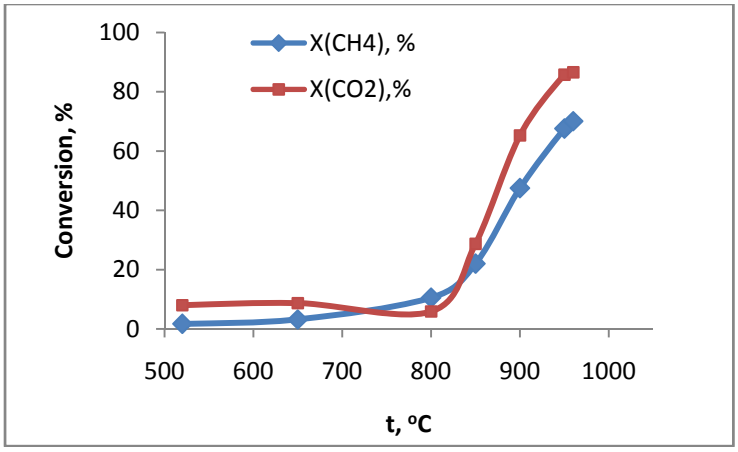

Figure 3 – The effect of temperature on BRM over the 2% Mo/HZSM-P-Al_2O_3 catalyst at CH_4:CO_2:H_2O=1.15:1:0.2, P=0.1 MPa, GHSV=1000h^{-1}

At using higher content of Mo – 5 mas.% under the same conditions (CH_4:CO_2:H_2O=1.15:1:0.2, P=0.1 MPa, GHSV=1000h^{-1}) an increase in activity of the 5%Mo/HZSM-P-Al_2O_3 catalyst was observed in BRM. Methane conversion became higher than carbon dioxide (Fig. 4): X_{CH4}=82.0%, while X_{CO2}=65.8% at 960°C.

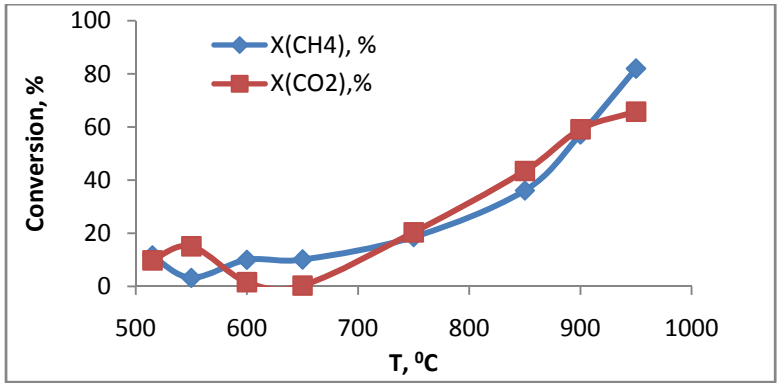

Figure 4 – The effect of temperature on BRM over the 5% Mo/HZSM-P-Al_2O_3 catalyst at CH_4:CO_2:H_2O=1.15:1:0.2, P=0.1 MPa, GHSV=1000h^{-1}

Thus, systematic studies of Mo/HZSM-P-Al_2O_3 catalysts with varying molybdenum contents from 1.0 to 5 wt.% allowed us to conclude that the activity is directly dependent on the amount of molybdenum, which is the active phase of the system (Table 4).

Table 4 – Comparative characteristics of Mo/HZSM-P-Al_2O_3 catalysts in BRM at CH_4:CO_2:H_2O=1.15:1:0.2, P=0.1MPa, t=960°C, GHSV=1000h^{-1}

Mo content, mas.%	Conversion, %	
	X_{CH4}	X_{CO2}
1	47.3	78.2
2	72.4	86.0
5	82.0	65.8

The physicochemical properties of the 2%Mo/HZSM-P-Al_2O_3 catalyst were studied after its long-term operation (30 hours) in BRM by electron microscopy and microdiffraction analysis. In addition to the structures observed in the fresh sample the new species with a size of 10-40 nm (Fig. 5), which can be attributed to a mixture of phases: MoO_2 (JCPDS, 32-671), η-MoC (JCPDS, 8-384), α-Mo_2C (JCPDS, 35-787), P (JCPDS, 18-964), SiC (JCPDS, 29-1127), Al_2Mo_3C (JCPDS 6-7) were detected by microdiffraction analysis.

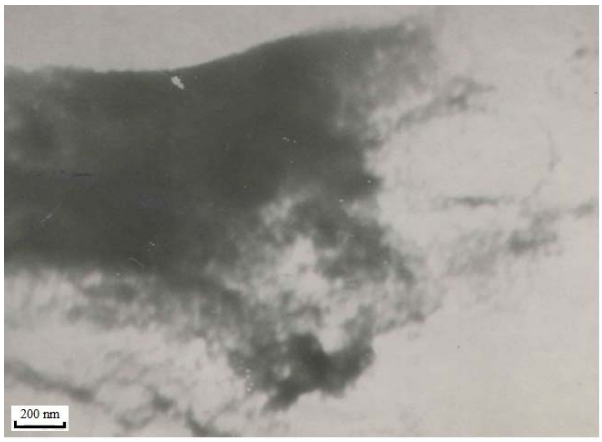

Figure 5 - TEM image of 2%Mo/HZSM-P-Al_2O_3 spent in BRM for 30 hours

It is more important the appearance of molybdenum carbides: MoC and Mo_2C. Molybdenum carbides are formed at temperatures above 600-650°C. Under the conditions of BRM molybdenum carbides may be formed due to interaction between atomic carbons formed as a result of methane destruction with Mo which is an active center of the catalyst.

It was shown in [22,23] that molybdenum catalysts coated with Mo carbides exhibit high activity in the carbon dioxide conversion of methane. Molybdenum carbides are highly active in methane conversion that was confirmed in this work by the long-term test of 2%Mo/HZSM-P-Al_2O_3 in BRM. But over time, the degree of methane conversion decreases as a result of the interaction of carbides with carbon dioxide to form carbon monoxide and non-active molybdenum oxides (Eq.2).

The stability of the 2%Mo/HZSM-P-Al_2O_3 catalyst was tested for long continuous operation (30 hours). The results prove that Mo-containing catalysts are sufficiently thermally stable; no destruction of their structure and particle agglomeration was observed by TEM. Measurement of the surface area of 2%Mo/HZSM-P-Al_2O_3 catalyst by the BET method showed that some changes occur in the spent sample – S=201.7m^2/g compared to the initial one –S=307m^2/g. Elucidation and elimination of the reasons leading to a decrease in the specific surface area of the catalyst after long-term operation will allow the development of methods to increase stability and activity of the Mo/HZSM-P-Al_2O_3 catalyst.

CONCLUSIONS

Phosphorus modified molybdenum catalysts can be of practical interest in the production of chemical and petrochemical products from any methane-containing feedstock including renewable biogas. The Mo/HZSM-P-Al_2O_3 catalysts developed perform the activity and selectivity in syngas production by dry and bireforming of methane. Preliminary stability test demonstrates their stable activity and selectivity for 30 hours of exploitation. Under certain conditions hydrocarbons and alcohols are formed over the catalysts. That allows considering the Mo/HZSM-P-Al_2O_3 as promising base for manufacturing a cheap stable catalyst for syngas production from methane or biogas by further appropriate modification of the catalyst developed.

Acknowledgement: This research was supported by the Ministry of Education and Science of the Republic of Kazakhstan, the Program # BR05236739 MES RK.

Е.Е. Нурмақанов[1], Г.Д. Закумбаева[1], Ш.С.Итқұлова[1], Л.В. Комашко[1]

[1]АҚ «Д.В. Сокольский атындағы жанармай, катализ және электрохимия институты», Алматы, Қазақстан

ФОСФОР ЖӘНЕ ЦЕОЛИТ ҚОСПАСЫМЕН МОДИФИЦИРЛЕНГЕН Mo/Al_2O_3- КАТАЛИЗАТОРЛАРДАҒЫ МЕТАННЫҢ ТҮРЛЕНУІ

Аннотация. Цеолит (HZSM) және фосфордың қоспаларымен модифицирленген алюминий тотығынан тұратын матрицаға қондырылған Мо-құрамды катализаторлар синтезделген болатын. Молибден мөлшері 1-5 мас.% шамасы аралығында тербеледі. Катализаторлардың физика-химиялық қасиеттері БЭТ, РФА, электронды микроскоп және микродифракциялық анализ әдістерімен зерттелді. Синтезделген катализаторлардың катализдік қасиеттері метанның көмірқышқылды және булы көмірқышқылды түрлену (конверсия) процестерінде тестілеуден өтті. Синтезделген катализаторлар молибденнің мөлшеріне және катализаторларды өңдеу тәсілдеріне байланысты бөлшектер шамасы 3-50 нм-ді құрайтын наножүйеге жататыны көрсетілді. Катализаторлар белсенділігі молибден мөлшері мен температураның ұлғаюына қарай өседі. Метан түрленуінің негізгі өнімі синтез-газ болып табылады. H_2/CO қатынасы бастапқы газ қоспасына су буын қосу есебінен өседі. Сондай-ақ, метанның сусыз риформингі кезінде реакция өнімдерінде C_2, C_6 көмірсутектердің және спирттердің азғантай мөлшері құрайды.

Түйін сөздер: Метанның Көмірқышқылды және Булы көмірқышқылды Түрленуі (Конверсиясы), Синтез-газ, Молибден, Цеолит, Фосфор.

УДК 544.478; 542.97; 665.612.3; 546.264-31
МРНТИ 31.15.28

Е.Е. Нурмаканов[1], Г.Д.Закумбаева[1], Ш.С. Иткулова[1], Л.В.Комашко[1]

[1]АО «Институт топлива, катализа и электрохимии им. Д.В. Сокольского», Алматы, Казахстан

КОНВЕРСИЯ МЕТАНА НА Mo/Al_2O_3 – КАТАЛИЗАТОРАХ, МОДИФИЦИРОВАННЫХ ДОБАВКАМИ ФОСФОРА И ЦЕОЛИТА

Аннотация. Были синтезированы Мо-содержащие катализаторы, нанесенные на матрицу, состоящую из оксида алюминия, модифицированного добавками цеолита – HZSM и фосфора. Содержание молибдена варьировалось в пределах 1-5 мас.%. Физико-химические свойства катализаторов изучались методами БЭТ, РФА, электронной микроскопии и микродифракционного анализа. Каталитические свойства синтезированных катализаторов тестировались в процессах углекислотной и пароуглекислотной конверсии метана. Было показано, что синтезированные катализаторы относятся к наносистемам, размеры частиц которых составляют 3-50 нм в зависимости от количества молибдена и методов обработки катализаторов. Активность катализаторов возрастает с увеличением содержания молибдена и температуры. Основным продуктом конверсии метана является синтез-газ. Соотношение H_2/CO возрастает при добавлении паров воды в исходную смесь. При сухом риформинге метана в продуктах реакции также содержатся в небольших количествах углеводороды C_2, C_6 и спирты.

Ключевые слова: Углекислотная и Пароуглекислотная Конверсия Метана, Синтез-Газ, Молибден, Цеолит, Фосфор.

Information about the authors:

Nurmakanov Y.Y. – D.V. Sokolsky Institute of Fuel, Electrochemistry and Catalysis, Almaty, Kazakhstan, yerzhan.nurmakanov@gmail.com, https://orcid.org/0000-0002-0404-1833

Zakumbayeva G.D. – D.V. Sokolsky Institute of Fuel, Electrochemistry and Catalysis, Almaty, Kazakhstan, Academician of NAS RK, Retired, g.d.zakumbaeva@gmail.com, https://orcid.org/0000-0001-5536-2664

Itkulova S.S. – D.V. Sokolsky Institute of Fuel, Electrochemistry and Catalysis, Almaty, Kazakhstan, s.itkulova@ifce.kz, https://orcid.org/0000-0001-7159-5249

Komasko L.V. – D.V. Sokolsky Institute of Fuel, Electrochemistry and Catalysis, Almaty, Kazakhstan, komashko535@mail.ru, https://orcid.org/0000-0003-0031-2816

REFERENCES

[1] Gao Y, Jiang J, Meng Y, Yan F, Aihemaiti A (2018) A review of recent developments in hydrogen production via biogas dry reforming. Energy Conversion and Management 171:133-155 DOI:10.1016/j.enconman.2018.05.083

[2] Nurmakanov YY, McCue AJ, Anderson JA, Itkulova SS, Kussanova SK (2016) Methane reforming by CO_2 or CO_2-H_2O over Co-containing supported catalysts. News of the National Academy of Sciences of the Republic of Kazakhstan. Series Chemistry and Technology 5:5-11.

[3] Iwarere S.A., Rohani V.-J., Ramjugernath D., Fulcheri L (2015) Dry reforming of methane in a tip-tip arc discharge reactor at very high pressure. International Journal of Hydrogen Energy 40:3388-3401

[4] Elvidge C.V., Bazilian M.D., Zhizhin M., Ghosh T., Baugh K., Hsu F.-C. (2018) The potential role of natural gas flaring in meeting greenhouse gas mitigation targets. Energy Strategy Reviews 20:156-162 DOI: 10.1016/j.esr.2017.12.012

[5] Jang WJ, Shim JO, Kim HM, Yoo SY, Roh SH (2018) A review on dry reforming of methane in aspect of catalytic properties. Catalysis Today 324:15-26 DOI: 10.1016/j.cattod.2018.07.032

[6] Gould A, Izar A, Weimer AW, Falconer JL, Medlin JW (2014) Stabilizing Ni catalysts by molecular layer deposition for harsh, dry reforming conditions. ACS Catalysis 4:2714-2717 DOI: 10.1021/cs500809w

[7] Nguyen HM, Pham GH, Ran R, Vagnoni R, Pareek V, Liu S (2018) Dry reforming of methane over Co-Mo/Al_2O_3 catalyst under low microwave power irradiation. Catalysis Science and Technology 8:5315-5324 DOI: 10.1039/c8cy01601a

[8] Brungs AJ, York APE, Claridge JB, Marques-Alvares C, Green MLH (2000) Dry reforming of methane to synthesis gas over supported molybdenum carbide catalysts. Catalysis Letters 70:117-122 DOI: 10.1023/A:1018829116093

[9] Muraza O, Galadima A (2015) Waste to liquid fuels: potency, progress and challenges. International Journal of Energy Research. 39:1451-1478 DOI: 10.1002/er.3360

[10] Abdulrasheed A, Abdul Jalil A, Gambo Y, Ibrahim M, Hambali HU, Hamid MYS (2019) A review on catalyst development for dry reforming of methane to syngas: Recent advances. Renewable and Sustainable Energy Reviews 108:175-193 DOI: 10.1016/j.rser.2019.03.054

[11] Aramouni NAK, Touma JG, Tarboush BA, Zeater J, Ahmad MN (2018) Catalyst design for dry reforming of methane: Analysis Review. Renewable and Sustainable Energy Reviews 82:2570-2585 DOI: 10.1016/j.rser.2017.09.076

[12] Park JH, Yeo S, Heo I, Chang TS (2018) Promotional effect of Al addition on the Co/ZrO_2 catalyst for dry reforming of CH_4. Applied Catalysis A: General 562:120-131 DOI: 10.1016/j.apcata.2018.05.036

[13] Zhang F, Song Z, Zhu J, Sun J, Zhao X, Mao Y, Liu L, Wang W (2018) Factors influencing CH_4-CO_2 reforming reaction over Fe catalyst supported on foam ceramics under microwave irradiation. International Journal of Hydrogen Energy 43:9495-9502 DOI: 10.1016/j.ijhydene.2018.03.171

[14] Mortensen PM, Dybkjaer I (2015) Industrial scale experience on steam reforming of CO_2-rich gas. Applied Catalysis A: General 495:141-151 DOI: 10.1016/j.apcata.2015.02.022

[15] Darujati ARS, Thompson WJ (2005) Stability of supported and promoted-molybdenum carbide catalysts in dry-methane reforming. Applied Catalysis A: General 296(2):139-147 DOI:10.1016/j.apcata.2005.07.057

[16] Du X, France LJ, Kuznetsov VL, Xiao T, Edwards PP, AlMegren H, Bagabas A (2014) Dry reforming of methane over ZrO_2-supported Co-Mo carbide catalyst. Applied Petrochemical Research 4:137-144 DOI: 10.1007/s13203-014-0060-3

[17] Frontera P, Macario A, Aloise A, Antonucci PL, Giordano G, Nagy JB (2013) Effect of support surface on methane dry-reforming catalyst preparation. Catalysis Today 218-219:18-29 DOI: 10.1016/j.cattod.2013.04.029

[18] Moradi G, Khezeli F, Hemmati H (2016) Syngas production with dry reforming of methane over Ni/ZSM-5 catalysts. Journal of Natural Gas Science and Engineering 33:657-665 DOI: 10.1016/j.jngse.2016.06.004

[19] Vosmerikov AV, Zaikowskii VI, Korobitsina LL, Yechevskii GV, Kozlov VV, Barbashin YE, Zhuryakov SP (2009) Nonoxidative Conversion of Methane Into Aromatic Hydrocarbons on Ni-Mo/ZSM5 Catalysts. Kinetics and Catalysis 50:725-733 DOI: 10.1134/S0023158409050140

[20] Zakumbayeva GD, Itkulova SS (2013) Catalytic conversion of hydrocarbon gases. Oil replacing processes. LAP Lambert Academic Publishing. ISBN: 978-3-659-33542-6

[21] Shul'man DA, Skuddin VV., Shamkina NA (2010) Poluchenie tonkih sloev karbidov molibdena na poverhnosti mikrofiltratsionnyh membrane. Uspehi himii I himicheskoi tehnologii, sbornik nauchnyh trudov. 24(5):46-51. (in Russ.)

[22] Gavrilov NN, Novikov FI, Skuddin VV, Shamkina NA, Shul'man DA (2011) Poluchenie katalizatorov na osnove karbida molibdena i volframa dlya uglekislotnoi konversii metana. Materialy kongressa po katalizu "Roskataliz". 2:28. (in Russ.)

N E W S
OF THE NATIONAL ACADEMY OF SCIENCES OF THE REPUBLIC OF KAZAKHSTAN
SERIES CHEMISTRY AND TECHNOLOGY
ISSN 2224-5286 **https://doi.org/10.32014/2019.2518-1491.77**
Volume 6, Number 438 (2019), 79 – 85

UDC 542.943; 547.211; 661.961; 661.993

G.U. Begimova[1,2], L.V. Komashko[1], S.A. Tungatarova[1,3]

[1]JSC «D.V. Sokolsky Institute of Fuel, Catalysis and Electrochemistry»,
st. Kunaev 142, 050010, Almaty, Kazakhstan;
[2]Kazakhstan Engineering Technological University, 93A al-Farabi ave., Almaty, Kazakhstan
[3]al-Farabi Kazakh National University, 71 al-Farabi ave., Almaty, Kazakhstan
zeynep80@mail.ru; zeynep80@mail.ru,

NICKEL-CONTAINING COMPOUNDS FOR THE CATALYTIC CONVERSION OF METHANE TO GAS SYNTHESIS

Abstract. In recent decades, many experiments have studied the catalytic materials synthesis' that are active, selective and stable in the conversion of gaseous hydrocarbons to organic liquids. The resulting nickel-based catalysts are discussed in terms of their preparation, physicochemical characteristics, and internal properties that the conversion of methane to synthesis gas.

Key words: methane, hydrogen, synthesis gas, self-propagating high-temperature synthesis, solution combustion.

Introduction

Methane is considered the most significant source of hydrocarbons in the process of catalytic partial oxidation, since it is the main component of natural gas, which exists on Earth in abundance. One of the most common methods for producing catalysts today is self-propagating high-temperature synthesis (SHS). This is an exothermic reaction, which is carried out in the modes of layer-by-layer combustion or thermal explosion, based on the use of the internal chemical energy of the starting reagents. The advantages of this method are - low power consumption, simplicity and a one-step synthesis cycle, high productivity, cheap equipment, high purity of the product [1].

The use of natural gas, synthesis gas allows to obtain a wide range of chemical products [2]. For such processes, the most common are catalysts based on nickel and noble metals. Nickel is the cheapest raw material for the manufacture of the catalyst, but the main disadvantage of this metal is its high coke formation, which contributes to the rapid "aging" of the catalyst.

Methane steam reforming (SR) is a well-established process for converting hydrocarbons to synthesis gas in industry.

$CH_4+H_2O \rightarrow CO+3H_2$ $\Delta H_{298}=+206$ kJ/mol

Recently there has been great renewal interest in the SR process because of its potential application in fuel cells [3]. However, this process has many disadvantages: firstly, in the process, an amusing amount of CO2 is generated along the way, which is difficult to separate; secondly high energy demand because SRM is a highly endothermic process.

The dry-reforming process (DR), on the other hand, produces the least amount of hydrogen per mole of methane consumed.

$CH_4+CO_2 \rightarrow 2CO+2H_2$ $\Delta H_{298} = +247$ kJ/mol

Although this process has two major disadvantages: extremely high energy cost and rapid catalysts deactivation through carbon deposition [4].

The search for numerous experiments over several decades to develop alternative processes led to the process of catalytic partial oxidation of methane (POM) [5].

$CH4 + 0.5O2 \rightarrow CO + 2H2$ $\Delta H_{1173K} = -23.1$ kJ/mol

This process is described as slightly exothermic [6] and occurs 10–100 times faster than steam reforming, which allows the use of small reactors.

The aim of this work was synthesis of catalysts based on Ni-Al-Pt compounds, organic part were glycine [7] or urea [8-10]. The synthesis of nanostructure materials was do method self-propagating high temperature synthesis (SHS) or «burning solution». That process is based on a self-sustaining exothermic reaction of the interaction of dissolved components based on systems containing an oxidizing agent (metal nitrate) and a reducing agent [11]. It allows one to obtain inexpensive oxide catalysts in the form of nanosized powders (particle size less than 100 nm), which have very high catalytic activity at ambient temperature.

Experimental

Catalyst preparation

A preliminary calculated amount of metal salts of Ni and Al crushed to a jelly-like state was injected with a few drops of a solution containing a salt of Pt and mixed. Then placed in a quart glass and sent to a preheated muffle furnace (600-900°C). After 5-7 minutes, spontaneous combustion occurred. Catalyst samples were tested on an FCU-1 unit with a gradual increase in temperature from 600 to 900°C at space velocities of 2500, 4500, 6500 h-1. Studies of the developed catalysts were carried out using various methods: elemental analysis, X-ray diffraction analysis (XRD), transmission electron microscopy on an EM-125K device using the "shooting in the lumen" method in the form of dry suspensions using microdiffraction. These analyzes were performed both before and after testing the synthesized catalysts in a flow reactor with a catalytic unit (FCU-1).

Results and discussion

It has always been believed that there are two sources of raw materials for organic chemistry, which are a source of huge reserves - coal and gas. The possibility of obtaining hydrocarbon raw materials from coal has long been developed, but the imperfection of the technology, economic factors and the stringency of the conditions do not allow to introduce these processes into the industry. Whereas the processing of, for example, acetylene from natural gas has long been put into production on an industrial scale. Although the process is also with very low selectivity and yield at high temperatures and pressure. Moreover, the existence in nature of enzymes that convert methane to methanol is well known. Therefore, the constant desire to create new highly efficient and selective processes for processing natural gas into useful alkane compounds is justified.

Currently, there is no industrial technology for producing synthesis gas by the method of carbon dioxide conversion of methane. Available developments are most often based on nickel catalysts used in the steam reforming process, they do not have sufficient selectivity and are quickly deactivated due to the formation of carbon, which covers active metal centers during catalysis, and accumulate in the pores of the catalyst, causing destructive changes and ultimately – decontamination [12].

According to the literature, it is known that the C-H bond energy in methane is approximately equal to the H-H bond energy in acetylene, benzene, and ethylene molecules. The ionization potential of methane is higher than that of benzene, ethylene and acetylene, but lower than the ionization potential of hydrogen. Methane has a lower proton affinity than a benzene and ethylene molecule, but more than hydrogen. From which it turns out that methane occupies an intermediate position between hydrogen and ethylene. Therefore, the activation of methane and its chemical reactions can be carried out in the presence of catalysts with 3d metals. In the periodic system, nickel is in a subgroup of elements such as palladium and platinum, which explains the similarity of the electronic configuration, especially the outer shells, as a result of which the elements of this group exhibit similar physical properties and chemical behavior [13]. Perhaps this explains the attempt to replace the expensive metals of the platinum subgroup with nickel.

The following are test results for the catalyst composition 50% Ni - 50% Al - (0.05%) Pt - glycine or urea catalyst. And also given elemental composition with different variation in quantity was considered.

Various elements in the catalysts form chemical bonds of varying degrees of strength. It is likely that someday it will be possible to explain the chemical properties of metal catalysts based on the ideas of

quantum mechanics, but now it is necessary to establish essentially empirical correlations. As elements used in catalysts, transition metals are of the greatest importance. In the synthesis of catalysts, glycine was used as organic fillers, which made it possible to obtain a huge amount of particles in the form of spinels and various frame structures.

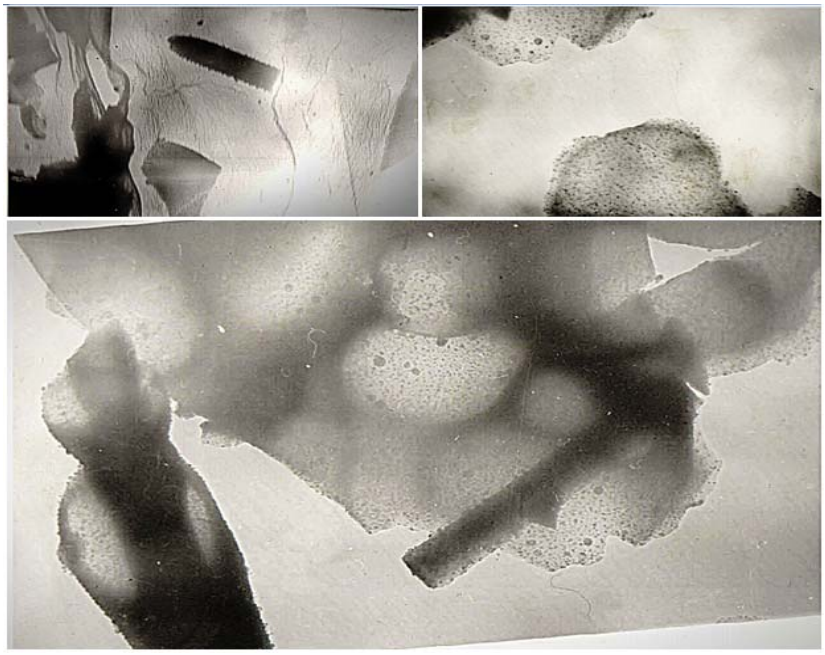

Figure 1 - TEM images of the 50 % Ni - 50 % Al – (0.05%)Pt- glycine catalyst before tests

On the other hand, the study of literary sources of aluminum oxide indicates a huge variety of the final compounds obtained, which is explained by the influence of everything: temperature, synthesis method, initial structure, pH of the solution used, and even the rate of solution merging and mixing. The influence of temperature in the range from 500 to 800°C on the structural composition of the catalyst was considered.

According to the analysis results, it was shown that at 500°C translucent films with seal sizes from 10-30 nm to 100 nm were shown. The microdiffraction pattern is represented by reflections and can be assigned to a mixture of phases: NiO (JSPDS, 4-835), χ-Al_2O_3 Alumina in the modification (JSPDS, 34-493), ϕ-$NiAl_{32}O_{49}$ (JSPDS, 20-777), PtO (JSPDS , 27-1331), Al_4C_3 (JSPDS, 38-799), AlN (JSPDS, 25-1133), Ni_3N (JSPDS, 10-280), NiO (JSPDS, 4-835).

In the samples obtained at 600°C, translucent films were shown with compaction sizes from 10-15 nm to 50 nm. The microdiffraction pattern is represented by reflections and can be attributed to a mixture of phases: $Al(OH)_3$ (JSPDS, 26-28), AlN (JSPDS, 25-1133), Pt_3O_4 (JSPDS, 21-1284), NiO (JSPDS, 4-835), ϕ-$NiAl_{32}O_{49}$ (JSPDS, 20-777), Ni_3N (JSPDS, 10-280), NiO (JSPDS, 4-835).

In the samples obtained at 700°C, translucent films were shown with compaction sizes from 10-15 nm to 50 nm. The microdiffraction pattern is represented by reflections and can be assigned to a mixture of phases: PtO (JSPDS, 27 -1331), $Al_{22}O_{39}N$ (JSPDS, 26-33), $NiAl_{26}O_{40}$ (JSPDS, 20-776), χ-Al_2O_3 Alumina in the modification (JSPDS, 4-880), $Al_9N_7O_3$ (JSPDS, 35-830), $NiAl_{32}O_{40}$ (JSPDS, 35-830) Pt (JSPDS, 27 -1331), Al_2Pt (JSPDS, 3-1006), NiO (JSPDS, 4-835)

Samples obtained at 800°C are translucent films with small particles on them ranging in size from 4-15 nm to 20 nm. The microdiffraction pattern is represented by reflections and can be assigned to a mixture of phases: NiO (JSPDS, 4-835), Al (JSPDS, 4-716), Al_3Ni_2 (JSPDS, 14-648), $NiAl_{26}O_{40}$ (JSPDS, 20-776), $Pt_{21}Al_6$ (JSPDS, 38-1179), $Al_{10}N_8O_3$ (JSPDS, 32-22), $NiAl_{32}O_{49}$ (JSPDS, 20-776), Pt (JSPDS, 4-802), $AlPt_2$ (JSPDS, 29-69). The most common types of particles formed are shown above as they decrease.

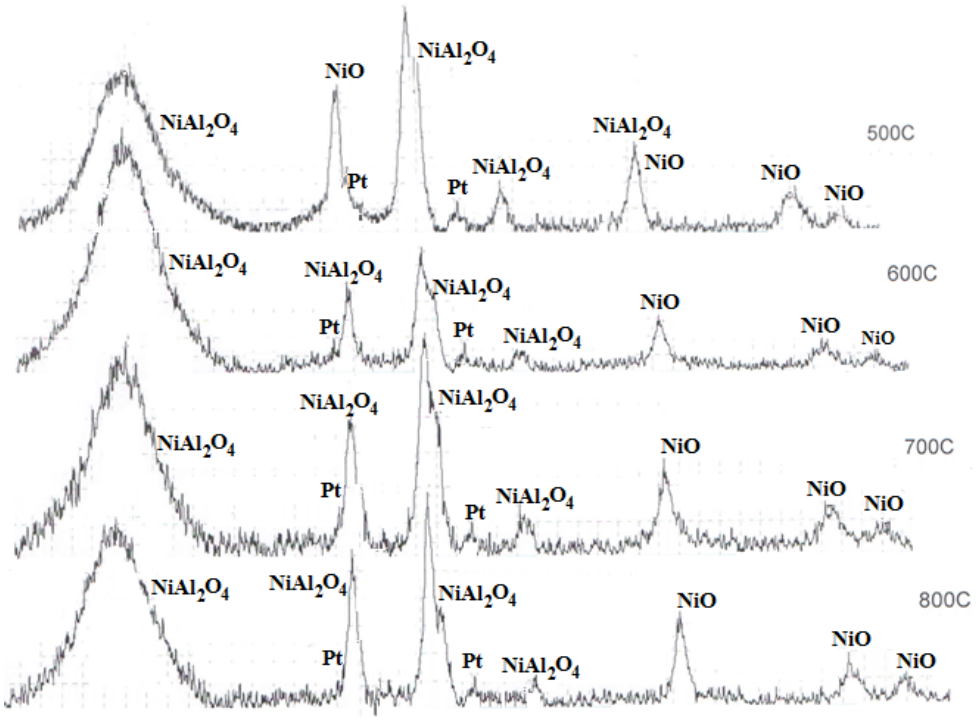

Figure 2 – XRD spectrum of the 50 % Ni - 50 % Al – (0.05%)Pt- glycine catalyst before tests

As can be seen from the experimental results, the temperature significantly affects the composition of the catalyst. At higher temperatures, metal atoms have time to recover, and also form more complex structures in the form of various spinels. It has been proven that reduced Ni can interact at high temperatures with the formation of $NiAl_2O_4$ spinels [14-16]. In fact, $NiAl_2O_4$ is not active in the reaction. But its reduced form tends to inhibit the formation of carbon deposits. This shows good stability, since reduced Ni from spinel tends to disperse, making sintering difficult. In addition, a synergistic effect exists between the carbon fraction and the metal-based fraction, which means that the experimental CO_2 and CH_4 conversions obtained in mixtures of carbon materials and metals are higher than the conversions calculated according to the law of mixtures (i.e., the addition of weighted individual transformations) [14,17].

X-ray diffraction analysis did not show significant differences between the samples. Figure 2 shows the spectra of the catalyst for 50% Ni - 50% Al - (0.05%) Pt-glycine. As a result of the data obtained, it is seen that the following phases are present in the catalysts: NiO (reflexes, Å: 2.41; 2.08; 1.48; 1.25; 1.21 - ASTM, 4-850); NiAl2O4 (reflexes, Å: 4.6220; 2.8420; 2.42100; 2.0065; 1.648; 1.5430; 1.4260 - ASTM, 10-339) and Pt (low-intensity reflexes, Å: 2, 26 ; 1.96 - ASTM, 4-802).

Despite the fact that such catalysts have good enough activity, they all undergo coking. Over time, this leads to the deactivation of the catalysts, which requires their regeneration and leads to an increase in production costs. A disadvantage of the known catalysts and carriers is that they are oxidized at high temperatures in a redox environment, which significantly reduces the contact strength between the particles [18-20]. In the continuation of the study, analyzes were carried out for the catalyst composition 50 % Ni - 50 % Al – (0.05%)Pt- glycine (500^{o}C) after the main multiple tests on the FCU-1 device.

Figure 3 (A, B) shows translucent films with seals 10-30 nm in size. And dense aggregates, on the edges of which there are particles with a size of 10-20 nm. The microdiffraction pattern is represented by a large set of reflections located along the rings and individual reflexes and can be assigned to a mixture of phases: δ-$NiAl_{26}O_4$ (JSPDS, 20-776), δ-Al_2O_3 (JSPDS, 4-877), Al_4C_3 (JSPDS, 38-799), ϕ-$NiAl_{32}O_{49}$ (JSPDS, 20-777), PtO (JSPDS, 27-1331), $Al_9N_7O_3$ (JSPDS, 35-83).

Figure 3 (C) shows a large and dense aggregate, along the edge of which both small particles with a size of 20-60 nm and large ones with signs of faceting of a size of 200-500 nm are observed. The

microdiffraction pattern is represented by rows of reflections and a large set of individual reflexes and can be assigned to a mixture of phases: large $NiAl_{10}O_{16}$ (JSPDS, 37-1292) or equally $9Al_2O_3 \cdot 2NiO$ (JSPDS, 22-451), γ-Al_2O_3 (JSPDS, 29-63) and (JSPDS, 10-425), AlN (JSPDS, 34-679) and χ-Al_2O_3 Alimina in the modification (JSPDS, 34-493). Small: Pt (JSPDS, 4-802), AlNi (JSPDS, 20-19), Ni_3N (JSPDS, 20-19), Ni_3C (JSPDS, 6-497), δ-$NiAl_{26}O_{40}$ (JSPDS, 20-776), Al (JSPDS, 4-787). However, after catalytic studies on the known catalyst, carbon deposition is observed, accompanied by the formation of nickel carbide and graphite-like carbon, which leads to the fact that the activity of the catalyst decreases (the catalyst is deactivated).

Figure 4 shows the accumulation of aggregates of elastic carbon nanotubes reaching a cross section of 20-40 nm, as well as a dense aggregate, along the edge of which particles of 10-50 nm in size and dense large round particles of 100-200 nm or more are observed . The microdiffraction pattern is represented by rings and a small set of reflections that can be attributed to a mixture of phases: PtO_2 (JSPDS, 23-1306), AlH_3 (JSPDS, 23-761), C - Zonsdaleite (JSPDS, 19-268) - tubes, $AlPt_2$ (JSPDS, 29-692), AlC_3 (JSPDS, 35-749) Ni3C (JSPDS, 6-497), ϕ-$NiAl_{32}O_{49}$ (JSPDS, 20-777), Al_2OC (JSPDS, 36-148).

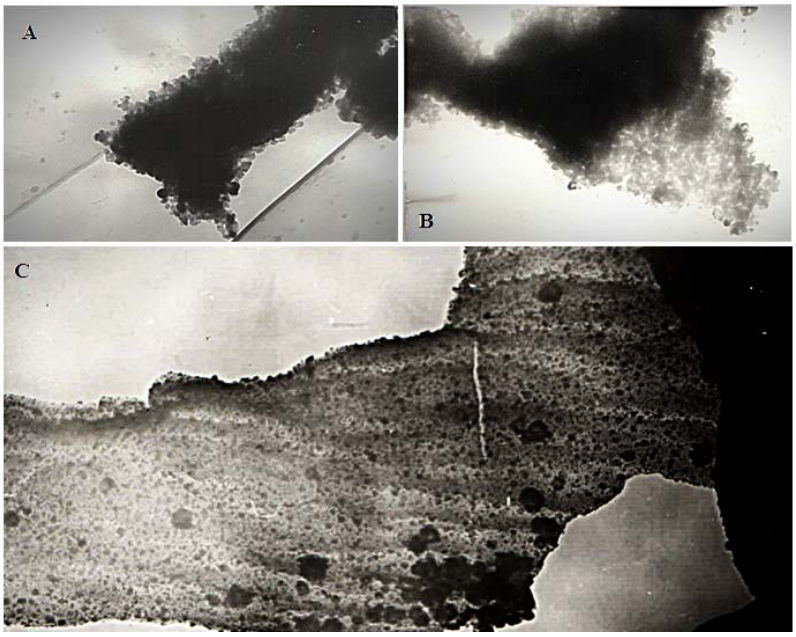

Figure 3 – TEM images of the 50 % Ni - 50 % Al – (0.05%)Pt- glycine catalyst after tests

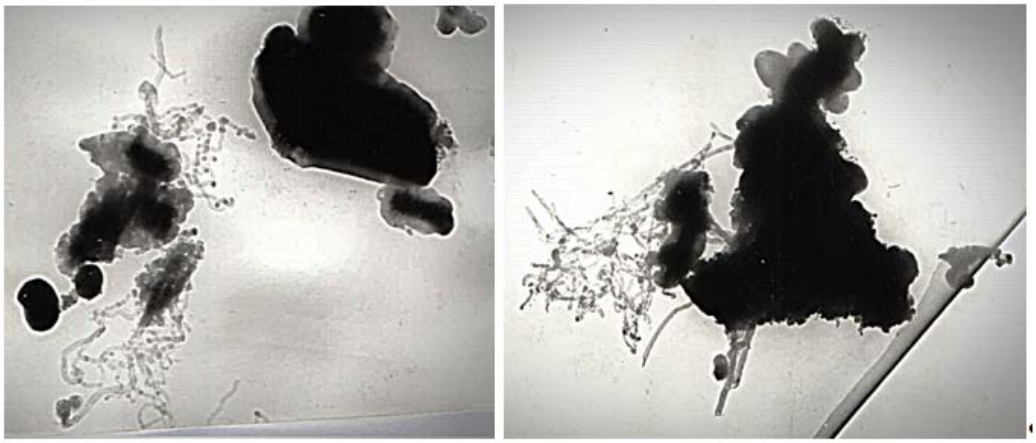

Figure 4 - TEM images of the 50 % Ni - 50 % Al – (0.05%)Pt- glycine catalyst after tests with carbon nanotubes

Conclusion

Based on the results of the study, the following conclusions can be drawn:

- organic fillers affect the composition and properties of the same catalysts;
- in catalysts prepared by the SHS method, temperature significantly affects the composition — moreover, if we study the most active centers of the catalyst for this system, we can synthesize a need composition;
- the catalyst was most active for conversion methane to synthesis gas from numerous combinations of catalysts with the following set of catalyst components from 50% Ni - 50% Al - (0.05%) Pt-glycine obtained by synthesis during combustion in solution at 800°C;
- the presence of carbon nanotubes in the spent catalyst samples was also revealed. The nanotubes are elastic, often wrapped in a spiral with a diameter of 50 - 70 nm.

Acknowledgments

The work was supported by the Ministry of Education and Science of the Republic of Kazakhstan (Grant No AP05132348).

ӘОК 542.943; 547.211; 661.961; 661.993

Г.У. Бегимова[1,2], Л.В. Комашко[1], С.А. Тунгатарова[1,2]

[1]АҚ «Д.В. Сокольский атындағы Жанармай, Катализ және Электрохимия Институты»,
Қонаев 142, 050010, Алматы, Қазақстан;
[2]Қазақстан Инженерлік-Технологиялық университеті, әл-Фараби д-лы, 93А, Алматы, Қазақстан;
[3]ал-Фараби атындағы Қазақ ұлттық университеті, әл-Фараби д-лы, 71, Алматы, Қазақстан

МЕТАННЫҢ СИНТЕЗ - ГАЗҒА КАТАЛИЗДІК КОНВЕРСИЯЛАУДА НИКЕЛЬҚҰРАМДЫ ҚОСЫЛЫСТАР

Аннотация. Соңғы онжылдықта көптеген тәжірибелерде газ тәрізді көмірсутектерді органикалық сұйықтықтарға тотықтыра айналдыру барысында белсенді, селективті және тұрақты болып табылатын каталитикалық материалдардың синтезі зерттелді. Метанның синтез-газға айналу конверсиясыда алынған никель негізіндегі катализаторларды дайындау және олардың физикалық-химиялық сипаттамаларына талдау жасау.

Түйін сөздер: метан, сутегі, синтез-газ, жоғарытемпературада өздігінен жану синтезі, ерітіндіде жану.

УДК 542.943; 547.211; 661.961; 661.993

Г.У. Бегимова[1,2], Л.В. Комашко[1], С.А. Тунгатарова[1,3]

[1]АО «Институт топлива, катализа и электрохимии им. Д.В. Сокольского»,
ул. Кунаева 142, 050010, Алматы, Казахстан;
[2]Казахстанский Инженерно-Технологический университет, пр. аль-Фараби, 93А, Алматы, Казахстан;
[3]Казахский Национальный университет им. аль-Фараби, пр. Аль-Фараби, 71, Алматы, Казахстан

НИКЕЛЬ-СОДЕРЖАЩИЕ СОЕДИНЕНИЯ ДЛЯ КАТАЛИТИЧЕСКОЙ КОНВЕРСИИ МЕТАНА В СИНТЕЗ ГАЗА

Аннотация. В последние десятилетия во многих экспериментах изучался синтез каталитических материалов, которые являются активными, селективными и стабильными при превращении газообразных углеводородов в органические жидкости. Полученные катализаторы на никелевой основе обсуждаются с точки зрения их приготовления, физико-химических характеристик и внутренних свойств, при которых происходит конверсия метана в синтез-газ.

Ключевые слова: метан, водород, синтез-газ, самораспространяющийся высокотемпературный синтез, сжигание раствора.

Information about authors:

Begimova G.U. – PhD, Scientific Researcher, Laboratory of Physical Methods of Research, JSC "D.V. Sokolsky Institute of Fuel, Catalysis and Electrochemistry", Kazakhstan Engineering Technological University, Almaty, Kazakhstan. Tel: +77272916632, zeynep80@mail.ru

Komashko L.V. - Scientific Researcher, Laboratory of Physical Methods of Research, JSC "D.V. Sokolsky Institute of Fuel, Catalysis and Electrochemistry", Almaty, Kazakhstan. Tel: +77272916632. ifce@ifce.kz

Tungatarova S.A. – Chief Researcher, Doctor of Chemical Sciences, Laboratory of Organic Catalysis, JSC "D.V. Sokolsky Institute of Fuel, Catalysis and Electrochemistry", Al-Farabi Kazakh National University, Almaty, Kazakhstan. Tel: +77272916632. tungatarova58@mail.ru

REFERENCES

[1] Rostrup-Nielsen J.R.(**1993**) Production of Synthesis gas, Catalysis Today V18..- p. 305 – 312. https:// doi.org/10.1016/0920-5861(93)80059-A (in Eng).

[2] Bradford, M.C.J. and Vannice, M.A. (**1999**) CO2 reforming of CH4, Catalysis Reviews, Science and Engineering. V. 41. №1. P. 1-42 (in Eng).

[3] Xu J.C., Yeung M.Y., Ni J., Meunier F., Acerbi N., Fowles M., Tsang S.C. (**2008**) Methane steam reforming for hydrogen production using low water-ratios without carbon formation over ceria coated Ni catalysts, Applied Catalysis A: General 345 p.119–127 (in Eng).

[4] Hu Y.H., Ruckenstein E. (**2004**) Catalytic conversion of methane to synthesis gas by partial oxidation and CO2 reforming, Advances in Catalysis 48 p. 297–345 (in Eng).

[5] York A.P.E., Xioa T., Green M.L.H. (**2003**) Brief overview of the partial oxidation of methane to synthesis gas, Topics in Catalysis 22 p. 345–358 (in Eng).

[6] Choudhary T.V., Choudhary V.R. (**2008**) Energy efficient syngas production through catalytic oxy-methane reforming reactions, Angewandte Chemie, International Edition 47 p.1828–1847 (in Eng).

[7] Fidalgo B., Menéndez J.A. (**2011**) Carbon Materials as Catalysts for Decomposition and CO_2 Reforming of Methane: A Review, Chinese J. Catalysis. V 32, Issues 1–2, p. 207-216. https:// doi.org/10.1016/S1872-2067(10)60166-0 (in Eng).

[8] Nikolaev S.A., Zanaveskin L.N., Smirnov V.V., Averyanov V.A., Zanaveskin K.L. (**2009**) Catalytic Hydrogenation of Alkyne and Alkadiene Impurities from Alkenes. Practical and Theoretical Aspects, Russian Chemical Reviews V.78. 3. – p. 248-265. (in Russ).

[9] Velasco J A, Fernandez C, Lopez L, Cabrera S, Boutonnet M, Jaras S (**2015**) Catalytic partial oxidation of methane over nickel and ruthenium based catalysts under low O2/CH4 ratios and with addition of steam, Fuel, 153:192-201. https://doi.org/10.1016/j.fuel.2015.03.009 (in Eng).

[10] Hiblot H, Ziegler-Devin I, Fournet R, Glaude PA (**2016**) Steam reforming of methane in a synthesis gas from biomass gasification, Int J Hydrogen Energ, 41:18329-18338. http://dx.doi.org/10.1016/j.ijhydene.2016.07.226 (in Eng).

[11] Lim M-W, Yong S-T, Chai S-P (**2014**) Combustion-synthesized Nickel-based catalysts for the production of hydrogen from steam reforming of methane, Energy Procedia, 61:910-913. https://doi.org/10.1016/j.egypro.2014.11.993 (in Eng).

[12] Tungatarova S A, Dossumov K, Baizhumanova T S, Popova N M (**2010**) Nanostructured supported Pt-, Ru- and Pt-Ru catalysts for oxidation of methane into synthesis-gas, J Alloys Compd, 504: 349–352. doi:10.1016 // j.jallcom.2010.04.223 (in Eng).

[13] Akhmetov N.S. (**2001**) General and inorganic chemistry, M.: Higher School, - p. 745 (in Russ).

[14] Tungatarova S A, Zheksenbaeva Z T, Baizhumanova T S, Grigoriyeva V P, Sarsenova R O, (**2017**) Heat generation in the catalytic combustion of light hydrocarbons, Chemical Engineering Transactions, 61:1915-1920. DOI: 10.3303/CET1761317 (in Eng)

[15] Lødenga R, Lunderb O, Leinb J E, Dahlc PI, Svenumb I H (**2018**) Synthesis of light olefins and alkanes on supported iron oxide catalysts, Catalysis Today, 299:47-59. http://dx.doi.org/10.1016/j.cattod.2017.06.039 (in Eng).

[16] Wei C, Luo J, Paul S, Liu Y, Khodakov A, Bordes E (**2017**) Synthesis and performance of vanadium-based catalysts for the selective oxidation of light alkanes, Catalysis Today, 298:145-157. http://dx.doi.org/10.1016/j.cattod.2017.05.004 (in Eng).

[17] Fidalgo B., Menéndez J.A. (**2010**) Syngas production by CO2 reforming of ch4 under microwave heating – challenges and opportunities, Appl. Catal. A 390, 78. pp: 121-149 (in Eng).

[18] Kim H.W., Moon Kang K., Kwak H.Y. (**2009**) Preparation of supported Ni catalysts with a core/shell structure and their catalytic tests of partial oxidation of methane, International J. Hydrogen Energy 34 p.3351–3359 (in Eng).

[19] Bordes E, Courtine P (**2000**) Influence of structural properties of catalysts at various stages of selective oxidation: from catalyst preparation to catalytic reactors, Top. Catal, 11:61-65. https://doi.org/10.1023/A:1027238217490 (in Eng).

[20] X. Zhang, C.S.M. Lee, D.M.P. Mingos and D.O. Hayward. (**2003**) Sustainable selective oxidations using ceria-based materials, Catal. Lett. 88, 129 https://doi.org/10.1039/C000 191K

N E W S
OF THE NATIONAL ACADEMY OF SCIENCES OF THE REPUBLIC OF KAZAKHSTAN
SERIES CHEMISTRY AND TECHNOLOGY
ISSN 2224-5286 **https://doi.org/10.32014/2019.2518-1491.78**
Volume 6, Number 438 (2019), 86 – 98

UDC 550.42:004.89

R.Z. Safarov[1], Zh.K. Shomanova[2], R.Zh. Mukanova[2], Yu.G. Nossenko[3], A. Ilieș[4], A.K. Sviderskii[2], N. Sarova[5]

[1]L.N. Gumilyov Eurasian National University, Nur-Sultan, Kazakhstan;
[2]Pavlodar State Pedagogical University, Pavlodar, Kazakhstan;
[3]Innovative University of Eurasia, Pavlodar, Kazakhstan;
[4]University of Oradea, Oradea, Romania;
[5] Kazakh National Medical University named after D. S. Asfendiyarov, Kazakhstan
e-mail: ruslanbox@yandex.ru

DESIGN OF NEURAL NETWORK FOR FORECAST ANALYSIS OF ELEMENTS-CONTAMINANTS DISTRIBUTION ON STUDIED TERRITORIES (ON EXAMPLE OF PAVLODAR CITY, KAZAKHSTAN)

Abstract. In the article we are presenting results of development appropriate method including neural network for creating predictive map of elements-contaminants distribution (on example of Cr) on the territory of Pavlodar city (Kazakhstan). Obtained method allows to get widen data. The data from 15 points were spread out into 500 points. The average relative error at verification process was 9.45%. Architecture of well working model of neural network is perceptron with one input neuron, which takes values of distances between given point and several nearest points, 10 hidden neurons, and 1 output neuron, which gives value of element concentration in specified point. Obtained data were used in QGIS for creation of IDW interpolated map, which visualizes the information about concentration distribution.

Keywords: neural network, contaminants, distribution, forecasting, modelling, GIS, environmental.

1. Introduction

The search for ways of solving environmental problems and developing scientific methodological approaches to studying the complex consequences of the anthropogenic activities of enterprises involves the study of the ecological state of the region [1–3]. Environmental researches now have special significance because environmental safety and rational use of nature resources are the most important factors, determinant prospective of successful development of economics and social sphere.

The Pavlodar city is the large industrial city on the North of Kazakhstan. It is known, that the main sources of environment contamination of the city and Pavlodar region are different waste of chemical-technological processes [4]. These can be products of related processes and by-reactions not used in subsequent processes. Also, it can be intermediates of reactions and polymerization processes, filer materials, industrial waste water, not reacted gases (Cl_2, NH_3 etc.) [5, 6]. Moreover, environmental contamination occurs as a consequence of mechanical losses of raw material and products due to leakages from equipment and communications. Effect of every kind of contaminant directly depends on its physical-chemical properties. Many gaseous chemicals can react in atmosphere with water vapor, oxygen, as well be affected under radiation converting into other more toxic substances.

Finding of borders of studied territory and identification of danger sources leading to damage are an initial and important stage in the process of assessment of environmental risks. A new approach in this field is to assess impact of factors affecting the environment of region through analysis of territorial distribution of contaminants with creation of maps. Map allows visualizing of effects of contaminants, to understand origin sources of the contaminants, to predict ways of distribution and meanings for prevention of negative consequences from various factors.

In the article we are describing a new approach for creating such kinds of maps using methods of computer modelling, in particular neural network. New ways of data analysis allow to obtain new generated data and are often used for solving problems when it is required to expand weak analytical data and get on output full picture of demanded information [7–9].

Neural network receives input information and analyses it in the way analogous to our brain. During the analysis network is trained (generates some new knowledge) and gives a new output information based on previous experience [10–12]. The main task of analyst using neural network for solving some problem is to design the most effective architecture of network. Namely, correctly choose the sort of neural network, algorithm of training, number of neurons and kinds of relations between them. This work has no formalized procedures and requires deep understanding of different architectures of neural networks, it includes lots of research and analytical work and can take quite much time [13–15]. The most common usages of neural networks are:

- classification – allocation of data by parameters;
- forecasting – possibility to predict following steps;
- recognition – determination of objects in a stack.

The computational item of neural network is neuron. It receives an information, makes simple calculations with it and pass it later. There are three types of neurons with specified functions – input, hidden and output. The principal scheme of simple neural network with two input neurons, two hidden and one output neuron is shown on the figure 1.

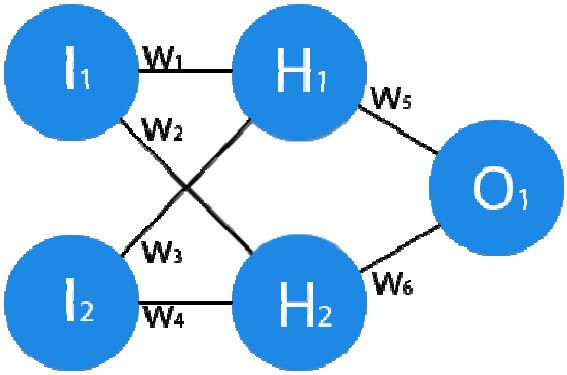

Figure 1 - The scheme of simple neural network

“W” on the figure are “weights”, which are parameters of the network. They are adjusted during the training stage for the network could be able to give correct values. In our work we use neural network for forecasting of distribution of elements-contaminants on the studied territory. The forecast is based on the data obtained with x-ray spectral elemental analysis of the soil samples taken from given locations. The aim of the work was to design appropriate model of neural network for obtaining at least 500 predicted values of element concentrations in 500 given coordinates on the territory of Pavlodar city.

2. Methods and materials

2.1 Sampling of soil

Sampling was carried out for estimation of quality and quantity analysis of elemental content of soils on the territory of Pavlodar city. Sampling was carried out according to requirements of conventional documents “GOST 17.4.4.02-84. Nature protection. Soils. Methods for sampling and preparation of soil for chemical, bacteriological, helmintological analysis”, “GOST 17.4.3.01-83. Nature protection. Soils. General requirements for sampling”, “GOST 5180-84. Soils. Laboratory methods for determination of physical characteristics”. The positions of sampling sites are shown on the figure 2 and specified in the table 1.

Figure 2 - Locations of sampling sites on the territory of Pavlodar city

Table 1 – Coordinates of positions of sampling sites

Number of sample	Name	X	Y
1	Lesozavod 1	76.919125	52.313194
2	Lesozavod 2	76.9083333333	52.3077777778
3	Constitution square 1	76.9338888889	52.2966666667
4	Constitution square 2	76.9367	52.2989166667
5	CHP2 1 (TEC2 1)	76.9630916667	52.3196361111
6	CHP2 2 (TEC2 2)	76.9625833333	52.3125277778
7	Zhayau Musa str. 1	76.9673194444	52.2497555556
8	Zhayau Musa str. 2	76.9707611111	52.2516555556
9	Railway Station 1	76.9552861111	52.3018861111
10	Railway Station 2	76.9570277778	52.235275
11	Narkodispancer 1	76.9926	52.2906138889
12	Narkodispancer 2	76.9894055556	52.290475
13	Gulliver TH 1	76.96925	52.2695777778
14	Gulliver TH 2	76.9688638889	52.27085
15	PNCP 1	76.9285722222	52.3449916667
16	PNCP 2	76.9279916667	52.3448638889
17	Usolka riv. 1	76.942475	52.2503555556
18	Usolka riv. 2	76.9501694444	52.2471638889
19	Lermontov str. 1	76.9636111111	52.2913888889
20	Lermontov str. 2	76.9553111111	52.2911972222
21	PTP 1	76.9619861111	52.3242555556
22	PTP 2	76.962475	52.3243888889
23	Satpayev str. 1	76.936725	52.292625
24	Satpayev str. 2	76.938175	52.3009916667
25	Naberezhnaya str. 1	76.9345222222	52.2815777778
26	Naberezhnaya str. 2	76.9375833333	52.2833
27	Mir str. 1	76.9444111111	52.2990027778
28	Mir str. 2	76.9447	52.2991111111
29	Toraigyrov str. 1	76.9552861111	52.2959166667
30	Toraigyrov str. 2	76.9594861111	52.2958333333

* Coordinate system EPSG:4326 - WGS 84 - Geographic

2.2 Elemental analysis of soil samples

The catalyst samples were studied on a low-vacuum scanning electron microscope with a thermal emission cathode (LaB6) JSM-6610LV from JOEL. The device is equipped with an energy dispersive microanalysis system (EDM), a wave dispersive microanalysis system, a backscattered electron diffraction analysis system with a reflected electron detector, an Everhart-Thornley secondary electron detector, a low-vacuum secondary electron detector and sample preparation equipment. Elemental analysis was performed using energy dispersive x-ray fluorescence spectroscopy on an energy dispersive microanalysis system INCA Energy 450. Spectra were obtained three times with the calculation of the average value.

2.3 Neural network designing

For creation of neural network Brain.js library was used. Brain.js is an opened JavaScript library that allows implementation of neural networks with different architectures right in the browser or with using Node.js. Simple browser program was prepared for implementation of developed neural net. The program allows to input initial data for training, verification and forecasting from text file with data written in CSV-like manner, columns are divided with commas. Moreover, average relative divergence is calculated after verification process, as well diagram of convergence of forecast with original data is created automatically using the Graph.js library. Using neural network based on initial data about element concentration from 30 input points, 500 points were predicted after calculations. These 500 points were used for plotting on the map.

2.4 Creating of element distribution map

Free geographic information system with open code QGIS 3.8.3-Zanzibar was used. QGIS is an open source, user-friendly geographic information system (GIS) distributed under the GNU General Public License. QGIS is a project of the Open Source Geospatial Foundation (OSGeo). It works on Linux, Unix, Mac OSX, Windows and Android, supports many vector and raster formats, databases and has many features. Input data were added as a layer with coordinate system EPSG:4326 - WGS 84 – Geographic. For better visualization of information data analysis with IDW interpolation method has been implemented. In the IDW (Inverse Distance Weighting) interpolation method, the sample points are weighted during interpolation such that the influence of one point relative to another declines with distance from the unknown point you want to create [16, 17]. The figure 3 demonstrates the principle of the IDW method.

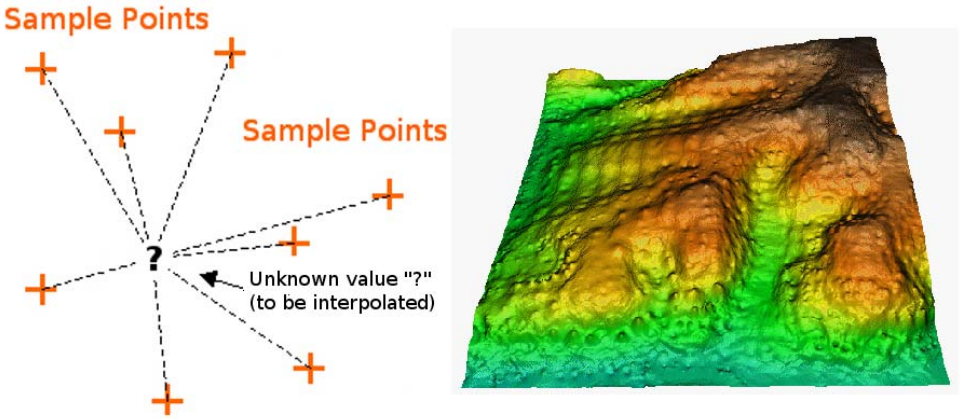

Figure 3. Inverse Distance Weighted interpolation based on weighted sample point distance (left).
Interpolated IDW surface from elevation vector points (right).
(Image Source: Mitas, L., Mitasova, H. (1999),
url: https://docs.qgis.org/2.18/en/docs/gentle_gis_introduction/spatial_analysis_interpolation.html)

Interpolation was visualized as a gradient of colors, monochannel pseudocolor mode of image was used. For map of chromium distribution following table of color distribution in dependence on concentration was assigned (table 2).

Table 2 – Distribution of colors in dependence on concentration in the method of interpolation visualization

Threshold concentration, %	Color	Color name	RGB color
0.00326683		blue	43,131,186
0.082261464		green	171,221,164
0.161256098		yellow	255,255,191
0.240250732		orange	253,174,97
0.319245366		red	215,25,28

3. Results and discussion

When we are describing distribution of concentrations of elements on the territory, practically we have to consider the data in three-dimensional space, where X and Y represent coordinates and Z is a third parameter – concentration in our case. Thus, we have to find the dependence between coordinates and concentration. First approach for creation of neural net, which could reveal that dependence is to give into input layer two parameters X and Y and get from output layer the value of concentration. In order to try the effectivity of developed neural network we have to find appropriate model with similar parameters. The convenient, simple and available model is some picture in gray scale. In this case a picture has its X and Y coordinates, when we are considering it as a matrix of pixels, and graduation of gray color is similar to concentration. Graduation of gray color lies in the range from 0 to 255 in RGB scheme [18].

So, the first picture we have chosen is quite simple and has dense relatively uniform sites of different shades of gray color (figure 4).

Figure 4 - Model image №1 for development of neural network

For this model we have taken 35 points as training data. The architecture of neural network included 2 neurons of input layer (X, Y coordinates), 3 hidden layers with 10, 20 and 4 neurons accordingly, 1 neuron on output layer (figure 5).

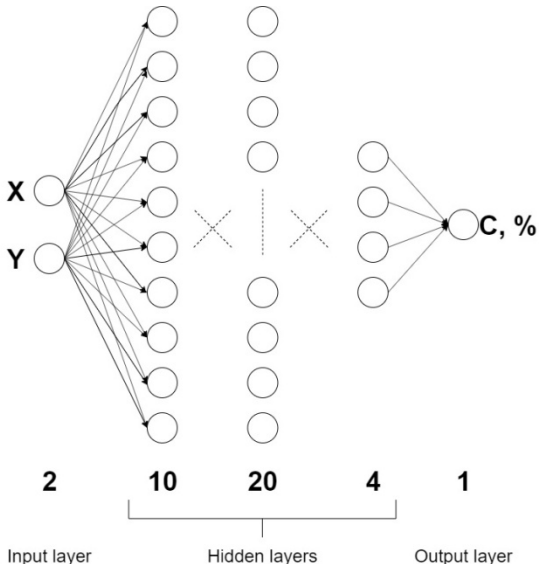

Figure 5 - Architecture of neural network model №1

Activation function was used sigmoid (1), because this function is widely used for neural networks aimed in prediction some values between 0 and 1 [19–22]. Graphical represent of the sigmoid function is showed on the figure 6.

$$S(x) = \frac{1}{1+e^{-x}} \tag{1}$$

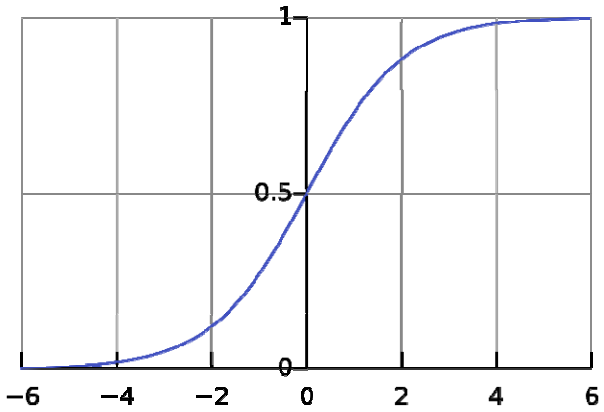

Figure 6 - Curve of sigmoid function

Using neural network model №1 after training we have obtained forecast for 10 points with average relative error 13.35%. The diagram of convergence of predicted data with original data is presented on the figure 7.

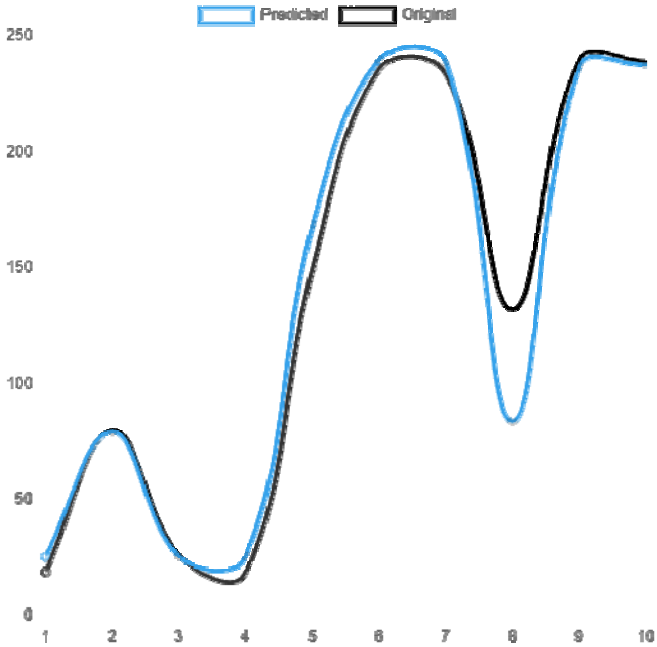

Figure 7 - The diagram of convergence of predicted data with original data on the neural network model №1 (x axis – number of verify point, y axis – shade of gray color in RGB)

Thus, neural network model 1 has shown good results with the first picture, so we have tried to use it with the second picture, which is more complicated and more similar to landscape distribution of some parameter: height, depth or may be the concentration of some element (figure 8). This picture is in the gray scale as well.

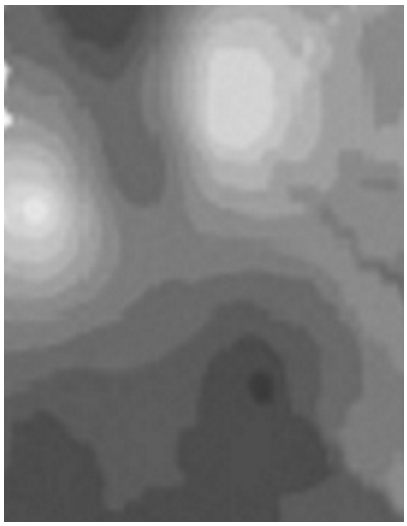

Figure 8 - Model image №2 for development of neural network

With the second model picture and using the previous architecture of neural network we have obtained the value of average relative error 20.49%. The diagram of convergence of predicted data with original data is presented on the figure 9.

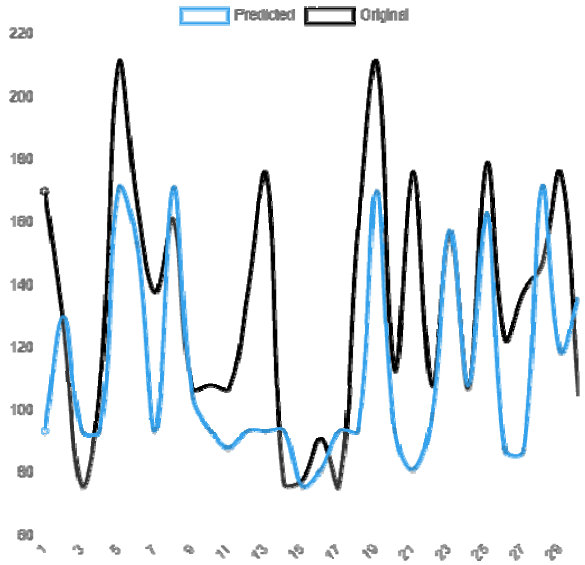

Figure 9 - The diagram of convergence of predicted data with original data on the neural network model №1 with picture 2 (x axis – number of verify point, y axis – shade of gray color in RGB)

On the diagram we can see that convergence in this case is much lover. Thus, it can be concluded, that the model №1 of neural network is appropriate just for simple characters of parameter distribution. That is why we are developed the second model of neural network and changed the approach for data analysis.

In the second model we used the interpolation method IDW for obtaining of demanded parameter value [23, 24]. But the calculations were made by neural network. This architecture has one neuron on input layer, which receives the values of distances between demanded point and each of 3 closest point. The distances were calculated by formula (2)

$$D = \sqrt{(x_2 - x_1)^2 + (y_2 - y_1)^2} \quad (2)$$

In accordance to this approach we have to get training data for each demanded point and train neural network for every point to prediction. However, taking into account the fact that training data contain only 3 input values it allows to simplify the model of neural network itself, so the second model of neural network has 1 neuron in input layer, 10 neurons in single hidden layer, and 1 output neuron. On the figure 10 we can see the convergence diagram for this case with picture №2.

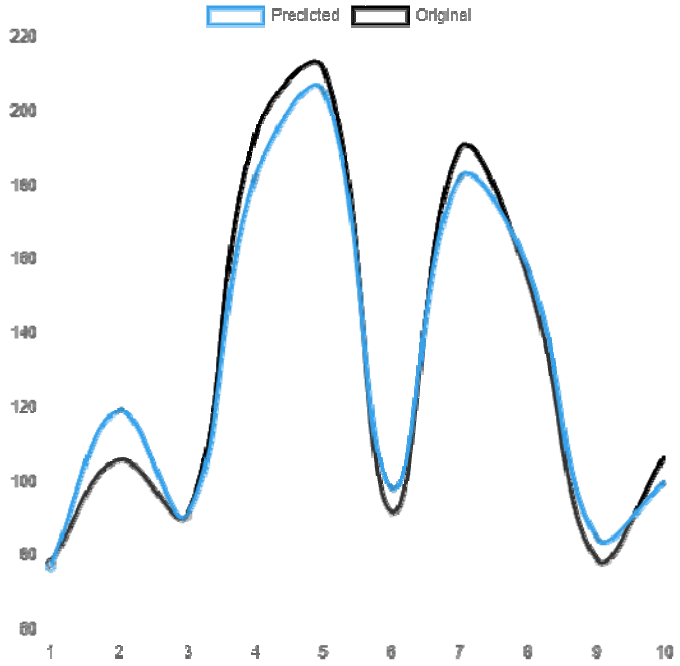

Figure 10 - The diagram of convergence of predicted data with original data on the neural network model №2 with picture 2 (x axis – number of verify point, y axis – shade of gray color in RGB)

In this situation we have obtained the value of average relative error 4.97% unless the picture was more complicated. Thus, this model of neural network was selected for using in analysis of concentration distribution of elements-contaminants on the studied territory.

Content of Cr in soils of studied territory was estimated using X-ray spectral microanalysis (table 3). These data were given into input of the neural network for training. On the figure 11 we can see the convergence diagram for verification process using model of neural network №2. The value of average relative error was 9.45%.

Table 3 – Data on Cr content in soils from sample sites 1-15 obtained using X-ray spectral microanalysis

Number of samples	X	Y	C, %
1	76.919125	52.313194	0.71
2	76.9083333333	52.3077777778	0.25
3	76.9338888889	52.2966666667	0.25
4	76.9367	52.2989166667	0.19
5	76.9630916667	52.3196361111	0.13
6	76.9625833333	52.3125277778	0.3
7	76.9673194444	52.2497555556	0.15
8	76.9707611111	52.2516555556	0.03
9	76.9552861111	52.3018861111	0.05
10	76.9570277778	52.235275	0.15
11	76.9926	52.2906138889	0.06
12	76.9894055556	52.290475	0.06
13	76.96925	52.2695777778	0.31
14	76.9688638889	52.27085	0.30
15	76.9285722222	52.3449916667	0.06

* Coordinate system EPSG:4326 - WGS 84 - Geographic

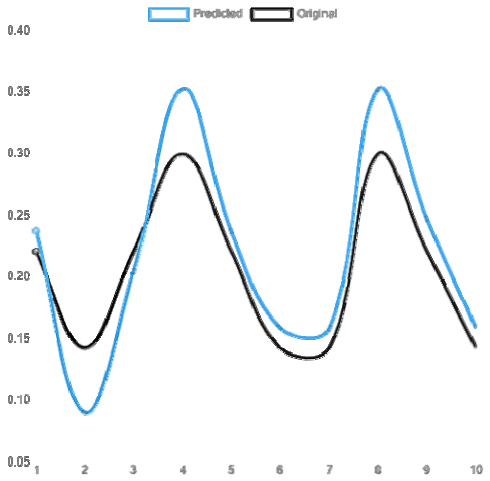

Figure 11 - The diagram of convergence of predicted data with original data on the neural network model №2 with data on Cr content in soils (x axis – number of verify point, y axis – concentration of Cr, %)

For prediction we have taken 500 points according to map represented on the figure 12. The batch process was performed with creation of prediction for every of 500 points. The obtained data with forecast of Cr distribution was plotted on the map in QGIS software. IDW interpolation was used in order to visualize the character of concentration distribution. The obtained interpolated map is represented on the figure 13. From the map it can be seen the large site with higher content of Cr. It is not necessary mean that the level exceeds the MPC level, but it gives the information about areas with higher and lower levels of the metal content. Control about MPC levels was not aimed in this research.

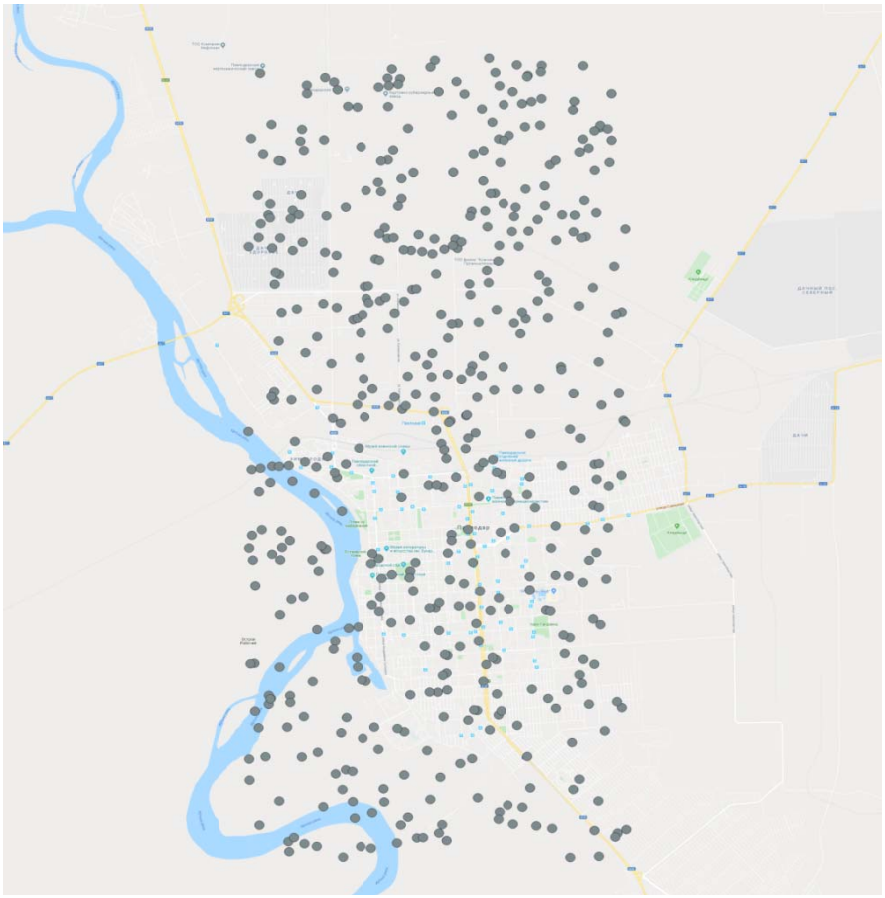

Figure 12 - Points where concentrations were calculated based on developed model of neural network

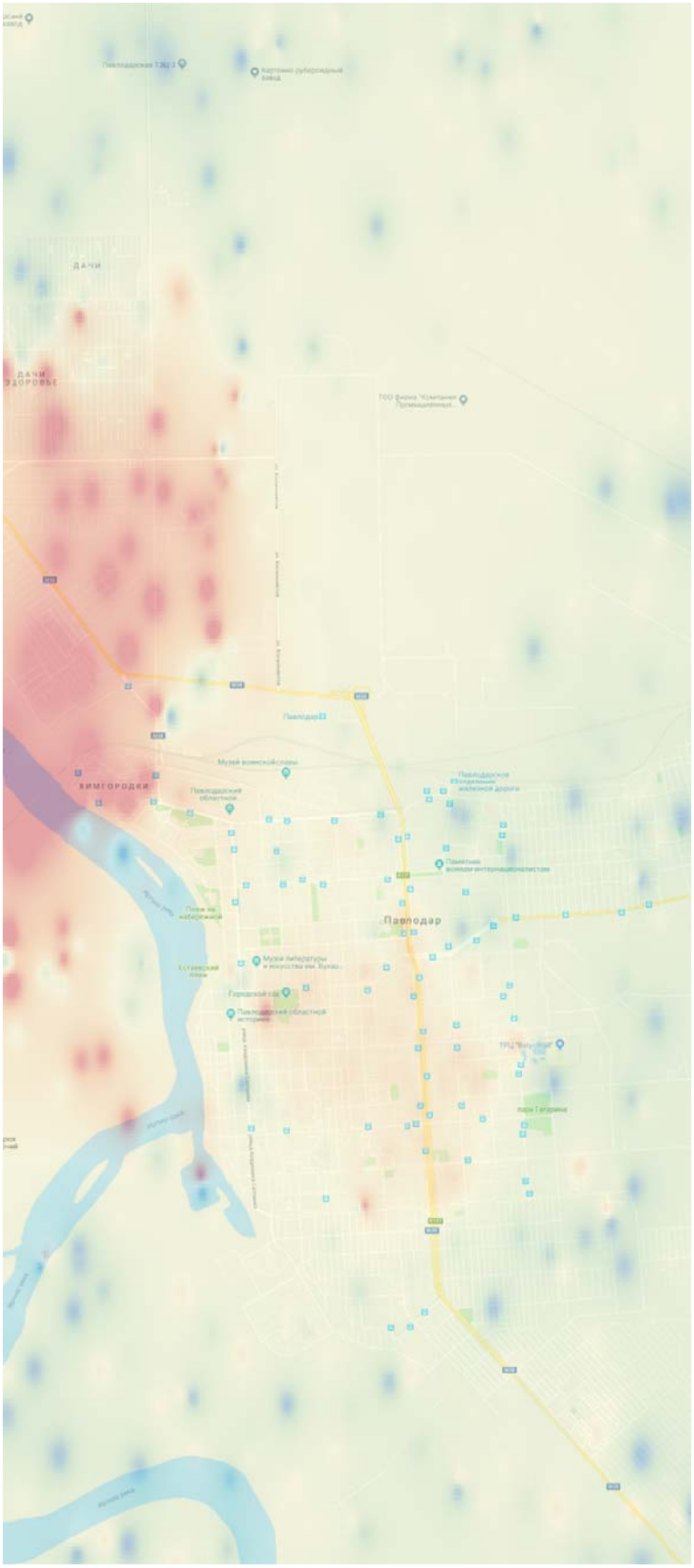

Figure 13 - Map of Cr concentration distribution in soils of Pavlodar city obtained on the basis of calculations of neural network model №2

Conclusion

Thus, during this work two models of neural network were developed. The method of calculating "point by point" using IDW approach and neural network №2 allows to predict complicatedly distributed data, which are usual when we are considering various geographical data: geochemistry, chemistry of environment, geology etc. That complexity is due to territorial distribution is influenced with many factors in very complex dependences. Using the developed method, it was possible to obtain 500 predicted points with values of chromium concentration on the different sites on the territory of Pavlodar city. The developed method allows to diminish level of error up to 9.45% (average relative error). The calculated data were inputted as a layer in QGIS. Based on the layer a new interpolated layer was created using IDW method. Thus, the colored map of chromium distribution on the territory of Pavlodar city was obtained in GIS. It allows to scale the map, get, print and save various views of the map.

Acknowledgments

The research work has been carried out in the frame of the project AP05134022 granted by Ministry of Education and Science of Republic of Kazakhstan.

УДК 550.42:004.89

Р.З. Сафаров[1], Ж.К. Шоманова[2], Р.Ж. Муканова[2], Ю.Г. Носенко[3], А. Илиеш[4], А.К. Свидерский[2], Н.Б. Сарова[5]

[1] Л.Н. Гумилев атындағы Еуразия ұлттық университеті, Нұрсұлтан, Қазақстан
[2]Павлодар мемлекеттік педагогикалық университеті, Павлодар, Қазақстан
[3] Инновациялық Еуразия университеті, Павлодар, Қазақстан
[4]Орадя университеті, Орадя, Румыния
[5]С.Ж. Асфендияров атындағы Қазақ ұлттық медицина университеті, Қазақстан

ЗЕРТТЕЛЕТІН АУМАҚТАРДА ЛАСТАУШЫ ЭЛЕМЕНТТЕРДІҢ ТАРАЛУЫН БОЛЖАМДЫҚ ТАЛДАУ ҮШІН НЕЙРОНДЫҚ ЖЕЛІНІ ӘЗІРЛЕУ (ПАВЛОДАР ҚАЛАСЫ МЫСАЛЫНДА, ҚАЗАҚСТАН)

Аннотация: Осы мақалада біз Павлодар қаласының аумағында (Қазақстан) ластаушы элементтердің (мысалы, Cr) таралуының болжамдық картасын жасау үшін нейрондық желіні қолданудың тиімді әдісін жасау нәтижелерін ұсынамыз. Әзірленген әдіс кеңейтілген деректерді алуға мүмкіндік береді. 15 нүкте бойынша деректер 500 нүктеде масштабталды. Верификация процесінің орташа салыстырмалы қателігі 9,45% құрайды. Нейрондық желінің жұмыс моделінің архитектурасы берілген нүкте мен бірнеше жақын нүктелер арасындағы қашықтықтың мәндерін қабылдайтын бір кіріс нейронымен перцептронды, жасырын қабаттың 10 нейронын және берілген нүктеде элементтің концентрациясының мәнін беретін 1 шығыс нейронды білдіреді. Алынған деректер концентрацияның таралуы туралы ақпаратты бейнелейтін IDW интерполяцияланған картасын құру үшін QGIS-те қолданылды.

Түйін сөздер: нейрондық желі, ластағыштар, бөлу, болжау, модельдеу, ГАЖ, экологиялық.

УДК 550.42:004.89

Р.З. Сафаров[1], Ж.К. Шоманова[2], Р.Ж. Муканова[2], Ю.Г. Носенко[3], А. Илиеш[4], А.К. Свидерский[2], Н.Б. Сарова[5]

[1]Евразийский национальный университет им. Л.Н. Гумилева, Нур-Султан, Казахстан
[2]Павлодарский государственный педагогический университет, Павлодар, Казахстан
[3]Инновационный Евразийский университет, Павлодар, Казахстан
[4]Орадя университет, Орадя, Румыния
[5]Казахский национальный медицинский университет им. С.Ж. Асфендиярова, Казахстан

РАЗРАБОТКА НЕЙРОННОЙ СЕТИ ДЛЯ ПРОГНОСТИЧЕСКОГО АНАЛИЗА РАСПРЕДЕЛЕНИЯ ЭЛЕМЕНТОВ-ЗАГРЯЗНИТЕЛЕЙ НА ИССЛЕДУЕМЫХ ТЕРРИТОРИЯХ (НА ПРИМЕРЕ ГОРОДА ПАВЛОДАР, КАЗАХСТАН)

Аннотация. В данной статье мы представляем результаты разработки эффективного метода с использованием нейронной сети для создания прогностической карты распределения элементов-загрязнителей (на примере Cr) на территории г. Павлодар (Казахстан). Разработанный метод позволяет получать расширенные данные. Данные по 15 точкам были масштабированы в 500 точек. Средняя относительная погрешность процесса верификации составляет 9,45

%. Архитектура рабочей модели нейронной сети представляет собой перцептрон с одним входным нейроном, который принимает значения расстояний между заданной точкой и несколькими ближайшими точками, 10 нейронов скрытого слоя и 1 выходной нейрон, который выдает значение концентрации элемента в заданной точке. Полученные данные использовались в QGIS для создания IDW интерполированной карты, которая визуализирует информацию о концентрационном распределении.

Ключевые слова: нейронная сеть, загрязнители, распределение, прогнозирование, моделирование, ГИС, экологический.

Information about authors:

Ruslan Zairovich Safarov – candidate of chemical sciences, Associate Professor of the Department of Management and Engineering in the field of environmental protection, L.N. Gumilyov Eurasian national university, ruslanbox@yandex.ru, https://orcid.org/0000-0003-2158-6330

Zhanat Kairollinovna Shomanova – doctor of technical sciences, professor of the Geography and chemistry department, Pavlodar state pedagogical university, zshoman@yandex.ru, https://orcid.org/0000-0001-8346-9688

Roza Zhumkenovna Mukanova - candidate of chemical sciences, Head of the Department of Geography and Chemistry, Pavlodar state pedagogical university, rozam14@mail.ru, https://orcid.org/0000-0001-9517-7359

Yuri Gennadievich Nossenko - candidate of chemical sciences, Innovative University of Eurasia, nosenko1980@yandex.ru, https://orcid.org/0000-0002-2491-7337

Alexandru Ilieș - Doctor of geography, professor, Dean of the Faculty of Geography, Tourism and Sport, University of Oradea, ilies@uoradea.ro, https://orcid.org/0000-0002-5920-5858

Aleksander Konstantinovich Sviderskiy - Doctor of Chemical Sciences, professor, Vice-rector for Research and International Relations, Pavlodar state pedagogical institute, katsostud@rambler.ru, https://orcid.org/0000-0001-5006-879X

Sarova Nurbanu – candidate of chemical sciences, Kazakh National Medical University named after D. S. Asfendiyarov, School of pharmacy. Lecturer, Department of Chemistry. nurbanu@mail.ru, https://orcid.org/0000-0002-7541-2224

REFERENCES

[1] Ramazanova N, Berdenov ZG, Ramazanov S, Kazangapova N, Romanova S, Toksanbaeva S, Wendt J. (2019). Landscape-geochemical analysis of steppe zone basin Zhaiyk. News of National Academy of Sciences of the Republic of Kazakhstan, 4(436):33–41. DOI:10.32014/2019.2518-170x.95(in Eng)

[2] Wu J, Lu J, Li L, Min X, Zhang Z, Luo Y. (2018). Distribution, pollution, and ecological risks of rare earth elements in soil of the northeastern Qinghai–Tibet Plateau. Human and Ecological Risk Assessment, 25(7):1–16. DOI:10.1080/10807039.2018.1475215 (in Eng)

[3] Wu S, Liang Z, Liu Y. (2019). Quantifying the risk of irreversible degradation for ecosystems: A probabilistic method based on Bayesian inference. Ecological Indicators, 107:105621. DOI:10.1016/j.ecolind.2019.105621 (in Eng)

[4] Mazhitova GZ, Janaleyeva KM, Berdenov ZG, Doskenova BB, Atasoy E. (2018). Assessment of the sustainability of landscapes of the North-Kazakhstan region to agricultural impact. News of The National Academy of Sciences of The Republic of Kazakhstan-Series of Geology and Technical Sciences, (3):90–95. (in Eng)

[5] Shomanova ZK, Safarov RZ, Auezhanova A, Zhumakanova AS, Nosenko YG, Tleulesov AK, Larichkin VV. (2017). Study of Composite Catalysts Containing Sludge of Ferroalloy Production in the Process of Cyclohexane Oxidation. News of the National Academy of Sciences of the Republic of Kazakhstan, Series of Chemistry and Technology, 426(6):55–61. (in Eng)

[6] Khodorov EI, Kvasha VB. (1996). Some problems in the quantitative estimation of the degree of no-waste production (cleanness) of chemical plants. Fibre Chemistry, 28(3):195–202. DOI:10.1007/BF01053569 (in Eng)

[7] Suleymenov IE, Sedlakova ZZ, Kopishev EE. (2019). New Polymer Materials for Optical Sensor Systems. Journal of Inorganic and Organometallic Polymers and Materials, 29(3):758–764. DOI:10.1007/s10904-018-1049-7 (in Eng)

[8] Herman GV, Ilies DC, Gaceu O, Ilies A, Mester C, Ilies M, … Dumitru M. (2019). Some considerations concerning the quality of groundwater in the Natura 2000 Lunca Barcaului (Barcaului Meadow) site, Romania. Journal of Environmental Protection and Ecology, 20(3):1102–1109. (in Eng)

[9] Ilieș DC, Oneț A, Wendt JA, Ilieș M, Timar A, Ilieș A, … Herman GV. (2018). Study on microbial and fungal contamination of air and wooden surfaces inside of a historical Church from Romania. Journal of Environmental Biology, 39:980–984. DOI:10.22438/jeb/39/6/MRN-658 (in Eng)

[10] Li H, Hu M, Huang Y. (2019). Automatic Identification of Overpass Structures: A Method of Deep Learning. ISPRS International Journal of Geo-Information, 8(9):421. DOI:10.3390/ijgi8090421 (in Eng)

[11] Tran M-N, Nguyen N, Nott D, Kohn R. (2019). Bayesian Deep Net GLM and GLMM. Journal of Computational and Graphical Statistics, :1–17. DOI:10.1080/10618600.2019.1637747 (in Eng)

[12] Alver A, Kazan Z. (2020). Prediction of full-scale filtration plant performance using artificial neural networks based

on principal component analysis. Separation and Purification Technology, 230:115868. DOI:10.1016/j.seppur.2019.115868 (in Eng)

[13] Gao C, Feng G, Ren Y, Liu L. (2019). Iris Segmentation Based on Improved U-Net Network Model. IEICE Transactions on Fundamentals of Electronics, Communications and Computer Sciences, E102.A(8):982–985. DOI:10.1587/transfun.e102.a.982 (in Eng)

[14] Suleimenov IE, Mun GA, Pak IT, Kabdushev SB, Kenessova ZA, Kopishev EE. (2017). Redistribution of the concentrations in polyelectrolyte hydrogels contacts as the basis of new desalination technologies. News of the National Academy of Sciences of the Republic of Kazakhstan, Series of Geology and Technical Sciences, 423(3):198–205. (in Eng)

[15] Fukuhara M, Fujiwara K, Maruyama Y, Itoh H. (2019). Feature visualization of Raman spectrum analysis with deep convolutional neural network. Analytica Chimica Acta, 1087:11–19. DOI:10.1016/j.aca.2019.08.064 (in Eng)

[16] Golla V, Arveti N, Etikala B, Sreedhar Y, Narasimhlu K, Harish P. (2019). Data sets on spatial analysis of hydro geochemistry of Gudur area, SPSR Nellore district by using inverse distance weighted method in Arc GIS 10.1. Data in Brief, 22:1003–1011. DOI:10.1016/j.dib.2019.01.030 (in Eng)

[17] Vural A. (2019). Evaluation of soil geochemistry data of Canca Area (Gümüşhane, Turkey) by means of Inverse Distance Weighting (IDW) and Kriging methods-preliminary findings. Bulletin of the Mineral Research and Exploration, 158:195–216. DOI:10.19111/bulletinofmre.430531 (in Eng)

[18] Martínez MÁ, Etchebehere S, Valero EM, Nieves JL. (2019). Improving unsupervised saliency detection by migrating from RGB to multispectral images. Color Research & Application, 44(6):875–885. DOI:10.1002/col.22421 (in Eng)

[19] Tallón-Ballesteros AJ. (2019). Metaheuristic algorithm to train product and sigmoid neural network classifiers. Expert Systems, 36(3):e12383. DOI:10.1111/exsy.12383 (in Eng)

[20] Elfwing S, Uchibe E, Doya K. (2018). Sigmoid-weighted linear units for neural network function approximation in reinforcement learning. Neural Networks, 107:3–11. DOI:10.1016/j.neunet.2017.12.012 (in Eng)

[21] Tallón-Ballesteros AJ. (2016). Contemporary training methodologies based on evolutionary artificial neural networks with product and sigmoid neurons for classification. AI Communications, 29(3):469–471. DOI:10.3233/AIC-150681 (in Eng)

[22] Tsai CH, Chih YT, Wong WH, Lee CY. (2015). A Hardware-Efficient Sigmoid Function with Adjustable Precision for a Neural Network System. IEEE Transactions on Circuits and Systems II: Express Briefs, 62(11):1073–1077. DOI:10.1109/TCSII.2015.2456531 (in Eng)

[23] Borges RC, Mahler CF, Caldas VG, da Silva AP, Bernedo AVB. (2018). Mapping of the concentration of natural radionuclides in the Fundão Island, RJ, Brazil supported by geoprocessing and IDW interpolation. Environmental Earth Sciences, 77(17):603. DOI:10.1007/s12665-018-7795-6 (in Eng)

[24] Madhloom HM, Al-Ansari N, Laue J, Chabuk A. (2017, December 22). Modeling spatial distribution of some contamination within the lower reaches of Diyala river using IDW interpolation. Sustainability (Switzerland). DOI:10.3390/su10010022 (in Eng)

N E W S
OF THE NATIONAL ACADEMY OF SCIENCES OF THE REPUBLIC OF KAZAKHSTAN
SERIES CHEMISTRY AND TECHNOLOGY
ISSN 2224-5286 **https://doi.org/10.32014/2019.2518-1491.79**
Volume 6, Number 438 (2019), 99 – 105

UDC 513.8

A.O. Kazenova[1], A.M. Brener[1], V.G. Golubev[1], Sh.K. Shapalov[2], D.R. Tortbayeva[1], G.D. Kenzhalieva[1], G.K. Ivahnuk[3]

[1]M. Auezov South Kazakhstan State University, Shymkent, Kazakhstan;
[2]SILKWAY INTERNATIONAL UNIVERSITY Shymkent, Kazakhstan;
[3]Petersburg State Institute of Technology (Technical University), Saint-Petersburg, Russian Federation
E-mail: aikerimkazenova@mail.ru, amb_52@mail.ru, golubev_50@mail.ru,
shermahan_1984@ mail.ru kafiedra.topid@mail.ru, nursara@mail.ru, ıvakhnyukg@list.ru

THE REGIMES OF THE REALIZATION OF DESUBLIMATION METHOD FOR ULTRADISPERSE POWDER PRODUCTION

Abstract. The paper deals with the investigation of the method of obtaining the ultrafine powders by the desublimationprocess. In the course of the experiments, the effect of temperature, pressure, and degree of supersaturation on the process kinetics and the dispersion size distribution function was investigated.The existence of the stage of the phenomenon of multiple coagulation with a high concentration of nucleates in a supersaturated vapor-gas mixture has been experimentally confirmed. Namely, it was established that with a large initial super-saturation, when a large number of embryos (monomers) of the dispersed phase are rapidly formed per unit volume of the apparatus, the contribution of multiparticle collisions is great. The obtained data may be very important for working out the engineering method for calculating and optimizing the regimes of aggregation processes to create highly homogeneous stable nanodispersions.

Keywords:desublimation, ultradisperse, nanodispersions, method, nano-powders, super-saturation, multiparticle.

1. Introduction

Currently, the use of chemical apparatus and reactors with the formation, aggregation and sedimentation of insoluble phases in the working volume of the apparatus is becoming increasingly widespread, especially in a number of modern technological processes [1-8]. Chemical equipment and reactors in which the formation, aggregation, and sedimentation processes of insoluble phases are carried out, especially in modern thin and nano-technologies, are widely used. In many cases, the processes of chemical technology are accompanied by the formation of a new solid dispersed phase. These can be phase transitions, as in the case of crystallization or desublimation, or processes of formation of slightly soluble substances during chemical reactions [9- 12].

Applications of dispersed media, namely: emulsions, suspensions, ultrafine materials and powders in modern industry cover a wide range of technologies. In particular, the following directions can be distinguished in the chemical industry [1-8]:

- obtaining nanodispersed powders of oxides and noble metal dioxides for structural, instrumental and functional bioceramics;
- creation of sorbents, catalysts and molecular sieves with a given nanostructure;
- development of methods for producing nano-dispersed rheological additives to create suspensions with desired rheological characteristics.

Nano-objects are characterized by small size, complex internal organization, the ability to very dense packaging, strong interactions with neighboring structures; on their basis, it can be created materials with new physical and chemical properties.

The most important features of the processes associated with dispersed media is the need for highly homogeneous and stable dispersions. These indicators play an extremely important role in modern pharmacopoeia, the production of high-quality fuel materials and in many other processes.

For the preparation of nano-powders with a high homogeneity of the fractional composition, desublimation methods seem to be very promising. The production of nano-powders in the gas phase is facilitated by the relatively low surface tension at the solid-gas interface [13]. An increase in surface tension leads to compaction of the nanoparticles in the aggregate. At the same time, high temperature accelerates diffusion processes, which contributes to the growth of particles and the formation of solid bridges between particles. The main problem of the method under consideration is the separation of nanoparticles from the gas phase under conditions where the concentration of particles in the gas stream is low and the gas temperature is sufficiently high. For trapping nanoparticles, special filtering devices are used (for example, metal-ceramic filters, electric precipitators), centrifugal sedimentation of solid particles in cyclone devices and hydrocyclones, special gas centrifuges.

In this paper, the method of obtaining the ultrafine powders by the desublimationprocess has been described.

2. Experimental method

Experimental studies were conducted to verify the adequacy of the theoretical concepts previously developed in our works [13], as well as to work out ways to optimize regimes of aggregation processes in dense dispersed systems with sources of the new phase. The desublimation method of obtaining ultrafine silica powder was chosen as objects for the study. In the course of the experiments, the effect of temperature, pressure, and degree of super saturation on the process kinetics and the dispersion size distribution function was investigated.

The experiment was organized on the well-known method of enriching high-silicon phosphorites [13]. The essence of this method is in the heat treatment of the raw material with ammonium fluoride followed by the conversion of silica contained in the raw material into ammonium silicofluoride. As next stage the sublimation of the obtained product was carried out.

For obtaining SiO_2, the especial reaction which at a certain temperature is carried out in the opposite direction with the rapid release of silicon dioxide was used [13]:

$$SiO_2 + 6NH_4F \Leftrightarrow (NH_4)_2SiF_6 + 4NH_3 + 2H_2O. \quad (1)$$

Earlier, in the work [13], the temperature threshold at which SiO2 emission prevails was determined . This threshold is 4500C.

A schematic diagram of the experimental setup and its photograph are presented in Figures 1 and 2.

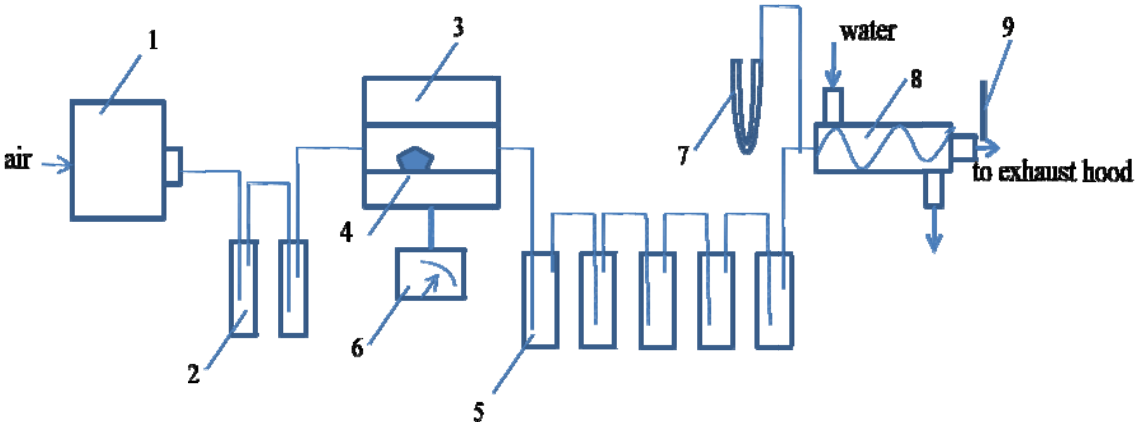

1- compressor, 2- Drexel flasks (for drying), 3- electric furnace, 4- boat with sample,
5- Drexel flasks (for capturing solid particles), 6- temperature conroller, 7- pressure gauge, 8- heat exchanger, 9- thermometer.

Figure 1- Scheme of the experimental installation.

Figure 2- Photograph of the experimental installation

The installation is operated as follows.

A ceramic tube is inserted into the furnace 3 where the boat (tube) 4 is placed with a sample prepared in accordance with the methodological recommendations indicated below. Next, the connection is made with the help of hoses of all elements of the installation, in accordance with the circuit diagram. Then the furnace is turned on and when the set temperature is reached (400-8000C) the compressor 1 is turned on.Compressor supplies the surrounding air in the room through the system of absorption flasks 2, which prevent moisture from entering the ceramic tube.

The resulting vapors from the sublimates $(NH_4)_2SiF_6$ from the furnace 3 enter the successively installed Drexel flasks 5, where they are desublimated.

Further the remaining fumes of silicon oxide go to the heat exchanger 7, where their final desublimation takes place, and then they go to the hood. The temperature in the furnace is maintained from 400 to 8000C. In the course of the experiment, the temperature in the furnace 3 is recorded, as well as the readings of the thermometer 1 at the exit from the refrigerator, and in addition, pressure is controlled at the inlet using a manometer 6. Sampling is performed periodically at each fixed temperature in the furnace.

The finished product is collected in glass cups and sent for analysis of the chemical and dispersion composition. The crystal structure is also analyzed.

A scanning electron microscope JSM-6490LV(SEM) is used as equipment for electron microscopic studies of the dispersion composition of desublimate. The appropriate method is based on scanning the surface of the sample with an electronic probe and detecting (recognizing) the broad spectrum of radiation arising from this.

Research and determination of measurement errors is carried out by standard methods.

The procedure for sample preparation is described below.

Investigating samples are prepared, then sublimated in a furnace and subject to desublimation. It makes in the following sequence:

a) the river sand is taken in an amount of 1 kg, it is sifted in order to separate from large impurities, and then it is washed with distilled water;

b) then it is washed with hot hydrochloric acid HCl with a concentration of 15-20% for 15-20 minutes and boiled for 15 minutes. Then the sample is defended in the flooded state for 2 hours, after which the liquid is drained;

c) the resulting sludge is washed with distilled water for 30-40 minutes in order to wash out the remaining impurities and acid residues;

g) then it is dried at a temperature of 105 ° C until the moisture content is in the range of 0.5-1%. The obtained sample should be gray;

e) then 1 part (weight) of the sample is mixed with 6 weight parts of ammonium fluoride;

e) the mixture is poured into a boat, which is placed in a furnace and sublimated at the temperature of 400-6000C until the strong smell of NH_3 appears;

g) white-colored vapors that are formed intensively are captured by their desublimation on a cooled surface for 1.5-2 hours in order to estimate the temperature of sublimation and desublimation, as well as for the most complete desublimation of the vapors.

The previous operation is repeated for 3-4 times. The sampling plan is shown in Table 1.

Table 1-The sampling plan while experiments on sublimation

№	Vapour temperature (C)	Sampling numbers by interval, min					
		The numerator is the first sampling stage, and the denominator is the second sampling stage					
		1	2	3	4	5	
1	T1=400	5/20	10/30	15/40	20/50	30/60	
2	T2=420	5/20	10/30	15/40	20/50	30/60	
3	T3=450	5/20	10/30	15/40	20/50	30/60	
4	T4=500	10	20	30	40	60	
5	T5=510	10	20	30	40	60	
6	T6=520	10	20	30	40	60	
7	T7=550	10	20	30	40	60	
8	T8=570	10	20	30	40	60	
9	T9=600	10	20	30	40	60	
10	T10=650	10	20	30	40	60	
11	T11=700	10	20	30	40	60	

3. Results and discussion

Some of the most illustrative images obtained as a result of the examination of samples using a scanning microscope are shown in Figure 3.

Inscriptions on photographs should be understood as follows. The first number is the temperature at which the sampling process is conducted, the next digit is the number of the Drexel flask in the capturing system.The obtained in the course of experiments characteristics and parameters of fractional composition of the silica dispersions, as well the microscope zoom, are automatically written in the fields of photographs.

The conducted investigations convincingly show that with a large initial super-saturation, when a large number of embryos (monomers) of the dispersed phase are rapidly formed per unit volume of the apparatus, the contribution of multiparticle collisions is great [11, 14]. This is clearly seen in Figure 3, made at high magnification. Namely, large clusters of particles consist of many small embryos. Moreover, the shape of large clusters-globules is rather rounded, which is possible only with simultaneous attachment of many small particles over the entire surface of larger clusters [15].

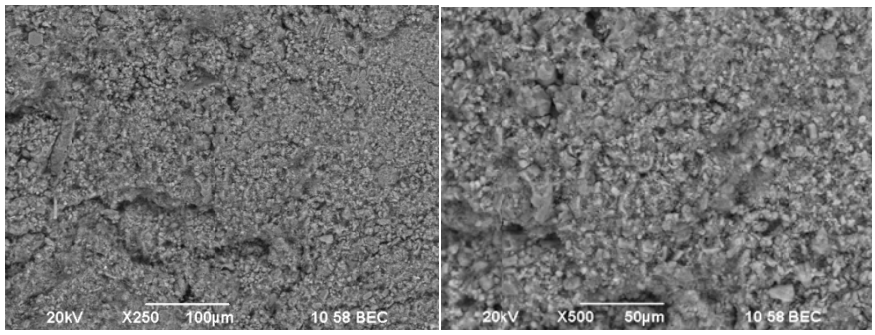

A) 300- 1

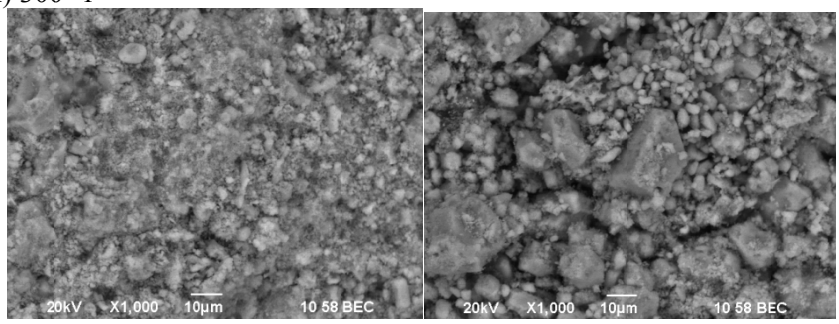

B) 300-1 300-2

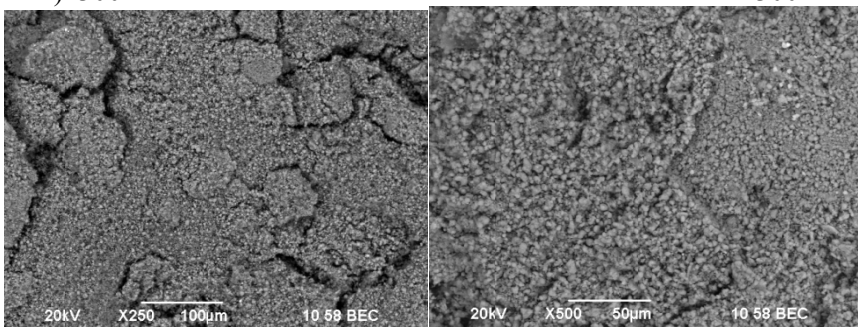

C) 500-1 500-2

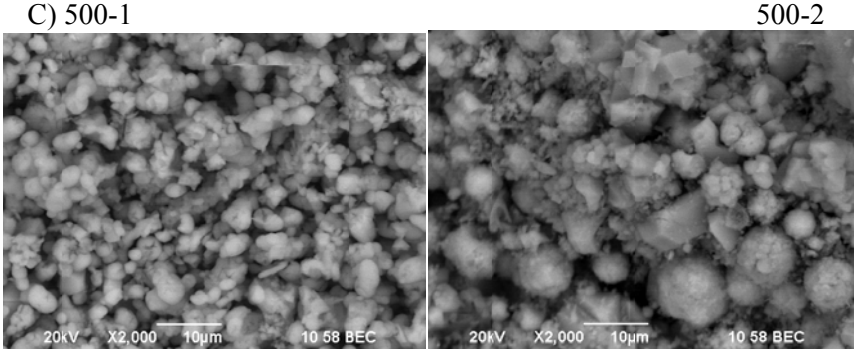

D) 500-3 500-4

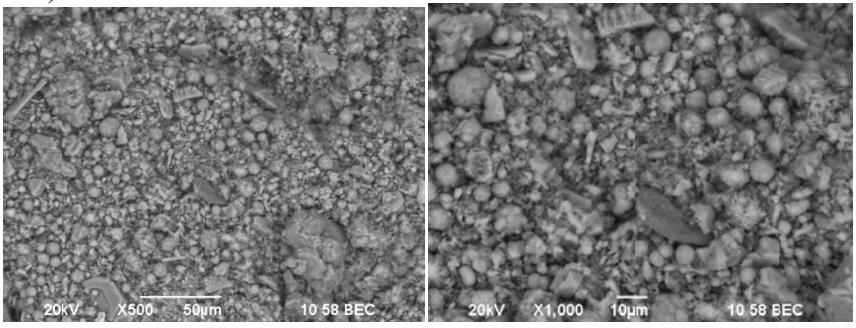

E) 500-5 (1, 2)

Figure 3 - Images of the desublimated samples

Then there is a sharp decrease in super-saturation, and the aggregation process begins to be limited by diffusion resistance in the gas phase. This leads to a sharp decrease in the value of coagulation nuclei, the intensity of the aggregation process drops sharply, and as a result, a dispersion of a fairly homogeneous fractional composition is obtained. The fact is that the characteristic time of the process is of the order of time, which is optimal for multiparticle aggregation.

At low initial super-saturation, the aggregation process is "eroded" in time, since binary collisions prevail. Therefore, the fractional composition of the resulting dispersion is very heterogeneous.

Conclusions

The existence of the stage of the phenomenon of multiple coagulation with a high concentration of nucleates in a supersaturated vapor-gas mixture has been experimentally confirmed. The results of experimental studies are well interpreted from the theoretical considerations. It can be the basis of the engineering methodology for calculating the operational parameters of the process. Especially, this conclusion is important for the aggregation in dense disperse systems and optimization of this process in order to create highly homogeneous stable nanodispersions.

The results of experimental studies of silicon dioxide desublimations confirmed the theoretical conclusion about the presence of a stage of rapid formation of primary nucleates and a subsequent stage of slow, diffusion-controlled growth of aggregates.

А.О. Казенова[1], А.М. Бренер[1], В.Г. Голубев[1],
Ш.К. Шапалов[2], Д.Р. Тортбаева[1], Г.Д. Кенжалиева[1], Г.К. Ивахнюк[3]

[1] М. Әуезов атындағы ОҚМУ, Шымкент, Қазақстан;
[2] SILKWAY Халықаралық университеті;
[3]Санк- Петербург мемлекеттік технологиялық институты (технологиялық университет),
Санк-Петербург қаласы

УЛЬТРАДИСПЕРЛІК ҰНТАҚ ӨНДІРУГЕ АРНАЛҒАН ДЕСУБЛИМАЦИЯ ӘДІСІНІСКЕ АСЫРУ РЕЖИМДЕРІ

Аннотация. Мақала десублимация әдісімен ультра дисперсті ұнтақтарды алу әдісін зерттеуге арналған. Эксперимент барысын датемператураның, қысымның және қанығу дәрежесінің процесс кинетикасына және дисперсияның мөлшері бойынша таралу функциясына әсері зерттелді.

Қанықпағанбу-газ қоспасында нуклеаттардың жоғары концентрациясы бар көпше коагуляция құбылысы кезеңінің болуы эксперименталды расталды. Атап айтқанда, үлкен бастапқы қанығу кезінде дисперсиялық фазаның эмбриондарының (мономерлерінің) көп саны аппарат көлемінің бірлігіне тез түзілетін кезде, көп бөлшекті қақтығыстардың үлесі үлкен.

Алынған мәліметтер біртекті фракциялық құрамы бар тұрақты нанодисперсияларды құру үшін агрегациялық процестердің режимдерін оңтайландыру және есептеудің инженерлік әдісін әзірлеу үшін өте маңызды болуы мүмкін.

Түйін сөздер: десублимация, ультрадисперсия, нанодисперсиялар, әдіс, наноұнтақтар, аса қанығу, көп бөлік.

Казенова[1], А.М. Бренер[1], В.Г. Голубев[1],
Ш.К. Шапалов[2], Д.Р. Тортбаева[1], Г.Д. Кенжалиева[1], Г.К. Ивахнюк[3]

[1]Южно-Казахстанский государственный университет им.М.Ауэзова, Шымкент, Казахстан;
[2] Международный университет SILKWAY Шымкент, Казахстан;
[3] Санк-Петербургский государственный технологический институт
(технологический университет), г.Санк- Петербург

РЕЖИМЫ РЕАЛИЗАЦИИ МЕТОДА ДЕСУБЛИМАЦИИ ДЛЯ ПРОИЗВОДСТВА УЛЬТРАДИСПЕРНОГО ПОРОШКА

Аннотация.Статья посвящена исследованию метода получения ультрадисперсных порошков способом десублимации. В ходе экспериментов было исследовано влияние температуры, давления и степени пересыщения на кинетику процесса и функцию распределения дисперсии по размерам. Существование стадии явления множественной коагуляции с высокой концентрацией нуклеатов в пересыщенной парогазовой смеси было подтверждено экспериментально. А именно, было установлено, что при большом

начальном пересыщении, когда большое количество эмбрионов (мономеров) дисперсной фазы быстро образуется на единицу объема аппарата, вклад многочастичных столкновений велик. Полученные данные могут быть очень важны для разработки инженерного метода расчета и оптимизации режимов агрегационных процессов для создания стабильных нанодисперсий с однородным фракционным составом.

Ключевые слова:десублимация, ультрадисперсия, нанодисперсии, метод, нанопорошки, сверхнасыщение, многочастица.

Informationaboutauthors:

Kazenova Aykerim - PhD student of the Department of "Technological Machines and Equipment", M.Auezov South Kazakhstan State University, aikerimkazenova@mail.ru, https://orcid.org/0000-0002-0637-5220

Brener Arnold - Doctor of Technical Sciences, professor of the Department of "Computing Systems and Software", M.Auezov South-Kazakhstan State University, amb_52@mail.ru, https://orcid.org/0000-0001-7041-0177

Golubev Vladimir Grigorievich - Doctor of Technical Sciences, professor of the Department of "Oil & Gas Business", M.Auezov South Kazakhstan State University, golubev_50@mail.ru, https://orcid.org/0000-0001-7370-3872

Shapalov Shermakhan, PhD Department of chemistry and biology, Silkway international university, Shymkent, Kazakhstan; shermahan_1984@mail.ru, https://orcid.org/0000-0002-3015-5965

Tortbayeva Dinara Ryskulbekkyzy - Candidate of technical science, associate professor of the Department of "Transport, transportation and traffic", M.Auezov South Kazakhstan State University, kafiedra.topid@mail.ru

Kenzhalieva Gulmira - Candidate of technical science, associate professor of t Department Department of «Life safety and environmental protection», M.Auezov South-Kazakhstan State University, nursara@mail.ru, https://orcid.org/0000-0003-0200-7145

Gregory Ivahnuk – doctor of technical science, professor of St. Petersburg State Institute of Technology (Technical University), ıvakhnyukg@list.ru , https://orcid.org/0000-0002-3401-158X

REFERENCES

[1] Voloshhuk V.M., SedunovJu.S. Processy koaguljacii v dispersnyh sistemah. L.: Gidrometeoizdat.- 1975, p. 435. (In Russian).

[2] Galkin V.A. UravnenieSmoluhovskogo.- M.: FIZMATLIT, 2001. 336 p. (In Russian).

[3] J.M. Ball, J. Carr, O. Penrose. The Becker-DoringClaster Equations: Basic Properties and Asymptotic Behaviour of Solutions// Commun Math. Phys. 104, 1986, p. 657-692. (In Russian).

[4] RudjakV.Ju. Statisticheskajateorijadissipativnyhprocessov v gazahizhidko-stjah.-Novosibirsk.: Nauka, 1987, 272 p. (In Russian).

[5] Kim L.A., Brener A.M. Vremennaja nelokal'nost' uravnenij perenosa tepla i massy v intensivnyh tehnologicheskih processah // TOHT, T. 30, №3, 1996, P. 258-262. (In Russian).

[6] Kim L.A., Brener A.M. Uchet perekrestnyh jeffektov v nelokal'nyh uravne-nijah perenosa tepla i massy.TOHT. 1998, T. 32, №3, p. 247-250 (In Russian).

[7] D. Jou, J. Casas-Vázquez, M. Criado-Sancho. Thermodynamics of Fluids Under Flow. Springer-Verlag: Berlin, Heidelberg, 2001, p. 231.

[8] UizemDzh. Linejnye I nelinejnye volny. M.: Mir, 1977. (In Russian).

[9] Gabov S.A., Vvedenie v teoriju nelinejnyh voln. M.: MGU, 1988. (In Russian).

[10] Brener A.M., 2011, Nonlocal model of aggregation in dispersed systems, Theoretical Foundation of Chemical Engineering, 45(3), 332-336.

[11] Brener A.M., 2014, Model of many-particle aggregation in dense particle systems, Chemical Engineering Transactions, 38, 145-150.

[12] Brener A.M., Dil'man V.V., 2016, Concept of building an aggregation kinetic model taking into consideration the dependence between aggregation activity and cluster ages, Theoretical Foundation of Chemical Engineering, 50(4), 439-443.

[13] Kazenova A., Brener A., Golubev V., Kenzhalieva G., 2017, Chemical Engineering Transactions, 57, 835-840.

[14] Golubev, V.G., Brener, A.M., 2002, Film condensation from a dusty vapor-gas mixture, Theoretical Foundation of Chemical Engineering, 36(2), 123-128.

[15] Caplrile B., Levi A.C., Liggieri L.L., 1986, Random Rain Simulations of Dendritic Growth, In: Pietronero L., Tosatti E. (Eds), Fractals in Physics, Elsevier Sci. Publ., 279-282.

[16] V. Bondarenko, O. I. Kutnyashenko, Y. I. Rudyk, S. V. Solyonyj//News of the National Academy of Sciences of the Republic of Kazakhstan. Series of geology and technical sciences. 2019 Vol. 2, N 434. P.120-130. ISSN 2224-5278. https://doi.org/10.32014/2019.2518-170X.45

МАЗМҰНЫ

СОДЕРЖАНИЕ

CONTENTS

Publication Ethics and Publication Malpractice in the journals of the National Academy of Sciences of the Republic of Kazakhstan

For information on Ethics in publishing and Ethical guidelines for journal publication see http://www.elsevier.com/publishingethics and http://www.elsevier.com/journal-authors/ethics.

Submission of an article to the National Academy of Sciences of the Republic of Kazakhstan implies that the described work has not been published previously (except in the form of an abstract or as part of a published lecture or academic thesis or as an electronic preprint, see http://www.elsevier.com/postingpolicy), that it is not under consideration for publication elsewhere, that its publication is approved by all authors and tacitly or explicitly by the responsible authorities where the work was carried out, and that, if accepted, it will not be published elsewhere in the same form, in English or in any other language, including electronically without the written consent of the copyright-holder. In particular, translations into English of papers already published in another language are not accepted.

No other forms of scientific misconduct are allowed, such as plagiarism, falsification, fraudulent data, incorrect interpretation of other works, incorrect citations, etc. The National Academy of Sciences of the Republic of Kazakhstan follows the Code of Conduct of the Committee on Publication Ethics (COPE), and follows the COPE Flowcharts for Resolving Cases of Suspected Misconduct (http://publicationethics.org/files/u2/New_Code.pdf). To verify originality, your article may be checked by the Cross Check originality detection service http://www.elsevier.com/editors/plagdetect.

The authors are obliged to participate in peer review process and be ready to provide corrections, clarifications, retractions and apologies when needed. All authors of a paper should have significantly contributed to the research.

The reviewers should provide objective judgments and should point out relevant published works which are not yet cited. Reviewed articles should be treated confidentially. The reviewers will be chosen in such a way that there is no conflict of interests with respect to the research, the authors and/or the research funders.

The editors have complete responsibility and authority to reject or accept a paper, and they will only accept a paper when reasonably certain. They will preserve anonymity of reviewers and promote publication of corrections, clarifications, retractions and apologies when needed. The acceptance of a paper automatically implies the copyright transfer to the National Academy of Sciences of the Republic of Kazakhstan.

The Editorial Board of the National Academy of Sciences of the Republic of Kazakhstan will monitor and safeguard publishing ethics.

Правила оформления статьи для публикации
в журнале смотреть на сайте:

www:nauka-nanrk.kz

http://chemistry-technology.kz/index.php/en/arhiv

ISSN 2518-1491 (Online), ISSN 2224-5286 (Print)

Редакторы: *М. С. Ахметова, Т. А. Апендиев, Аленов Д.С.*
Верстка на компьютере *А.М. Кульгинбаевой*

Подписано в печать 05.12.2019.
Формат 60x881/8. Бумага офсетная. Печать – ризограф.
5,25 п.л. Тираж 300. Заказ 6.

Национальная академия наук РК
050010, Алматы, ул. Шевченко, 28, т. 272-13-18, 272-13-19